2013

Novel Ribosome Biogenesis in the Lyme Disease Spirochete Borrelia burgdorferi

Melissa Lynn Hargreaves
The University of Montana

NOVEL RIBOSOME BIOGENESIS IN THE LYME DISEASE SPIROCHETE *BORRELIA BURGDORFERI*

By

MELISSA LYNN HARGREAVES

B. S. Montana State University, Bozeman, Montana, 2006

Dissertation

presented in partial fulfillment of the requirements
for the degree of

Doctor of Philosophy
Integrative Microbiology and Biochemistry

The University of Montana
Missoula, MT

June 2013

Approved by:

Sandy Ross, Dean of The Graduate School
Graduate School

D. Scott Samuels, Chair
Division of Biological Sciences

Mike Minnick
Division of Biological Sciences

Stephen Lodmell
Division of Biological Sciences

Michele McGuirl
Division of Biological Sciences

Kent Sugden
Chemistry and Biochemistry

Hargreaves, Melissa, Ph.D., Spring 2013 Integrative Microbiology/Biochemistry

Novel ribosome biogenesis in the Lyme disease spirochete *Borrelia burgdorferi*

Chairperson: D. Scott Samuels

Here we demonstrate the first characterization of an RNase III enzyme from a spirochete and its role in processing rRNA transcripts from the unusual rRNA gene operons of *Borrelia burgdorferi*. In most bacteria, the three rRNA transcripts (16S, 23S, and 5S rRNAs) that form the ribosome are produced as a single transcript from an operon with minimal spacing between genes. In the *B. burgdorferi* genome, however, a single 16S rRNA gene is encoded more than 3 kb from the bicistronic 23S-5S rRNA operons. The 23S-5S operons are tandemly duplicated, yielding an uneven number of rRNA genes, a feature unique to Lyme disease *Borrelia*. Additionally, the 16S and tandem 23S-5S operons appear to be synthesized as two separate transcripts. Our data show that *B. burgdorferi* RNase III processes the 3′ end of the 16S, 23S, but not the 5S, rRNA transcripts, as in other bacteria. However, 16S rRNA 5′ end processing proceeds by an as yet unidentified mechanism, which is an unprecedented finding. We hypothesize that this deviation from the canonical 16S rRNA processing pathway is likely an adaptation of *B. burgdorferi* to rRNA gene rearrangement during genome reduction and transition to a host-restricted lifestyle. In agreement with this finding, the 16S rRNA gene is transcribed as part of a larger operon containing unrelated genes, suggesting alternative regulation of the rRNA transcripts. Additionally, we show that the 23S rRNA is transcribed from identical promoters present in front of both tandem 23S rRNA genes and that this creates our observed 2.5 to 3-fold excess of 23S rRNA compared to 16S rRNA. Finally, single deletion mutants in each of the 23S rRNA genes were constructed. Surprisingly, deletion of the first 23S rRNA gene produces a severe growth phenotype and increased erythromycin susceptibility *in vitro* and a strain that is non-infectious *in vivo*. A mutant with a deletion in the second 23S rRNA gene shows no phenotype. The 23S rRNA genes have begun to acquire single nucleotide polymorphisms. However, their pattern currently indicates that they are the products of genetic drift. We conclude that the mechanism of rRNA transcription is unique in *B. burgdorferi*.

Acknowledgements

First and foremost, I would like to thank my advisor, Scott Samuels, for introducing me to the weird and wonderful world of *Borrelia* biology, for his support these past five years, and for helping me mature into a better scientist by providing an excellent example of what a scientist should be. He also deserves thanks for his endless generosity, patience, and kindness, particularly in helping me develop a more concise writing style.

I would also like to thank my committee members, Mike Minnick, Steve Lodmell, Michele McGuirl, and Kent Sugden, for their advice, guidance, and time. I could not have completed key experiments without the technical advice of Jean-Marc Lanchy and Mary Ellenbecker. A special thank you should also go to Emily Hedrick and Walt Hill for their help with the primer extension experiment. I would like to thank our collaborators David Bechhofer and Paula Schlax for the generous gift of materials.

All of the current and past members of the Samuels lab deserve thanks for creating an amazing lab environment to work in, particularly: Laura Hall, Dan Drecktrah, Meghan Lybecker, Cassie Abel and Amanda Brinkworth. A special thanks to Richard LeCoultre as well, for helping me to grow as a mentor and teacher, for being an amazing mentee, and for his hard work on key RNase III experiments.

Finally, I would like to thank my family and friends for believing in me and cheering me on during my time in graduate school. And, of course, endless thanks go to my wonderful husband, Gregory Hargreaves, for helping me maintain my sanity during all of the trials of my graduate school years. I could not have survived my degree without his constant support and inspiration.

Table of Contents

List of Tables

List of Figures

Chapter 1

Introduction

Borrelia burgdorferi and the enzootic cycle

Borrelia burgdorferi is the causative agent of Lyme disease (9, 10, 11). Lyme disease accounts for more than 90% of reported vector-borne disease in the United States (12, 13). *B. burgdorferi* belongs to the genetically distinct Spirochaetae phylum, which includes other notable genera associated with disease such as *Leptospira* (leptospirosis), *Treponema* (syphilis, Yaws), and *Brachyspira* (intestinal spirochetosis) (14, 15, 16, 17, 18, 19, 20, 21). The Spirochaetae are widely distributed throughout the world and exhibit diverse lifestyles, from free-living saprophytes residing in stagnant water to a parasitic enzootic life cycle dependent on an arthropod vector and mammalian host. Members of this phylum are characteristically defined by the unusual periplasmic location of their flagella, which contributes to their unique bacterial shape and motility (22, 23, 24).

The *Borrelia* genus itself is divided into two major phyletic groups generally based on their capability of causing human disease; *B. burgdorferi*, *B. afzelii*, *B. garinii, B. bissettii, B. valaisiana, B. lusitaniae,* and *B. spielmanii* have been isolated as agents of Lyme disease (or LD-like disease), whereas *B. duttoni*, *B. recurrentis*, and *B. hermsii* are the primary species associated with borrelial relapsing fever. *B. andersonii* and *B. japonica* are closely related to the LD *Borrelia* but have not yet been associated with disease (13, 25). As all of these organisms (except *B. recurrentis*) depend on a tick vector during their natural life cycle, incidence of disease is linked to the distribution of each

vector, which is related to the availability of suitable habitat (25, 26). The tick vectors for Lyme disease *Borrelia* species are the hard-bodied ticks of the *Ixodes* genus, which are distributed throughout the Northern Hemisphere in regions containing temperate forests with high humidity (13, 25, 26, 27).

B. burgdorferi is maintained in nature through an enzootic cycle involving its tick vector and small vertebrate hosts (13, 25). The two-year tick life cycle is central to the seasonal pattern of *B. burgdorferi* transmission into a warm-blooded host (26, 27). Lyme disease in humans initially manifests with the development of a bull's-eye rash known as erythema migrans at the site of the tick bite and can be accompanied by flu-like symptoms (12). If detected early, Lyme disease can be readily treated with antibiotics such as doxycycline (28). However, if left untreated, further complications such as arthritis, carditis, and neurological sequelae can develop (12).

The genome of *B. burgdorferi* lacks discernible genes for production and secretion of toxins, so the symptoms of Lyme disease are considered to be the consequence of immunological responses to spirochete infection (12, 13, 29, 30). For acute Lyme disease, the erythema migrans results from activation of local dermal macrophages and dendritic cells along with the recruitment of other circulating immune cells (12, 31). The accompanying flu-like illness is thought to be the result of cytokine production in response to hematogenous dissemination of *B. burgdorferi* (12). In untreated patients, the arthritis, carditis, and neuropathies are likely the outcome of localized immune activation, and, in the case of long-term arthritis, the development of autoimmunity to uncleared spirochete remnants in the joints (12, 30).

During transmission from the salivary glands of the tick vector to a mammalian host, *B. burgdorferi* utilizes the multitude of anti-immune factors in tick saliva to initially evade the immune response (13, 32, 33, 34, 35). In addition, *B. burgdorferi* outer surface lipoprotein C (OspC) can bind the tick protein SALP15, which allows the bacterium to evade antibody attachment (13, 34, 35, 36). Other surface lipoproteins (BbCRASPs; complement regulator-acquiring surface proteins) bind factor H, inhibiting the complement cascade (12, 13, 36, 37).

After initial dermal penetration, *B. burgdorferi* rapidly replicates and eventually moves toward the interface between the posterior dermis and the circulatory system, entering the bloodstream (12, 13, 37, 38). Rather than produce tissue-digesting enzymes, *B. burgdorferi* binds plasminogen and its activation molecule (to create plasmin), as well as induces matrix metalloproteinases, which are produced by a variety of cells and are involved in normal tissue remodeling (13, 30, 37, 39, 40). Activated plasmin is a protease that allows *B. burgdorferi* to penetrate the cells lining the dermal capillaries and promotes hematogenous spread of the organism (37). OspC has recently been shown to bind plasminogen (41).

B. burgdorferi eventually exits the circulatory system and takes up residence in tissue (37, 38). The spirochete possesses the ability to bind collagen and seems to find potential ‘protective niches’ within the mammalian host where it can persist (37, 42, 43). At this point, OspC is downregulated and other *B. burgdorferi* surface molecules are switched as needed in an effort to avoid the host immune response (37, 44). Similar to relapsing fever *Borrelia* species, *B. burgdorferi* has the capacity to recombine the gene

for a plasmid-expressed outer membrane lipoprotein (*vlsE*) in order to confer antigenic surface variation in response to undefined mammalian signals (37, 45, 46).

The enzootic cycle begins when a female *Ixodes* tick lays eggs on the ground amongst leaf litter. Uninfected larval ticks hatch during late summer or early autumn and immediately seek out a blood meal, usually from small rodents or birds. If this reservoir animal has been previously infected with *B. burgdorferi*, the larval tick can acquire the spirochete during the blood meal (13, 25, 26). *B. burgdorferi* in its reservoir host likely sense chemoattractants from the feeding tick and migrate towards the bite location (13). In order to colonize the tick, however, *B. burgdorferi* must alter its gene expression to switch from survival in the mammal to persisting in the tick (47, 48), including upregulating metabolic pathways to utilize alternative carbon sources (13, 49, 50). One of the predominant proteins responsible for enabling this transition is outer surface lipoprotein A (OspA), which allows *B. burgdorferi* to bind to tick midgut epithelium and probably provides shielding from anti-*Borrelia* antibodies that may be present in the host blood meal, thus permitting successful colonization of the tick vector (51, 52, 53, 54).

As the larval tick molts into a nymph, *B. burgdorferi* is maintained in the tick's midgut. Persistence requires *B. burgdorferi* to survive in a nutrient-limiting environment within the flat, unfed nymph over the winter months (13, 35). However, the spirochete is not dormant during this phase as certain genes are specifically upregulated to cope with this environment. *B. burgdorferi* utilizes glycerol, which is present in the tick midgut and serves as a natural antifreeze, as a carbon source (13, 49, 50). There is a poorly understood stringent response in *B. burgdorferi* that might also contribute to spirochete survival under these harsher conditions (13, 55, 56, 57, 58).

Once the molt is complete and winter has transitioned to spring, the nymphal tick must feed again, usually on another rodent or bird, but occasionally on humans or other animals (13, 25). Nymphs climb low-level vegetative matter and quest for their next meal by protruding their legs until they catch on the fur or skin of a suitable host (25). After attachment the tick begins to feed and the *B. burgdorferi* residing in its midgut alter their gene expression to prepare for transmission (47, 48). Most conspicuously, OspA is downregulated and OspC is upregulated (59, 60, 61, 62, 63, 64, 65, 66). A complex cascade involving the alternative sigma factors RpoN and RpoS regulates this switch (67). After approximately 48 hours of feeding, the spirochete moves from the tick midgut to the salivary glands and is successfully transmitted into its host to begin the process of infection (13, 68). Following its second blood meal, the nymphal tick molts once again into the adult form. At this stage, only the female tick will feed again, generally on large mammals such as deer, mate, lay their eggs, and die (13, 25). *B. burgdorferi* is not vertically transmitted in ticks and must be acquired anew by larvae from an infected warm-blooded host (69).

Both reservoir host species along with the tick vectors contribute to the continued maintenance of *B. burgdorferi* and other Lyme disease *Borrelia* species in nature (13, 25, 26, 27). The white-footed mouse, *Peromyscus leucopus*, is the primary North American *B. burgdorferi* reservoir species and seems to asymptomatically maintain the spirochete over its lifetime after the initial infection (70, 71, 72). Additionally, in Europe, migratory birds that become infected with the spirochete *B. garinii* contribute to the spread of *Borrelia* isolates to new regions (13, 25, 26). However, not all hosts are capable of promoting maintenance of *B. burgdorferi* within the enzootic cycle. Humans and dogs are

thought to be dead-end hosts, as they are not part of the normal ecological niche of the enzootic cycle and clinical treatment will eliminate the spirochete before another tick can feed (13). Some lizard species in the Southwestern United States are capable of initial infection with *B. burgdorferi* but possess anti-*Borrelia* immune factors that rapidly lead to spirochete death, removing these spirochetes from the transmission pool (73).

The complex genome of *Borrelia burgdorferi*

In order to survive in and transition between the two disparate environments of the tick vector and mammalian host, the genome of *B. burgdorferi* must encode a diverse array of genes (13, 36, 48). In fact, *B. burgdorferi* possesses what is considered the most complex prokaryotic genome (29, 74, 75, 76). However, as *B. burgdorferi* has adapted to a parasitic lifestyle within its vector and host, natural genetic reduction has taken place, resulting in a core chromosome with very few intergenic spaces and only a few rRNA genes (29, 77, 78). Consequently, *B. burgdorferi* has become metabolically restricted and is fastidious to grow in laboratory cultures (79, 80). Unlike most bacteria, which harbor a single, circular chromosome molecule, the genome of *B. burgdorferi* consists of a relatively small (~900 kb), linear chromosome harboring the majority of housekeeping and metabolic genes as well as ~12 linear and ~9 circular plasmids (ranging from 5 to 20 kb) (29, 74, 75, 77). At least one of the circular plasmids is a prophage (75, 77, 81, 82). This genomic arrangement is unique and many of the linear plasmid genes have no homologs outside of *Borrelia* species (29, 74, 77). However, the gene content of the chromosome is relatively consistent among *Borrelia* species (77).

The linear chromosome of *B. burgdorferi* strain B31 carries 846 protein-coding genes, 31 tRNA genes, and 5 rRNA genes (discussed in detail below) (1, 29, 77, 83). It has a low GC-content (28.6%) and protein-coding genes account for 93% of the coding sequence, which is a common trend for a genome that has been severely reduced (77, 84, 85). The metabolic capacity of *B. burgdorferi* is limited; it must scavenge all amino acids, nucleotides, vitamin cofactors and fatty acids (80). It also lacks the enzymes of the citric acid cycle. Consequently, the genome contains many types of transporters for nutrient uptake, including metabolic intermediates (29, 77, 80). Glycolysis is carried out through fermentation of sugars via the Embden-Meyerhof pathway (80). There is a lack of genes involved in iron scavenging and metabolism, and *B. burgdorferi* does not require iron for growth (80, 86). Intriguingly, the linear chromosome and linear plasmids possess covalently closed telomeres, which are generated by a plasmid-encoded resolvase (ResT) (76, 77, 87). In addition to the chromosome, lp54, cp26, and cp32 (plasmid nomenclature includes lp for linear plasmids or cp for circular plasmids along with the size in kb in strain B31) are present in all strains, and are thought to potentially serve as a ‘mini chromosome‘ (74, 75, 77).

The genetic content of the plasmids is more variable than the chromosome and these contain paralogous sequences, pseudogenes, and a few essential genes (29, 75, 77). Most of the genes encoding the plethora of outer surface lipoproteins (36) are also carried on the plasmids. Some of the plasmids are required for mammalian infectivity (lp25 and lp28-1) (45, 88, 89), whereas others are vital to survival within the tick environment (lp25 and lp28-4) (77, 90). The circular plasmids have fewer pseudogenes than the linear plasmids, and genes are closely packed on these plasmids (29, 74, 77). *B. burgdorferi*

encodes multiple copies of cp32 and single copies of both cp9 and the essential cp26 (74, 77). The cp32 plasmids appear to be prophages that are similar to the λ-phages, including a contractile tail and a late operon (81, 82, 91, 92). Isolated phages contain cp32 DNA and are capable of transducing this DNA between *Borrelia* strains (82). The cp32 plasmids carry genes for surface-exposed proteins, including the one responsible for binding to complement factor H (36, 74, 77).

The novel rRNA gene organization of *Borrelia burgdorferi*

The unusual *Borrelia* ribosomal RNA gene organization is, considering the parasitic lifestyle, perhaps not surprising. As bacteria adapt to a host-restricted life, their genomes undergo a natural reduction that can lead to the development of unusual rRNA arrangements through a variety of mechanisms ((93) and below). The rRNA genes are located in the central portion of the chromosome, which is more GC-rich than the remainder of the chromosome, and are present in the canonical order (16S-23S-5S), but are arranged in a considerably different organization than in other bacterial species, which could affect metabolism (1, 83, 94, 95). Figure 1, below, depicts the ribosomal RNA region of *B. burgdorferi*. The 16S rRNA gene is separated from the 23S-5S rRNA operon by more than 3 kb (5 kb in the other Lyme disease species *B. garinii* and *B. afzelii*) (1, 83, 94, 95). Two tRNA genes ($tRNA_{Ala}$ and $tRNA_{Ile}$) are located downstream of the 16S rRNA gene and Bugrysheva *et al.* (5) determined that the 16S rRNA and $tRNA_{Ala}$ are produced as a single transcript, while $tRNA_{Ile}$ is generated as its own transcript. Notably, in addition to the tRNAs, four predicted protein-coding genes are

present in this spacer region: two that appear to be truncated ORFs (located between the tRNA genes), a DNA-3-methyladenine glycosylase (*bb0422*), and a haloacid dehalogenase-like hydrolase (*bb0421*). The latter enzyme may hydrolyze phosphorylated metabolic intermediates, including acetyl phosphate (96), which plays a role in regulating gene expression during transmission (97). The first 5S rRNA gene (*rrfB*) follows the 23S rRNA gene (*rrlB*) with a short spacer between the two. However, there is an additional 23S-5S operon (*rrlA-rrfA*) downstream with a short 179-bp spacer, a feature that has not been observed for any other bacterial species sequenced to date (1, 95). The tandem 23S-5S rRNA operon region is transcribed as a single precursor RNA (5), but the mechanism separating the two rRNAs has not yet been characterized.

Figure 1: Chromosomal arrangement of *B. burgdorferi* ribosomal RNAs

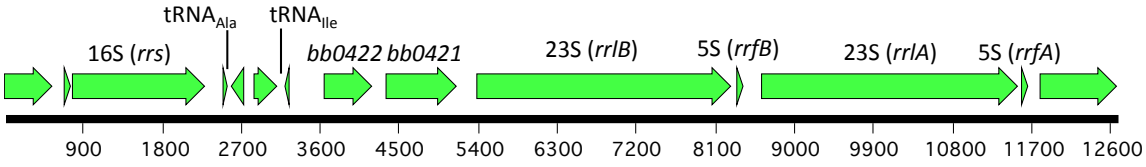

The rRNAs of *B. burgdorferi* are located near the center of the linear chromosome. The 16S gene is followed by two tRNA genes and there appears to be 2 truncated ORFs between them. The remaining genes in the spacer region include *bb0422* (a DNA-3-methyladenine glycosylase) and *bb0421* (a haloacid dehalogenase-like hydrolase). The tandem 23S-5S operon, a phenomenon restricted to Lyme disease *Borrelia* species, is 3 kb downstream from the 16S gene.

In general, this unusual rRNA arrangement appears to be conserved across Lyme disease species (1, 94, 95, 98, 99). Recent sequences of other Lyme disease *Borrelia* species (*B. valaisiana*, *B. bissettii,* and *B. spielmanii*) show that they also exhibit this

unique operon structure (100). However, one isolate of *B. afzelii* (ACA-1) appears to encode two 16S genes that are 398 nucleotides (nt) apart followed by a 2.8 kb spacer. A single 23S-5S pair is located after this spacer (101). Only one complete *B. burgdorferi* genome (strain 156a) encodes a single 23S-5S rRNA operon following the 16S and spacer region, although this has not been experimentally confirmed by restriction mapping (99). The related relapsing fever *Borrelia* species (*B. hermsii*, *B. turicatae*, and *B. anserina*) encode only a single 23S-5S rRNA operon and the spacer between the 16S rRNA gene and 23S-5S rRNA operon is 1 kb (1, 94). In addition, Lyme disease species *B. japonica* and *B. andersonii* have undergone recent mutational events to their rRNA genes (102). Marconi *et al*. (102) discovered several interesting rRNA gene variations in isolates of these species: absence of one of the tandem 23S-5S rRNA operons, intervening sequences in the 23S rRNA genes that are subsequently spliced out to produce the mature 23S rRNA, and missing 5S rRNA genes.

A null mutation in one of the 23S rRNA genes of *B. burgdorferi* does not affect growth rate, suggesting that the spirochete is able to compensate for loss of one gene, perhaps by regulating transcription of the remaining 23S rRNA gene (103). Growth phase rather than growth rate controls rRNA levels in *B. burgdorferi* (5). A major remaining question is how *B. burgdorferi* compensates for possessing an uneven number of 16S, 23S, and 5S rRNA genes to enable a 1:1:1 stoichiometric ratio in the final ribosomes without wasting resources by overproducing the 23S-5S rRNA transcripts.

Unusual rRNA gene arrangements in other bacteria

Non-canonical rRNA arrangements in bacteria are not without precedence and seem to be a property of bacteria with specific characteristics: host- or environment-restricted organisms, low GC-content, slow growth, and small genome size (93). *B. burgdorferi* exhibits all of these characteristics along with very few pseudogenes, and the few it does contain are restricted to its numerous plasmids (29, 74, 77). The slow growth exhibited by these organisms is thought to be the result of the limited number of rRNA genes (78). Indeed, a slow-growth phenotype was observed for the model organisms *Escherichia coli* and *Bacillus subtilis*, when rRNA operons were deleted so that each mutant possessed only a single rRNA operon (from seven in *E. coli* and ten in *B. subtilis*) (104, 105, 106). Additionally, rRNA operon placement within the bacterial chromosome can also affect growth rate. Nanamiya *et al.* demonstrated that a lower cellular ribosome concentration is observed in *B. subtilis* when the coding distance between the origin of replication and a single rRNA operon is increased (106).

In many host-restricted genera such as *Mycoplasma*, *Rickettsia*, and *Buchnera*, evolution has driven a reduction in genome size, preventing them from surviving outside of their specific host environments but allowing them to thrive in an environment of limited nutrients. As a consequence of genome reduction, rRNA operons are often rearranged, driven by homologous recombination (93). The rRNA operon region is a hot spot for recombination as tRNA genes can serve as recognition sites for mobile genetic elements leading to rRNA gene rearrangement (93, 107, 108). Gene duplications in this region also support recombination (93, 109). A recent survey of 16S rRNA genes from

over 1100 sequenced bacterial genomes of diverse phyla showed that a variety of evolutionary processes have rearranged and altered this conserved gene. Specific examples include tandem duplication of the 16S rRNA gene followed by homologous recombination, inversion of an rRNA operon, transposon insertion, gene deletions and substitutions, degeneration of the anti-SD sequence, and transfer of a 16S rRNA gene to the chromosome from a plasmid (110). The evolutionary forces that shaped the unusual rRNA gene arrangement in *B. burgdorferi* are currently undefined, but it is likely that the rearrangement occurred during genome reduction and host adaptation.

A smaller genome means the organism can survive with a paucity of rRNA genes, although at least one of each must, of course, remain. These evolutionary pressures favor the development of bizarre rRNA arrangements in organisms undergoing active genome reduction (93). There are multiple examples of unique genome rearrangements that have resulted from genome reduction and rRNA recombination. Some of the more notable cases include *Thermoplasma acidophilum*, where all three rRNA genes are separated on the chromosome, *Rickettsia prowazekii, Anaplasma marginale* and *Mycoplasma gallisepticum*, where the 16S rRNA gene is separated from the 23S-5S rRNA operon, similar to *Borrelia*, *Mycoplasma fermentans*, which possesses two copies of the rRNA genes and where the 16S-23S rRNA operons are separated from the 5S genes and the 16S-23S rRNA operons are in an usual tail-to-tail arrangement on the chromosome, and *Mycoplasma hyopneumoniae*, where the 5S rRNA gene is separated from the 16S-23S rRNA operon (111, 112, 113, 114, 115, 116). Among the other genera of the Spirochaetae phylum, all three rRNA genes are separated from one another and gene copy number varies between *Leptospira* serovars (117, 118, 119).

However, none possess the conserved tandem duplication of the 23S-5S rRNA operon as observed in Lyme disease *Borrelia* species (1). Intriguingly, separation of the 16S rRNA gene and 23S-5S rRNA operon is conserved among *Rickettsia* species, suggesting that this genomic architecture, which is also observed among most *Borrelia* species, might be advantageous for host-restricted bacteria (120).

Heterogeneity of bacterial rRNA operons

Expansion of bacterial rRNA genes into multiple operons over time has led to sequence heterogeneity among rRNA operons in *E. coli* and *B. subtilis* (106, 121, 122). Single rRNA operon deletion mutants in both genera do not exhibit a discernible growth phenotype (123, 124). In fact, neither increasing nor decreasing the ribosomal RNA operon copy number by three in *E. coli* caused a change in the amount of rRNA required for maximum growth rate (125, 126). In the case of the gene depletion study, the remaining rRNA operons were transcribed with increased frequency to keep up with the demands of the cell (126). This finding has led to the hypothesis that multiple copies of rRNA operons might be beneficial to the bacterial cell by providing the ability to cope with a variety of environmental stresses, including changing nutritional conditions (127, 128). In accordance with this hypothesis, the structure of the *rrn* operon 5′ regulatory regions and transcription factor binding efficiencies differ between the *rrn* operons in *E. coli* (129). In addition, *rrn* promoters are used differently between nutrient abundant and limiting conditions (130). Furthermore, *B. subtilis rrn* operon promoters respond differentially to a variety of physiological conditions; specifically, only some of the

operons are downregulated in response to starvation conditions (131). Finally, *B. subtilis* single rRNA operon mutants show differences in sporulation, which also suggests a functional significance to the heterogeneous character of the rRNA genes (106). We hypothesize that regulation of the tandem 23S rRNA genes in *B. burgdorferi* contributes to some form of environmental response system, particularly considering the dual-host lifestyle of the spirochete; this would provide a compelling rationale for the strong conservation of the 23S-5S rRNA tandem operon duplication observed in Lyme disease *Borrelia* species.

Bacterial rRNA transcription regulation

Functional ribosomes are, not surprisingly, essential to cell viability and growth. However, the bacterial cell also faces a variety of favorable or unfavorable environmental conditions during growth, and must be able to properly modulate the amount of ribosomes that are produced. rRNAs (as well as tRNAs) account for more than 95% of total cellular RNA and their syntheses consume a majority of the cell's resources (132). As a bacterial cell reaches stationary phase, and nutrients become limited, fewer ribosomes can be advantageous, as the amount of translation needs to be reduced to account for the decrease in free metabolites for biosynthesis. Additionally, the nucleotides of rRNA and amino acids of ribosomal proteins (r-proteins) from unneeded ribosomes can be recycled in order to continue essential, yet low-level, transcription and translation (133).

A recent study with *E. coli* by Piir *et al.* examined the normal course of ribosome degradation during bacterial exponential growth and stationary phase (134). Using a turbidostat to enable a constant rate of growth for *E. coli*, the ribosomes were found to be most stable during exponential growth in an abundance of nutrients. However, as *E. coli* enters stationary phase, more than 50% of the ribosomes produced during exponential growth are degraded, but those that remain are stable for several hours (134). The growth rate of cells was shown using mathematical models to be limited by translational capacity (135). More specifically, the synthesis and amount of free rRNA available for r-protein binding limits r-protein synthesis and growth rate (136, 137, 138, 139). Therefore, for an efficient translation system, during both favorable and unfavorable growth conditions, rRNA transcription must be carefully regulated.

There have been multiple studies on rRNA transcriptional regulation in both *E. coli* and *B. subtilis* that have shown differences in the mechanisms used between the two genera, suggesting that the regulation of the rRNA genes in bacteria differs depending on the needs of the respective organism. However, two small molecule regulators have been described in bacteria that regulate transcription of the rRNA genes: induction is regulated by the concentration of an initiating nucleotide triphosphate (iNTP) and repression by guanosine pentaphosphate or guanosine tetraphosphate (known as (p)ppGpp) (133, 140).

Transcription initiation, in general, depends on the presence of an initiating nucleotide triphosphate (iNTP). The cellular concentration required to stimulate transcription between promoters varies, but appears to be quite high for the rRNA genes (133, 140, 141). This nucleotide varies between bacterial genera, with ATP or GTP serving as the iNTP in *E. coli rrn* promoters (130, 142) and GTP serving as the sole iNTP

in *B. subtilis* (143). Presence of high concentrations of the iNTP in both *E. coli* and *B. subtilis* signify to the promoter that the required phosphate-rich NTPs are available in the cell to power the energy requirements of translation (140, 143). Therefore, transcription will be upregulated.

In addition to iNTP concentration in cells, rRNA promoters are sensitive to another small regulatory molecule, guanosine pentaphosphate or guanosine tetraphosphate (known as (p)ppGpp). This GTP/GDP derivative serves as an alarmone in the cell and downregulates rRNA gene transcription during times of nutrient limitation in a system known as the "stringent response" (144, 145, 146, 147). The enzymes responsible for generating and hydrolyzing (p)ppGpp are known as RelA and SpoT, though these can exist as a chimeric single enzyme known as the RelA-SpoT Homolog (RSH), the latter of which is observed in Firmicutes and *B. burgdorferi* (57, 145, 147, 148, 149, 150).

E. coli rRNA gene transcription from two promoters (P1 and P2) at each *rrn* operon is tightly regulated. P1 is utilized during exponential growth and is downregulated during stationary phase; P2, on the other hand, is a weaker promoter that displays clear responses to amino acid availability (stringent control), rRNA gene dose (feedback control), and changes in growth rate (growth rate-dependent control) (140, 151). This bimodal system allows *E. coli* to fine-tune rRNA transcription during each phase of growth. In addition to the typical σ^{70} core promoter region (with -35/-10 hexamer sequences) in the *E. coli* rRNA promoters, a "discriminator" sequence is present in a GC-rich region downstream from the -10 element (140, 152). Several upstream elements are also present and include the UP element, an AT-rich sequence that binds the C-terminal

domain (CTD) of the RNA polymerase (RNA pol) α subunit and is located near the -35 hexamer. Further upstream are 3 to 5 copies of the Fis (factor for inversion stimulation) transcription factor binding sites. Dimers of the Fis protein also interact with the CTD of the RNA pol α-subunit. Finally, the spacing between the -35/-10 elements is 16 nucleotides instead of the typical 17 nucleotides.

All of these promoter elements provide an approximate 300-fold increase in transcription of the rRNA genes in *E. coli* and help regulate the levels of rRNA through differential expression during growth phase or nutrient availability (i.e., Fis protein expression is increased during high nutrient availability) (reviewed in 133, 140). In *E. coli*, rRNA transcription during the stringent response is directly inhibited by (p)ppGpp. Formation of the RNA pol transcription open complex is blocked when (p)ppGpp binds to the transcription cofactor, DksA, which interacts with RNA pol and the "discriminator" sequence to destabilize transcription at rRNA promoters (145, 146, 152, 153).

While the *E. coli* rRNA promoter region contains many elements for transcriptional regulation, the *B. subtilis* rRNA promoter regions appear to lack some of these key features, including an UP element and Fis-binding sites (143). The mechanism for *B. subtilis* rRNA transcription regulation seems to instead revolve solely around the concentration of GTP/GDP in the cell. As previously discussed, GTP is the iNTP for *B. subtilis* rRNA transcription initiation and synthesis of (p)ppGpp will decrease the available pool of GTP/GDP for both translation and rRNA gene transcription, downregulating rRNA levels. Additionally, direct downregulation of rRNA transcription seems to occur via a binding of (p)ppGpp to RNA pol without the aid of a cofactor (143).

(p)ppGpp also binds to several GTP-binding ribosome associated proteins such as initiation factor 2 (IF2) or Obg, which would also stall translation (148, 154, 155).

In *B. burgdorferi*, the relationship between rRNA transcription and the stringent response is not entirely clear. The 16S rRNA and tandem 23S-5S rRNA operons are transcribed as two separate transcripts (5). *B. burgdorferi* lacks a "discriminator" sequence at the proposed 16S rRNA promoter indicating that rRNA transcription may be more similar to *B. subtilis* than *E. coli* (5, 29, 148). While (p)ppGpp and a RelA-SpoT homolog (RSH, also referred to as Rel_{Bbu}) are present in *B. burgdorferi*, the stringent response is different in the spirochete (5, 55, 56, 57, 156); low levels of glucose and amino acids do not seem to stimulate (p)ppGpp synthesis (56, 156). RSH is sufficient to regulate (p)ppGpp levels in *B. burgdorferi* and enables the organism to successfully transition from exponential growth to stationary phase (57). Levels of 16S and 23S rRNA are also reduced upon entry into stationary phase, as expected (5).

Co-transcriptional rRNA processing and ribosome assembly in bacteria

In most bacterial species, the three rRNA genes are encoded in a single operon in the following order: 16S-23S-5S with minimal intergenic sequences. There are usually several tRNA genes encoded between rRNA genes, but their number and location varies among operons. Once rRNA transcription has been initiated, a single long transcript containing the 16S-23S-5S precursor rRNA is produced and subsequently processed by ribonucleases to separate each rRNA subunit. The endoribonuclease, ribonuclease III (RNase III) is responsible for initial processing of the 16S and 23S rRNA transcripts prior

to ribosome assembly (7, 157, 158). Endonucleolytic processing occurs co-transcriptionally, first separating the pre-16S transcript from the pre-23S-5S transcript and then separating the pre-23S transcript from the pre-5S as the entire polycistronic RNA is transcribed (159). As the ribosomal RNAs are generated, a stem joining the complementary 5′ and 3′ ends of each rRNA forms, creating double-stranded substrates for RNase III (160). RNase III processes both strands simultaneously, releasing each rRNA. Exonucleases (and a few endonucleases) then further process the remaining stem to create the mature rRNAs (reviewed in 161). Unlike pre-16S and pre-23S rRNAs, pre-5S rRNA is initially processed by other endonucleases (RNase E in *E. coli* and RNase M5 in *B. subtilis; B. burgdorferi* possesses a homolog of the latter enzyme) (162, 163). This enzymatic processing has been well characterized in both *E. coli* and *B. subtilis*, which have similar mechanisms but require different enzymes for post-RNase III processing (reviewed in 161). After the initial endonucleolytic processing, each rRNA continues to fold into its native conformation, aided by the ribosomal proteins that assemble on the nascent RNA. Exonucleases have better access to their substrates in this partially folded environment, allowing rRNA processing to transpire in an ordered manner (164, 165).

There are a variety of covalent chemical modifications made to both the rRNA and r-proteins as the ribosome assembles (reviewed in 166). Ribosome assembly is sequential, with distinct sets of proteins binding to each subunit in a specific temporal manner. The 16S rRNA sequentially binds 21 ribosomal proteins (the “S” proteins) during maturation and assembles into the 30S ribosomal subunit. The 23S rRNA and 5S rRNA assemble into the 50S subunit. Thirty-three ribosomal proteins (the “L” proteins)

associate with the 50S subunit in a progressive manner similar to the 30S rRNA subunit. Following maturation of each ribosome component, the 50S and 30S ribosomal subunits assemble into the 70S ribosome, which is part of translational initiation and requires a variety of initiation factors, the initiator $tRNA^{met}$ and the mRNA (reviewed in 166).

Ribonucleolytic processing of the rRNAs

16S rRNA

RNase III processing in *E. coli* initially leaves extra nucleotides on both the 5′ (115 nt) and 3′ (33 nt) ends of the pre-16S rRNA transcript; single-stranded endoribonucleases E and G are responsible for the subsequent trimming of the 16S rRNA 5′ end (167, 168). RNase G rapidly processes the 16S rRNA 5′ end after RNase E removes the first 66 nucleotides (167). In *B. subtilis*, the processing pathway is slightly different, as no homologs of RNases E or G exist in this organism (169, 170). Instead, RNase J1, an essential enzyme with broad activities within *B. subtilis* (mRNA processing and turnover), fulfills the role of the absent RNases E and G (171, 172, 173, 174). RNase J1 is an endoribonuclease that also exhibits 5′-to-3′ exonuclease activity, though it is currently the subject of debate whether the primary activity in processing the 16S rRNA is exonucleolytic or endonucleolytic (172). RNase J1 processes the 16S rRNA transcript following its assembly with proteins into the 30S subunit (171). Both RNase E and RNase J process the 5′ end of all three rRNA transcripts in *Mycobacterium smegmatis* (175).

Maturation of the 16S rRNA 3′ end in bacteria has only recently been characterized and appears to be the same in both *E. coli* and *B. subtilis*. A novel but highly conserved single-stranded endoribonuclease, YbeY, is required for 16S rRNA 3′ end maturation (176, 177). Translation is impaired in the absence of YbeY due to the production of defective 30S ribosomal subunits (178). Following RNase III processing of the 16S rRNA transcript, YbeY cleaves near the mature 3′ end of the rRNA while it is in the context of the assembled 30S subunit (176). This specificity has been predicted to be guided by a small subunit ribosomal protein or the GTPase Era, which may expose the 3′ end (176, 179). Additionally, the exonucleases RNase R and PNPase, along with YbeY, are likely candidates for the final 16S rRNA 3′ end processing (176, 177). YbeY has a role in 70S subunit quality control by initiating degradation of the ribosomal RNA after inducing multiple nicks in the single-stranded rRNA that are then unwound by the RNase R helicase domain (176). YbeY also aids in transcription antitermination of the rRNA precursor substrate (180). In *Pseudomonas syringae,* a single ribonuclease, RNase R, is capable of the complete 3′ end processing of 16S rRNA (181).

23S rRNA

After separation of the individual pre-23S and pre-5S rRNAs from the larger transcript, each rRNA is further processed by nucleases before associating with one another and thirty-three large subunit ribosome proteins to form the 50S ribosomal subunit. RNase III cleavage of the 23S rRNA leaves 3 to 7 nt on the 5′ end and 7 nt on the 3′ end in *E. coli* and 64 nt on the 5′ end and 32 nt on the 3′ end in *B. subtilis* that must be further trimmed by exo- and endonucleases (182, 183). In *E. coli*, RNase G finishes

the 5′ end and RNase T and RNase PH generate the mature 3′ terminus (165, 184, 185). Exonuclease processing proceeds in an ordered manner, with maturation of the 3′ end of the 23S rRNA preceding maturation of the 5′ end in *E. coli* (186). *B. subtilis* utilizes a single enzyme, Mini-III, which is an endonuclease composed of an RNase III-like catalytic domain, to process both the 5′ and 3′ ends. In spite of the similarity of this enzyme to RNase III, no overlap in cleavage sites is observed as Mini-III binds different RNA sequences (183). As with the secondary processing enzymes of the 16S rRNA transcript, Mini-III initiates 23S rRNA cleavage more efficiently in the context of the assembled 50S subunit (187). Post-RNase III processing of the pre-23S rRNA still transpires in the absence of Mini-III. The combined activities of RNases J1 (5′-to-3′ exoribonuclease activity), RNase PH (3′-to-5′ exoribonuclease activity), and YhaM (3′-to-5′ exoribonuclease activity) are capable of generating a mature 23S rRNA in the absence of Mini-III in *B. subtilis* (188).

5S rRNA

Pre-5S rRNA is initially separated from the primary transcript by RNase III cleavage of the 23S rRNA 3′ end (189). Following this cleavage event and initial assembly of the 5S rRNA into the 50S subunit, RNase E in *E. coli* and RNase M5 in *B. subtilis* cleave both the 5′ and 3′ ends near the base of the conserved 5S rRNA double-stranded stem structure (189, 190, 191). *E. coli* also requires RNase T cleavage of the 5S rRNA 3′ end to remove three remaining nucleotides from the mature transcript (164). The activity of RNase M5 is similar to that of Mini-III (183). *B. burgdorferi* possesses an unannotated RNase M5 homolog and no detectable RNase E/G homologs, so this

organism likely follows a more *Bacillus*-like pathway for rRNA processing. A more thorough discussion of the ribonucleases of *B. burgdorferi* and a potential model for ribonucleolytic processing in *B. burgdorferi* are discussed in a later section.

Effect of unprocessed 16S, 23S, and 5S rRNA ends on ribosome assembly

As discussed above, RNase G (encoded by the *rng* gene) is important in generation of the mature 5′ end of the 16S and 23S rRNA transcripts (167, 168, 184). In a Δ*rng* background, 66 nt remain on the 5′ end of the pre-16S rRNA. However, this does not affect ribosome assembly (192, 193). Gutgsell and Jain (193) postulate that an RNase G-independent mechanism enables generation of a mature 5′ end in some of the 16S rRNA transcripts, allowing normal ribosome formation for a subset of the population, thus diluting the effect of the *rng* mutation. However, translational fidelity is lost in an *E. coli rng* mutant (192). The effect of the 5′ end of the 23S rRNA on ribosome assembly was not examined in this study. While the absence of RNase G can leave 77 nt on the 5′ end on the 23S rRNA, RNase III can compensate for this defect by cleaving all but 3 or 7 nt on the 5′ end (182, 184). As discussed above, YbeY processing of the 16S rRNA 3′ end is essential in bacteria, so mutants cannot be generated and no precursor sequences can be studied (176, 177).

In both RNase PH and RNase II mutants, ribosome assembly was much slower than in wild-type *E. coli*, while the RNase T mutant showed a much more minor growth phenotype (193). From these data, Gutgsell and Jain (193) conclude that ribosome assembly is most affected by defects in early processing events, that a 2 nt or less

precursor extension on the 23S rRNA is tolerated by the ribosome, and that these precursor sequences might serve as a mechanism of quality control by slowing ribosome assembly in strains with defective 23S rRNA processing. Gutgsell and Jain (193) further propose a model for the delayed ribosome assembly in mutants with 2 nt or longer extensions on the 23S rRNA 3′ end. As the 3′ end of the 23S rRNA protrudes outside of the ribosome, they postulated that this extension does not affect activity of the ribosome. However, as ribosome assembly is a sequential and ordered process, they hypothesize that a 23S rRNA 3′ end extension might cause a steric clash that slows down or inhibits assembly of the mature ribosome. Therefore, in addition to ribonucleolytic processing, rRNA precursor sequences might also promote ordered ribosome assembly as well as quality control. In contrast to this finding, extra nucleotides on the 5′ and 3′ end of the 5S rRNA transcript in both *E. coli* and *B. subtilis* appear to have no effect on the assembly of ribosomes, as fully functional ribosomes are made in the absence of RNase T and RNase M5 (164, 191). This suggests that the processing of the 16S and 23S rRNAs is more important for the generation of functional ribosomes than the processing of 5S rRNA.

Endoribonuclease III – enzyme activity and characteristics

While *B. burgdorferi* possesses a paucity of genes for endoribonucleases compared to other bacteria (see below), it does possess a homolog of RNase III from both *B. subtilis* (44% identity) and *E. coli* (35% identity). RNase III, encoded by the *rnc* gene, specifically recognizes and cleaves double-stranded RNA (194). Homologs exist in even the smallest bacterial genomes, including *Mycoplasma* species (195). RNase III is

conserved across all bacterial phyla and the homologs Dicer and Drosha, present in eukaryotic cells, are responsible for miRNA processing (196, 197, 198, 199). The enzyme operates as a homodimer of ~25-kDa subunits that primarily interact through hydrophobic regions (200). In general, RNase III contains an N-terminal catalytic domain with endonuclease activity (defined by a conserved signature motif EGLEFLGD$^{S}/_{A}$) and a C-terminal domain with four RNA-binding motifs (195, 199, 200, 201). Two of these motifs recognize sequences specific for their cognate RNAs (RNA-binding motifs 3 and 4; RBM3 and RBM4), whereas the other two bind RNA less specifically by recognizing RNA structural features (RBM1 and RBM2) (201, 202, 203). The endonuclease domain rotates upon binding to double-stranded RNA via a linker region that joins it to the RNA-binding domains. Amino acid substitutions of prolines in the linker region still allow binding of double-stranded RNA, but cleavage activity is abolished, likely due to the lack of the proper conformational change (204).

Substrate recognition relies on the absence of anti-determinant nucleotide pairs (specific bases that cause improper alignment of the active site and inhibit cleavage) in the double-stranded stem near the cleavage site (termed the 'proximal' and 'distal' boxes) as well as the presence of appropriate bases at the scissile site (205, 206, 207, 208, 209). These features are present in the *B. burgdorferi* 23S rRNA stem. Crystallographic studies suggest that seven hydrogen bonds per subunit contact the 2′-hydroxyl groups of the substrate, with two loops inserted into the minor grooves. RBM1 and RBM4 interact with the proximal and distal boxes, respectively (201, 205). RBM3 interacts with nucleotides at the cleavage site and may stabilize recognition/binding (201). Gan *et al*. (201) proposed the following model for formation of the enzyme-substrate complex based on

their crystallographic data: the non-specific RBMs bind a double-stranded RNA molecule, which is brought into the endonuclease domains where it contacts the specific RBMs and is precisely situated for cleavage. Catalysis is Mg^{2+}-dependent, involving coordination of two Mg^{2+} ions per catalytic site with specific acidic residues and water molecules. This arrangement instigates a phosphoryl transfer mechanism that ends in hydrolysis of one phosphodiester bond from each strand of RNA (201, 208, 210, 211). This requires both monomers for double-stranded processing, with two residues from RBM3 of one subunit (selecting the scissile bond) coordinating with two aspartic acid and two glutamic acid residues from the second subunit (performing the cleavage reaction) (201, 210). Cleavage of phosphodiester bonds creates a two-nucleotide overhang from one-full turn of RNA double helix, an 11 bp nucleic acid stretch that fits into the catalytic valley (212).

Remarkably, while RNase III performs an essential function in the bacterial cell, it is not always required for growth as alternative RNA processing pathways are available in some bacteria. In *E. coli* and *Staphylococcus aureus*, but not *B. subtilis, rnc* mutants are able to grow at a reduced rate. The *rnc* growth defect is thought to be the result of aberrant ribosomes (7, 157, 213, 214, 215, 216). In many cases, the 23S-5S rRNAs are not properly separated in these null mutants, leading to the appearance of an unprocessed 30S rRNA species (157, 195, 213, 214, 215). RNase III is highly conserved and homologs from different organisms can often, but not always, functionally substitute for each other and genetically complement *rnc* mutants (217). For example, RNase III homologs from *Rhodobacter capsulatus* and *B. subtilis* are capable of cleaving RNA substrates from *E. coli* at the expected site. However, *E. coli* RNase III cannot process

substrates from *R. capsulatus* and *B. subtilis*, indicating that species-specific factors play a role in proper RNA processing (218, 219, 220). RNase III is autoregulated by processing a hairpin stem-loop structure on the 5′ end of the *rnc* mRNA, which reduces levels of the transcript in both *E. coli* and *S. coelicolor* (221, 222, 223). In *rnc* point mutants, more RNase III is produced, as this control mechanism is absent and the hairpin stem-loop stabilizes the transcript (221, 222, 223).

The constellation of bacterial ribonucleases

The standard complement of endo- and exoribonucleases from *B. subtilis* and *E. coli* were subjected to a BLAST screen against the *B. burgdorferi* genome sequence. Tables 1 and 2 show the standard complement of ribonucleases in each model organism, their function, and whether an annotated or unannotated homolog exists in *B. burgdorferi*.

Table 1. Endoribonucleases

*Indicates a *B. burgdorferi* endoribonuclease homolog identified in this work

Ribonuclease	Present in *B. burgdorferi*	Annotated in *B. burgdorferi*	Model organism	Primary Processing Role	References
RNase III	**Yes**	**Yes**	*E. coli* *B. subtilis*	Initial 16S and 23S rRNA processing and global mRNA processing	(161, 173, 196, 206)
RNase P	**Yes**	**Yes**	*E. coli* *B. subtilis*	5′ pre-tRNA processing	(224)
RNase Z	**Yes**	**Yes**	*E. coli* *B. subtilis*	3′ end pre-tRNA processing	(224)
YbeY	**Yes**	**Yes**	*E. coli* *B. subtilis*	3′ end 16S rRNA processing; ribosome quality control; rRNA	(176, 177, 180)

				transcript antitermination	
RNase Y	**Yes**	**No***	*B. subtilis*	riboswitch processing and global mRNA processing	(225)
RNase M5	**Yes**	**No***	*B. subtilis*	5S rRNA double-stranded processing	(161)
Ribonuclease	**Present in *B. burgdorferi***	**Annotated in *B. burgdorferi***	**Model organism**	**Primary Processing Role**	**References**
RNase J1/J2	No	N/A	*B. subtilis*	5′ end 16S rRNA processing and global mRNA processing and decay	(225)
RNase E/G RNase E/G	No No	N/A N/A	*E. coli* *E. coli*	16S, 23S, and 5S rRNA and tRNA processing; mRNA and non-coding RNA processing and decay	(196, 226, 227)
MazF/EndoA	No	N/A	*E. coli* *B. subtilis*	Decay of mRNA during stress; toxin with RNase activity	(228)
ChpBK	No	N/A	*E. coli*	Decay of mRNA during stress; toxin with RNase activity	(170)
YoeB	No	N/A	*E. coli*	Decay of mRNA during stress; toxin with RNase activity	(170)
RNase I	No	N/A	*E. coli*	Nonspecific activity; Periplasmic RNase; role in scavenging?	(206)
RNase M	No	N/A	*E. coli*	Altered form of RNase I	(229)
RNase LS	No	N/A	*E. coli*	Cleavage of T4 bacteriophage mRNA; *E. coli* mRNA decay	(230, 231)
RNase HI	No	N/A	*E. coli*	Processing of RNA in RNA-DNA duplexes	(206, 232)
RNase HII	Yes	Yes	*E. coli* *B. subtilis*	Processing of RNA in RNA-DNA duplexes	(232)
RNase HIII	No	N/A	*B. subtilis*	Processing of RNA in RNA-	(232)

				DNA duplexes	
RNase Bsn	No	N/A	*B. subtilis*	Extracellular secreted enzyme	(233)
YhcR	No	N/A	*B. subtilis*	Sugar-nonspecific nuclease; located in the cell wall; Ca^{2+} activated	(234)

Table 2. Exoribonucleases

*Indicates a *B. burgdorferi* exoribonuclease homolog identified in this work

Ribonuclease	**Present in *B. burgdorferi***	**Annotated in *B. burgdorferi***	**Model organism**	**Primary Processing Role**	**References**
PNPase	Yes	Yes	*E. coli* *B. subtilis*	decay of single-stranded RNA; 3′ to 5′ activity	(196, 235)
RNase PH	No$^{\Delta}$	N/A	*E. coli* *B. subtilis*	3′ end of tRNA processing	(196)
RNase R	No	N/A	*E. coli* *B. subtilis*	rRNA and mRNA decay; 3′ to 5′ activity	(196, 235)
RNase II	No	N/A	*E. coli*	decay of RNAs (unstructured); 3′ tRNA processing; 3′ to 5′ activity	(196, 235)
RNase T	No	N/A	*E. coli*	23S and 5S 3′ end processing; tRNA processing; 3′ to 5′ activity	(161, 206)
RNase D	No	N/A	*E. coli*	tRNA 3′ end processing; 3′ to 5′ activity	(206)
OligoRNase	No	N/A	*E. coli*	Terminal steps of mRNA decay	(236)
YhaM	No	N/A	*B. subtilis*	Role unclear; 3′ to 5′ activity	(237)
RNase J1/J2	No	N/A	*B. subtilis*	decay of RNAs; 5′ to 3′ activity	(225)

$^{\Delta}$BLAST search shows high homology of this enzyme to PNPase from *B. burgdorferi*

Complement of ribonucleases in *B. burgdorferi*

In comparison with the endo- and exoribonuclease complement of model organisms *E. coli* and *B. subtilis*, the number of ribonucleases in *B. burgdorferi* is limited

(see Tables 1 and 2 above). While *B. burgdorferi* possesses homologs to the highly conserved and essential endoribonucleases RNases III, P, Z, HII, and YbeY from *E. coli* and *B. subtilis*, as well as RNases Y and M5 from *B. subtilis*, it lacks homologs to RNases E or G and J1 or J2. The lack of RNases E and G is not surprising; RNase Y has been determined to serve the same purpose in *B. subtilis* as RNase E in *E. coli* and both enzymes are membrane-bound and form degradosome complexes with a variety of other enzymes (238). However, RNases J1/J2 perform central roles in *B. subtilis* (225). The lack of a *B. burgdorferi* homolog to RNases J1/J2 or similar enzymes in *E. coli* is puzzling.

In terms of exoribonuclease homologs in *B. burgdorferi*, the suite is even more limited. PNPase is the only enzyme that is a clearly discernible exoribonuclease in *B. burgdorferi*. However, performing a BLAST alignment with *B. subtilis* RNase PH identified *B. burgdorferi* PNPase with a 24% identity, so perhaps this enzyme performs a dual role in *B. burgdorferi*. The two enzymes are derived from the same family and have similar functions; additionally, PNPase contains an RNase PH domain (235). The only other exoribonuclease conserved between *E. coli* and *B. subtilis* is RNase R, which is an exonuclease that is efficient in cleaving structured RNAs (235). Perhaps *B. burgdorferi* PNPase performs the role of this exonuclease as well, since both exhibit 3′ to 5′ activity.

We propose that *B. burgdorferi* either possesses novel exoribonucleases that have yet to be identified or the suite of ribonucleases in *B. burgdorferi* serve more than the standard roles. From the discernible set of ribonucleases in *B. burgdorferi*, we predict that RNase III, YbeY, RNase M5, and PNPase are all involved in rRNA processing. The many roles of RNase Y are still in the process of being defined, but it has so far been

linked to riboswitch degradation and global mRNA turnover (239, 240, 241, 242, 243, 244, 245, 246). It is possible that this enzyme is also involved in rRNA processing in *B. burgdorferi*, performing a role similar to that observed for RNase E (161). Perhaps PNPase association in a degradosome-like complex with RNase Y and other enzymes (238) might allow for greater substrate tropism in *B. burgdorferi*.

Hypothesis and significance

RNase III is a crucial enzyme in most bacterial cells. *B. burgdorferi* encodes an obvious homolog of this enzyme with extensive homology to model organisms leading us to predict that it would have similar important functions in rRNA processing and selected mRNA processing. Our data support this hypothesis, as the *B. burgdorferi rnc* gene is capable of heterologously complementing a *B. subtilis rncS* mutant. We generated an *rnc* null mutant in order to take a genetic approach toward defining RNase III function in *B. burgdorferi*, specifically initial endonucleolytic processing of the pre-16S and pre-23S rRNA transcripts. We hypothesized that *B. burgdorferi* RNase III processes the pre-16S and pre-23S rRNA transcripts in a canonical fashion in spite of the unusual rRNA gene arrangement. While our results suggest that RNase III is responsible for processing the pre-23S rRNA transcript as in other bacteria, it is only essential for processing the 3′ end of the 16S rRNA in *B. burgdorferi*; the 5′ transcript end appears to be generated through a novel, undefined mechanism. We expect this finding reflects the unusual arrangement of the orphaned 16S rRNA gene as part of a larger operon. RNase III does not process the pre-5S rRNA transcript in *B. burgdorferi*, as expected.

As noted above, there are only a few sequenced bacterial genomes that contain unusual rRNA arrangements. The Lyme disease *Borrelia* species (*B. burgdorferi*, *B. afzelii*, *B. garinii,* and others) appear to be the only bacteria with a tandem chromosomal duplication of their 23S-5S rRNA operon. The tandem duplication of the 23S-5S rRNA operons creates a potential imbalance in the ratio of rRNAs if transcription is not coordinated with the unlinked 16S rRNA gene. We hypothesized that transcription of the 16S and 23S genes was differentially regulated in *B. burgdorferi* to maintain a 1:1:1 ratio of the three rRNAs in the cell. To explore rRNA transcription from the tandem 23S rRNA genes in *B. burgdorferi*, we created null mutants for each of the 23S-5S genes, leaving one complete copy of the three rRNA genes in each strain. Surprisingly, our data demonstrate that transcripts from both 23S rRNA gene copies are transcribed and incorporated into ribosomes. Additionally, a single mutation in the first 23S rRNA gene exhibits definite growth and viability phenotypes both *in vitro* and *in vivo*. Finally, the ratio of 16S:23S:5S rRNAs is not equimolar in *B. burgdorferi*, which is unexpected. However, each 23S-5S operon is predicted to have a strong, identical RpoD promoter (σ^{70} promoter), providing a model for this unbalanced transcription.

In this dissertation, we present the first characterization of an RNase III enzyme from a spirochete. We also expand upon the limited knowledge of rRNA gene regulation in *B. burgdorferi*, including insight into tandem 23S-5S gene duplication, a biological feature unique to Lyme disease *Borrelia* species. Dissecting the mechanism by which ribosomes are generated and the role of ribonuclease III in *B. burgdorferi* is important because the spirochete displays unique biological solutions for other molecular processes and the data presented in this work may offer further insight into ribosome generation in

other parasitic bacteria that have undergone genome reduction and rRNA gene rearrangement.

Chapter 2

Materials and Methods

Bacterial strains and culture conditions. Low-passage *B. burgdorferi* strains B31-A3 (247), B31-5A4 (89) and 297 (BbAH130) (67), the *rnc* mutants, and the *rrlA* and *rrlB* mutants were cultivated at 34°C in Barbour-Stoenner-Kelly II (BSK II) liquid medium containing 6% rabbit serum (RS) (79) without gelatin (248). Cell density was assayed as previously described by enumeration using a Petroff-Hausser counting chamber (2, 3). Purified ribosomes were harvested from a high passage, noninfectious *B. burgdorferi* clone, B31-A (249).

B. subtilis strain BE589 and the *rncS* mutant BE600 (7), a generous gift from Dr. David Bechhofer (Mount Sinai School of Medicine), were grown at 30°C or 37°C in lysogeny broth (LB) (250) or Spizizen's minimal medium (SpC and SpII) (251, 252).

Escherichia coli Rosetta^{TM} (DE3) from EMD4Biosciences was grown at 37°C in LB medium containing 50 μg ml^{-1} ampicillin and 68 μg ml^{-1} chloramphenicol and used to overexpress recombinant *B. burgdorferi* RNase III. *E. coli* TOP10F′ and DH5α were grown at 37°C in LB medium containing 50 μg ml^{-1} kanamycin and used for cloning.

Table 3: Oligonucleotides used in this study

Name	Sequence (5′-3′)
BB705 U1260F	TTTAAAGGTTGAAAATGAAG
BB705 92R+AatII+AgeI	ACCGGTCAAGACGTCTAAAGTCAATGCTCAAATT
BB705 617F+AatII	GACGTCTTTTTTGTGTGGAACTTTAT
BB705 D1945R+AgeI	ACCGGTATGAATCTAGGGAAAAACA
rnc 1F+NdeI	CATAGAAAAAAAAATCTTCTGA
rnc 738R	TTAAAGGTTAATGTTTTCCA

pflgB5′+AgeI	ACCGGTACCCGAGCTTCAAGGAA
rrs 107R	TTACTCACCCGTTCGCCACTGAATGTA
rrl 76R	GCTTTTCGCAGCTTACCACGACCTTC
rrl 198R	TTAGATGGTTCACTTCCCCTGGTATCGC
rrf 88R	CGAACTCGCAGTACCATCAGCGAATAAG
rrf 49R	TGTGTTCGGAATGATAACAGGTGTTTCCTC
rrf 51R	TCTGTGTTCGGAATGATAACAGGTGTTTCC
rrf 112R	CCCTGGCAATAACCTACTCTCCCGC
rrs 1365F	TGAATACGTTCTCGGGCCTTGTACACA
rrl 2770F	ACGTTCGGAAAGGATAACCGCTGAAAG
rrf 60F	CTTATTCGCTGATGGTACTGCGAGTTCG
rrf 8f	GGTTAAAGAAAAGAGGAAAC
rrl 76R	GCTTTTCGCAGCTTACCACGACCTTC
bb702 351F	ATTTTTACCAAGTAGTGCAG
bb703 48F	GCGGAGTATAAATATGAGAA
bb703 145R	ATCCACATTTTAAACAAATC
bb704 46F	GAGCAACTTGATAAAAAAGA
bb704 177R	CTCTGGAATCTTATCATCAA
rnc 143R	AACTCATTAGAATACGACGA
rnc 1F+ClaI	ATCGATGAAAAAAAAATCTTCTGA
rnc 738R+XbaI	TCTAGATTAAAGGTTAATGTTTTCCA
rnc 1F+NdeI	CATATGAAAAAAAAATCTTCTGA
rnc 735R+SapI	GCTCTTCCGCAAAGGTTAATGTTTTCCATAG
T7 prom	TAATACGACTCACTATAG
23S stem+T7	AGGAAGACAAAAATATGGCCAAAGTTGCCTTT GACCATATTTTTATCTTCCATCCTATAGTGAGT CGTATTA
rrlB U884F	TTAAAAATATAAGGAGCCAA
rrlB U29R+AatII+AgeI	ACCGGTTATGACGTCAATTTGTTTATGCAACAT A
rrl 3043F+AatII	GACGTCGAGAGTAGGTTATTGCCAG
rrlB D391R+AgeI	ACCGGTCAGCACTTCTATGCTTTAAT
rrlA U882F	ACTCTGTAAGTGTAAAGGCA
rrlA U19R+AatII+AgeI	ACCGGTTTCGACGTCTATTTTGCCAATTTATTT
rrlA D3975R+AgeI	ACCGGTTCCCTGTGAATTAATAAAA
bb0427 687F	AGAATATCAAATTGGCAAAC
bb0426 90R	CAAGAAATTTCAAAACCTCA
bb0426 437F	TGTGGATTAAGTTTAAAGGA
bb0425 29R	CTTAACTCTTCCCTTCTCTC
bb0425 10F	GAGAGAAGGGAAGAGTTAAG
rrs 146R	AATAGTTATCCCCATCTCAT
rrl U30F	TGGCAAAATAGAGATGGAAG
rrl 654F	TGCGAGTTATCATGTCTAGC
rrl 1299F	AAGTTTGATGGAGGTATCAG
rrl 958R	CCCTAGCTCAATTAGTGCTC

rrl 1606R	CACTCATCATCACATCTTAGC
rrl 2234R	AACAAGGGTGGTATTTCAAG
rrl 2676F	ATTTGAGAGGAGCTATCTTT
rrl 2814F	CCTCAAGATGAGATATCCTT
rrf 60F	CTTATTCGCTGATGGTACTGCGAGTTCG
rrf 70R	AGCGAATAAGAGCTTAACTT
rrfB D276R	TCTATTTTGCCAATTTATTT
rrfA D196R	TCCCTTATTAAAAACAACAG
rrl 1983F	GCGAAATTCCTTGTCGGGTAA
rrl 2047R	TGAGACAGCGTCCAAATCGTT
rrs 1066F	TGCTGTGAGGTGTTGGGTTAAG
rrs 1139R	CCCCACCATTACATGCTGGTA
16S rRNA probe	CCCGCAACGAGCGCAACCC
23S rRNA probe	TTCCGACCCGCACGAATGGTG
rrl 1071R	TGTTGGTCTGGGTTGTTT
rrl 2903R	TTAGTCAGCTTAATATATTGCT
flaB 278F	TGGCAGTTCAATCAGGTAACG
flaB 551R+T7	TAATACGACTCACTATAGGCTTCATCTTGGTTT GCTCC
flaB 423F	TTCTCAAAATGTAAGAACAGCTGAAGA
flaB 542R	TGGTTTGTCCAACATGAACTC
BBA60-5’ (lp54)	ATGAGCAAAAAAGTAATTTTAATAT
BBA60-3’ (lp54)	CACTAATTCTTTTTGAATTACTAAT
BBB03-5’ (cp26)	ATGCCTCCAAAAGTGAAGATAAAAA
BBB03-3’ (cp26)	TAGCTTATAATTAAAAATTATTGAT
BBC10-5’ (cp9)	ATGCAAAAAATAAACATAGCTAAAT
BBC10-3’ (cp9)	ATCTTCTTCAAGATATTTTATTATA
BBD11-5’ (lp17)	GTGTATACTGACCCAAGGTCAATTA
BBD11-3’ (lp17)	CAATAATGTGATATTTTTAAGAAAT
BBE16-5’ (lp25)	TTGCTGCCATTTCTCACTTGGTAA
BBE16-3’ (lp25)	ATAAAAGCGACAGGTTATCGTGCAG
BBG13-5’ (lp28-2)	ATGGCGCTGATTACATTAATTGTCG
BBG13-3’ (lp28-2)	AATCTTGAAGAACCTTGCATCTTTA
BBH18-5’ (lp28-3)	CTGAAAATGAAGGAGAAGCGGGTGG
BBH18-3’ (lp28-3)	TAGGCTAATACCAATTCGTACAAAT
BBI28-5’ (lp28-4)	ATGAAATGCCATATAATTGCAACTA
BBI28-3’ (lp28-4)	AATCCGACAGATCTGGTTTGTCCAG
BBK12-5’ (lp36)	TTCTTATCCCTGACTTTCACTTTTGAGG
BBK12-3’ (lp36)	TCCTTTACTTCTATGTTTTTACTTTCCTTGGT
BBT03-5’ (lp5)	ATGAATGGAATAATTAACGATACAC
BBT03-3’ (lp5)	AATATTAGGATGAAGATTATAAATT
BBU06-5’ (lp21)	TGTGGTTGCTAAAACCCAAGCGT
BBU06-3’ (lp21)	TTGTTTCTAATTGCTCTGAATTGCATCC
Bb PC *flaB*-5’	GATTATCAATCATAATACATCAGC
Bb PC *flaB*-3’	TCTAAGCAATGACAAACATATTGG

297-PC-*vlsE* (+1)(lp28-1)	GGAGCAATATTTGTTTTTGTTAATTG
297-PC-*vlsE* (-1)(lp28-1)	CTAATTTCTGCTATAGCACCTTGTAC
297-PC-p21-5' (cp18-2)	TGAGCAAAGTAGTGGTGAGAT
297-PC-p21-3' (cp18-2)	CTTCTGCTTTTCCTGTTGATAC
297-*mlp7*orfCspec(cp32-1)	GGCCCATCCAATTTTATGTAAATTTG
297-"R"orf3specRC(cp32-1)	GCTCCCTTCTAATACTTTTCTATAA
297-PC-*elpA*2-5'(cp18-1)	ATGCTACAGTATTAAAACCCGAG
297-PC-*elpA*2-3'(cp18-1)	GCCTGGTCTTGGAGAATAATG
297-PC-2.10-5' (cp32-4)	TGCAAGAATTATGCAAGTGGTGAAG
297-PC-2.10-3' (cp32-4)	AAACACCTTGAGCCACTTGCTC
297-"P"-orf3specR+C (cp32-5)	AGATTTCAAGCGCTCCTTCAACAAA
297-"P"-mlp5 orfC spec (cp32-5)	GCCTTATAAGGAACATAGGTTAAAGG
297-orfC-mlp2	GGTGCTTTAGACACAAGAGATGTG
297-mlp2orf3spec R+C	GAACAAATTTCAGATTTAACATTTATCG
297-*mlp10*orfCspec(cp32-2)	CAAGCGAGTTTATTCCCCTTAAA
297-"L"orf3specRC(cp32-2)	ATTCTAATATTGTCCACTTTATGAAAT
297-PC-*ospF*-5'(cp32-3)	CAGAACAAAATGTAAAAAAAACAGAGCAAG
297-PC-*ospF*-3'(cp32-3)	CCCAAACTATTAGCACACTGCCAAG
297-orfC-mlp4spec	GTCAAATTTAAGCTGTTTTAGCAGTG
297mlporf3specR+C	TATTTACTAATGTATTTTTCAATTTTTCA

Heterologous complementation of a *B. subtilis rnc* mutant. A *B. subtilis rncS* null mutant carrying pBSR40, a temperature-sensitive plasmid that replicates at 30°C (7), was *trans*-complemented with the *B. burgdorferi rnc* gene. We transformed pBK36-*Bbrnc*, the *B. burgdorferi rnc* gene fused to the isopropyl-β-D-thiogalactoside (IPTG)-inducible *spac* promoter on the shuttle vector pBK36, into *B. subtilis* as previously described (252). Briefly, competent *B. subtilis* cells were obtained by growth in SpC minimal medium to stationary phase at 37°C with vigorous agitation. The cells were inoculated into pre-warmed SpII minimal medium containing 0.1M $CaCl_2$ and incubated at 37°C for an additional 90 min. Following incubation, cells were centrifuged and the supernatant (containing competency factors) was removed and saved. The pellet was resuspended in a

smaller volume of the saved supernatant and mixed with 10% glycerol. Competent cells were rapidly frozen in liquid nitrogen and stored at -80°C for up to 3 months.

To transform competent *B. subtilis*, cells were quickly thawed in a 37°C water bath. Once thawed, one volume of SpII + EGTA (without $CaCl_2$) minimal medium was added and gently mixed. Approximately 16 μg of pBK36-*Bbrnc* was added to the tube. Cells were incubated for 20 min at 37°C in a shaking incubator. Following incubation, cells were diluted 10^{-3} and 10^{-4} and plated on LB media with or without 5 μg ml^{-1} neomycin. All clones tested contained both the *B. subtilis rncS* plasmid (pBSR40) and the *B. burgdorferi rnc* plasmid (pBK36-*Bbrnc*). To cure the pBSR40 plasmid, transformants were shifted to the non-permissive temperature of 45°C (7, 252) and incubated for 8 h. Successful *B. subtilis* transformants that retained the pBK36-*Bbrnc* plasmid and lost the pBSR40 plasmid were confirmed by PCR and antibiotic susceptibility (growth on 5 μg ml^{-1} neomycin and absence of growth on 5 μg ml^{-1} erythromycin).

Growth was assayed for the following *B. subtilis* strains: an *rncS* merodiploid (wild type carrying the *rncS* in *trans*: BE589 with pBSR40), the *rncS* null mutant carrying the *rncS* in *trans* (BE600 with pBSR40), wild type carrying the *B. burgdorferi rnc* gene in *trans* (BE589 with pBK36-*Bbrnc*); the *rncS* null mutant carrying both *rncS* in *trans* and the *B. burgdorferi rnc* gene in *trans* (BE600 with pBSR40 and pBK36-*Bbrnc*); and the *rncS* null mutant carrying the *B. burgdorferi rnc* gene in *trans* (BE600 with pBK36-*Bbrnc*). Overnight lawns of each strain that had been incubated at 37°C were used as inocula for the growth assay. For each strain, 30-ml cultures were prepared in LB containing 5 μg ml^{-1} neomycin and inoculated at an OD_{600} of approximately 0.2. A SpectraMax M2e spectrophotometer (Molecular Devices) was used to measure OD_{600}

from 1-ml samples that were collected every 30 min or (for the BE600 with pBK36-*Bbrnc*) 1 h. A log-scale graph of the data utilizing the mean and standard deviation was plotted using KaleidaGraph (version 4.01) software.

Generation of *rnc*, *rrlA,* and *rrlB* null mutants in *B. burgdorferi*. We employed a standard technique that utilizes homologous recombination between target sequences upstream and downstream of a gene of interest to replace the target gene with an antibiotic resistance cassette, generating a null mutant for the gene of interest (248, 253, 254). The *rnc* gene (*bb0705*), *rrlA* gene, and *rrlB* gene were individually disrupted by replacement with *flgBp-aacC1*, which confers gentamicin resistance (247) as previously described (255, 256). Briefly, genomic regions encompassing 0.9 to 1.3 kb upstream and downstream of each target gene were amplified by PCR using Taq polymerase (Sigma-Aldrich), cloned into pCR®2.1-TOPO, and ligated together using T4 DNA ligase (New England Biolabs). The gentamicin resistance cassette was ligated into a synthetic AatII site between the two flanking sequences. The plasmid was linearized with SapI and electroporated into *B. burgdorferi* as previously described (248).

Transformants were cloned in liquid BSK II medium in 96-well plates (51) containing 40 μg ml^{-1} gentamicin at 34°C in a 1.5% CO_2 atmosphere and screened by PCR for successful homologous recombination. Clones for each *rnc* mutant appeared in approximately 90 d at 34°C, which is considerably longer than the 10 to 14 d typically required for positive cultures to grow. Clones for the *rrlA* and *rrlB* mutants were present within the expected 10 to 14 d. Positive clones were confirmed by RT-PCR of total RNA using a RETROscript™ kit (Ambion) and assayed for the presence of genomic plasmids

by PCR (88, 89). Two independent *rnc* null mutants from *B. burgdorferi* strains B31-A3 and 297 were isolated. The *rrlA* and *rrlB* mutants were isolated from *B. burgdorferi* strain 297.

***B. burgdorferi* growth assay** To compare the growth rates of the *rnc, rrlA, and rrlB* null mutants with wild-type *B. burgdorferi*, a growth curve of each strain was charted at 34°C as previously described (3#192). Briefly, both strains were inoculated into BSK II liquid medium and incubated at 34°C until each had reached a cell density of ~5.0×10^7 cells ml^{-1}. Each culture was then diluted and inoculated into three replicates containing BSK II at a cell density of approximately 1.0×10^4 cells ml^{-1}. Cultures were grown at 34°C and each culture was counted every 24 h. *B. burgdorferi* were enumerated by diluting each culture in Dulbecco's phosphate-buffered saline (138 mM NaCl, 2.7 mM KCl, 8.1 mM Na_2HPO_4, and 1.5 mM KH_2PO_4; dPBS) and counting on a Petroff-Hausser counting slide (Hausser Scientific) at 400× magnification under dark-field on an Olympus CX31 microscope as previously described (2, 3). Cell counts were multiplied by 5×10^5 to obtain cells ml^{-1}. The mean and standard deviation of the three replicates for each strain was calculated and a growth curve of the data plotted using KaleidaGraph (version 4.01) software.

Microscopy. *B. burgdorferi* cells were stained using a wheat germ agglutinin (WGA)-Alexa Fluor® 594 conjugate (Invitrogen) (46). Briefly, a small volume of late-log or early stationary phase *B. burgdorferi* cells were washed once in pre-warmed dPBS + 5 mM $MgCl_2$ and resuspended in dPBS containing WGA-Alexa Fluor® 594 lectin conjugate at

1:200 dilution. The cells were incubated for 5 min at 37°C before pelleting by centrifugation. Following centrifugation, the supernatant was removed and discarded. Cells were resuspended in a small volume of pre-warmed dPBS and placed on pre-cleaned slides with coverslips. Images were captured using an Olympus BX51 microscope through a 100 × objective equipped with a DP72 digital camera, controlled by DP2-BSW software. Images were processed and cell length measured using ImageJ (National Institutes of Health; http://rsbweb.nih.gov/ij/). Figures were prepared using Pixelmator (Pixelmator Team, Ltd.). For each strain (wild type and *rnc* null), the length of fifty spirochetes was measured using the microscope standard of 94 pixels = 10 μm and the data were analyzed using KaleidaGraph software (version 4.01).

Identification of 5′ and 3′ ends of rRNAs. The 5′ and 3′ ends of each of the rRNAs (16S, 23S, and 5S) were determined by 5′ and 3′ Rapid Amplification of cDNA Ends (RACE). *B. burgdorferi* cells (wild type and the *rnc* null mutant) were grown to mid-log cell density and lysed with TRIzol® (Ambion); total RNA was extracted with chloroform, isopropanol, and 70% ethanol before being resuspended in RNase-free water. Prior to 3′ RACE, total RNA was polyadenylated with a Poly(A) Tailing Kit (Ambion). For the RACE protocol, nested primers and reverse transcriptase from the BD SMART^{TM} RACE cDNA Amplification kit were utilized to generate cDNA from the total RNA. The cDNA was amplified by PCR using a universal primer set included in the kit and gene-specific primers (designed with the Primer3 function in the MacVector version 12.7; Table 3) specific for a sequence either downstream of the 5′ end or upstream from the 3′ end of each rRNA gene. PCR products were resolved on a 2% agarose gel, visualized

with an LAS-3000 digital camera (Fujifilm), purified with a QIAquick gel extraction kit (Qiagen), and cloned into pCR®2.1-TOPO. Clones were sequenced at the Murdock DNA Sequencing Facility (The University of Montana) with an Applied Biosystems Genetic Analyzer (GeneScan) and sequence data were analyzed using MacVector (version 12.7).

Junctional RT-PCR of the tandem 23S-5S rRNA operon and *rnc* gene regions. Total *B. burgdorferi* RNA was collected as described above. Following resuspension in water, the RNA was treated with Turbo™ DNase (Invitrogen) and isolated by phenol-chloroform extraction and ethanol precipitation. A SuperScript® III Reverse Transcriptase (RT) kit (Invitrogen) was used to generate cDNA from total RNA. "No RT" controls were also prepared for each sample to ensure complete DNase treatment. PCR amplification using primer sets (Table 3) covering the region upstream of the 16S rRNA gene, the intergenic spacer between the first 5S gene (*rrfB*) and the second 23S gene (*rrlA*), as well as the region upstream of *rnc* yielded products that were resolved on 2% agarose gels, stained with ethidium bromide, and detected using an LAS-3000 (Fujifilm).

Generation of an artificial 23S rRNA substrate. An artificial 23S stem-loop that serves as an RNase III substrate was generated as previously described (8). Oligonucleotides with a T7 promoter (Table 3) were used to generate a template for transcribing a ^{32}P-labeled RNA molecule. The sequence was composed of the 23S 5′ and 3′ complementary ends that form the stem portion of the rRNA transcript with a loop of four unmatched nucleotides. Oligonucleotides were annealed in water by heating for 5 min at 65°C and

then quick-cooled on ice. A MEGAscript® *in vitro* transcription reaction (Ambion) with ^{32}P-α-UTP (Perkin-Elmer) was incubated overnight at 37°C. Following subsequent DNase treatment (Turbo DNase; Invitrogen), the substrate was extracted from a 15% TBE-urea polyacrylamide gel overnight using gel elution buffer (0.5 M ammonium acetate, 1 mM EDTA, and 0.2% sodium dodecyl sulfate) and ethanol precipitated. Detection of the substrate in the gel prior to extraction was performed using a phosphorimager (FLA-3000; Fujifilm). Following precipitation, RNA was resuspended in TE buffer (10 mM Tris-HCl, pH 8.0, and 1 mM EDTA).

Purification of recombinant RNase III protein. Recombinant RNase III protein was purified using the IMPACT^{TM} (Intein Mediated Purification with an Affinity Chitin-binding Tag) kit (New England Biolabs). This system utilizes a self-cleaving intein tag linking a chitin-binding domain to the C-terminus of a recombinant protein (*B. burgdorferi* RNase III). Briefly, cultures of *E. coli* carrying pTXB1 with the *B. burgdorferi rnc* were induced with 0.4 mM IPTG for 4 h at 37°C and lysed by sonication. The lysate was loaded on chitin beads and washed with column buffer (20 mM Tris-HCl, pH 8.5, 500 mM NaCl, and 1 mM EDTA), leaving recombinant protein bound to the resin. DTT was added to the column to initiate self-cleavage of the intein tag, which separated the tag and protein. The unbound recombinant protein was then washed off the column using column buffer, leaving the intein and chitin-binding domain attached to the resin.

RNase III cleavage assay. An RNase III cleavage assay was performed as previously described (8). The artificial 23S rRNA substrate was briefly heated (30 s) at 100°C and rapidly cooled on ice to fold into a stem-loop structure. Substrate RNA (300 nM) and various amounts of recombinant RNase III (0 nM, 0.5 nM, 1nM, 5 nM, 10 nM, 20 nM, and 25 nM) were combined in cleavage buffer (30 mM Tris-HCl, pH 8, 160 mM NaCl, 0.1 mM EDTA, 0.1 mM DTT, and 0.1 mM tRNA) and incubated for 5 min at 37°C to bind enzyme and RNA. Addition of 10 mM $MgCl_2$ initiated the cleavage reaction. Reactions were stopped after 5 min by adding gel loading buffer containing EDTA. Samples were resolved on a 15% (w/v) polyacrylamide gel containing 7 M urea and visualized on a phosphorimager (FLA-3000; Fujifilm).

Sequencing of the tandem 23S-5S rRNA operons from *B. burgdorferi* strain 297. Primers (Table 3) covering overlapping regions both flanking and within the tandem 23S-5S operons of *B. burgdorferi* strain 297 were amplified by PCR. PCR products were resolved on a 1% agarose gel, purified with a QIAquick gel extraction kit (Qiagen), and cloned into pCR®2.1-TOPO. Clones were sequenced at the Murdock DNA Sequencing Facility (The University of Montana) with an Applied Biosystems Genetic Analyzer (GeneScan) and sequence data were analyzed using MacVector (version 12.7). A master sequence for the tandem 23S-5S rRNA operons was assembled using MacVector (version 12.7). This sequence was submitted to GenBank (http://www.ncbi.nlm.nih.gov/genbank/) and has been assigned accession number JX564636.

Tandem 23S-5S rRNA operon single-nucleotide polymorphism (SNP) analysis. Complete 23S-5S rRNA operon sequences for all sequenced *B. burgdorferi* strains (B31, JD1, N40, and ZS7) were downloaded from GenBank (http://www.ncbi.nlm.nih.gov/genbank/) and analyzed, along with the tandem 297 23S-5S rRNA operon sequence determined in this work, using ClustalW alignment software included in MacVector (version 12.7).

Determination of the ratio of 16S to 23S rRNA transcripts. Total *B. burgdorferi* RNA was collected, DNase treated, and used to synthesize cDNA as described above for three wild-type *B. burgdorfer*i strains (297, B31-A3, B31-5A4) and the *rrlA* and *rrlB* null mutant strains (297). Prior to cDNA synthesis, RNA was analyzed for DNA contamination with *B. burgdorferi* flagellin gene-specific primers (Table 3). Primers and TAM-FAMRA-labeled probes for 16S and 23S rRNA (Table 3) were designed using PRIMER EXPRESS 3.0 version (Applied Biosystems). Genomic DNA and cloned 16S and 23S rRNA genes were used as controls to establish standard curves. Each quantitative real-time PCR (qRT-PCR) contained 13 µl TaqMan® Gene Expression Master Mix (Invitrogen), 10 µM forward and reverse primers, 2.5 µM probe, 1 ng of genomic or cDNA template or 10 ng, 1 ng, or 0.1 ng cloned 16S or 23S rRNA gene controls in a total volume of 25 µl. Samples were run in triplicate. TaqMan qRT-PCR was performed in a 96-well plate and run with standard cycle parameters using an Applied Biosystems 7300 Real-Time PCR System. Data collected by the instrument software was processed and exported into Microsoft® Excel where the ratio of 16S to 23S rRNA was calculated for each strain.

Analysis of 23S rRNA SNPs. Purified *B. burgdorferi* strain B31-A ribosomes, generously given to us by Paula Schlax (Bates College), were phenol/chloroform extracted before ethanol precipitation and resuspension in water to isolate purified rRNA. Additionally, total RNA was collected from *B. burgdorferi* strain B31-5A4 as described above. A primer (Table 3) was designed to be complementary to a region less than 25 nucleotides away from a sequenced single nucleotide polymorphism (SNP) in the *B. burgdorferi* strain so that we could differentiate between transcript products from each 23S rRNA gene. All RNA samples were diluted to a concentration of 0.5 μM before use in the experiment.

A primer extension assay was conducted according to a standard protocol based on Sigmund *et al*. (257) by Emily Hedrick of the Hill laboratory (The University of Montana, Missoula). Briefly, reactions containing AMV-RT (Promega) and 10 x extension buffer (1.3 M Tris-HCl, pH 8.5, 0.1 M $MgCl_2$, and 0.1 M DTT in water) were assembled for each of the RNA samples containing 2 μl of the appropriate 5′-^{32}P-labeled DNA oligonucleotide (Table 3). Samples were extended for 30 min at 42°C. Sequencing lanes containing each of the four dNTPs (1 mM) were also run for comparison. SNPs were detected by adding excess (10 mM) of a single ddNTP complementary to the first expected chain termination site (ddGTP and ddATP for strain 297 SNPs; ddGTP for strain B31 SNPs) for each primer. After extension, samples were electrophoresed on an 8% (w/v) polyacrylamide sequencing gel containing urea for 1 hr and 45 min (55 watts) and detected on a Fuji FLA-3000G phosphorimager with Image Gauge software (Fuji Biomedical).

***In vitro* competition assay.** An *in vitro* competition assay was performed with *B. burgdorferi* wild-type strain 297, *rrlA* null mutant, and *rrlB* null mutant based on the protocol described in Criswell *et al.* (258). Each culture was grown at 34°C in 10 ml BSK-II to a cell density of 10^8 cells ml^{-1} and passaged at a density of 10^5 cells ml^{-1} into a fresh 10 ml culture for continued growth at 34°C. No gentamicin selection was used during this part of the assay so that no selective advantage would be conferred during strain competition. Once the passaged cultures reached a density of 10^8 cells ml^{-1}, cells were enumerated using a Petroff-Hausser counting chamber as described above and inoculated at a density of 10^5 cells ml^{-1} into 10 ml of fresh BSK-II in the following combinations: wild-type 297 alone, *rrlB* null mutant alone, *rrlA* null mutant alone, wild-type 297 and *rrlB* null mutant, wild-type 297 and *rrlA* null mutant. Competition between the *rrlA* and *rrlB* mutants was not performed due to the growth defect observed in the *rrlB* mutant. All cultures were inoculated at the same cell density. Duplicate cultures were inoculated for each treatment.

Competition cultures were grown at 34°C until they reached a density of 10^8 cells ml^{-1}, then passaged into a fresh 10 ml culture at a density of 10^5 cells ml^{-1} for continued growth at 34°C, usually a period of 72 h to 96 h. This process was repeated for a total of twelve passages, which correlates to approximately 120 generations. At 6 and 12 passages (60 and 120 generations, respectively), cells were enumerated, diluted, and plated in semisolid media with and without 40 μg ml^{-1} gentamicin selection. Briefly, plating BSK (containing a BSK II base, rabbit serum, 5% sodium bicarbonate, and 1.7% agarose) was aseptically prepared, heated to 55°C, and 15 ml was aliquoted into each sterile plate in the presence or absence of 40 μg ml^{-1} gentamicin (248). The remaining

plating BSK was cooled to 42°C for plating a top layer. *B. burgdorferi* cells from each culture were enumerated and diluted so that plating 100 µl would correspond to 10^{-4} and 10^{-3} dilutions in the semisolid media. A volume of 20 ml plating BSK (with and without 40 µg ml^{-1} gentamicin) and 100 µl of each *B. burgdorferi* dilution were briefly mixed and plated onto the solidified bottom layer of media in each plate.

After the top layer solidified, plates were incubated at 34°C in 1.5% CO_2 for two weeks before manual counting of colonies. The wild-type 297 was plated with no selection, each *rrl* mutant was plated with 40 µg ml^{-1} gentamicin, and each competition mixture was plated without selection and with 40 µg ml^{-1} gentamicin. A ratio of each *rrl* mutant as compared to wild-type 297 for each competition culture was calculated by taking the number of colonies on the gentamicin plate and dividing it by the number of colonies in the plate with no selection.

Murine infectivity assay. Three *B. burgdorferi* strains were needle-inoculated into C3H-HeJ female mice to examine infectivity of the *rrlA* and *rrlB* null mutant strains as compared to the parental wild-type 297 strain. All three strains assayed were screened for the presence of all plasmids prior to needle inoculation, including the essential infectivity plasmids (lp54, lp25, and lp28-1) (88, 89). Cultures were initially grown at 23°C in BSK II (pH 7.6), passaged once at this temperature, then passaged again into BSK II (pH 7.6) at 34°C. A final passage at 34°C was carried out in BSK II (pH 6.8) to prepare strains for needle inoculation into mice. Once cultures reached a cell density of 5-7 × 10^7 cells ml^{-1}, they were enumerated using a Petroff-Hausser counting chamber (described above), and diluted to 2 × 10^7 cells ml^{-1}. Cultures were loaded into insulin syringes to a volume of 50

µl, which is equal to 10^4 *B. burgdorferi* cells per injection. Three mice per strain were inoculated by intraperitoneal injection while awake.

Ear punches were taken three weeks post-inoculation. An isofluorane chamber was prepared using an isofluorane-soaked sponge underneath a metal grate in a large beaker. A tight lid was placed on top of this container. Each mouse was individually placed within the chamber and anesthetized by the isofluorane gas. Their movement was carefully monitored to ensure full anesthesia but not overdose. The mouse was then placed within a sterilized biosafety cabinet, its ear thoroughly wiped with an ethanol swab, and a sterile ear puncher used to take a piece of the mouse's ear. The mouse was then placed back into its cage to recover. Ear biopsies were cultured in 3 ml of BSK II containing 50 µg ml^{-1} rifampicin, 20 µg ml^{-1} phosphomycin and 2.5 µg ml^{-1} amphotericin B . Cultures were incubated at 34°C for a minimum of one week.

At five weeks post inoculation, mice were humanely sacrificed using CO_2 gas. Each mouse was then placed in a biosafety cabinet and a second ear punch was taken. Tibiolateral joints and bladders were also collected at this time. The dissecting tools and mouse skin near the point of incision were sterilized with 70% ethanol prior to organ collection. Each organ and ear biopsy was cultured as described above. All experiments performed on these mice were in compliance with and approved by The University of Montana Animal Care and Use Committee.

After one week at 34°C, wet mounts were prepared for each culture and examined carefully for the presence of spirochetes by dark-field microscopy. Cultures that were positive were discarded after data collection. Cultures that were negative for spirochetes were incubated for additional time and checked on a weekly basis for a maximum of four

weeks post-collection. After the final microscopic examination, a PCR screen using *B. burgdorferi* flagellin gene-specific primers (Table 3) was performed to ensure the absence of genomic DNA. Positive cultures were used as a PCR control. Briefly, 1 ml of culture was centrifuged, resuspended in 200 µl dPBS, and 1 µl was used for PCR analysis.

Antibiotic susceptibility assay. Susceptibility of wild-type 297 and the *rrlA* and *rrlB* null mutants to two antibiotics that target the large subunit of the ribosome (chloramphenicol and erythromycin) was assayed using a protocol similar to established methods (249, 259). The assay was performed in a 96-well plate, with 11 concentrations of each antibiotic (in a two-fold dilution series) and one well with no antibiotic as a positive control. Each strain was duplicated for each antibiotic and inoculated in two complete rows of the plate. The bottom two rows of each plate contained no *B. burgdorferi*, only media and antibiotics, to serve as a negative control. Antibiotic concentrations were determined based on published minimum inhibitory concentration (MIC) data for erythromycin (0.004 µg ml^{-1}) (4) and chloramphenicol (1.25 µg ml^{-1}) (6). These concentrations were used as midpoints for the assay yielding a range of 0.00013 µg ml^{-1} to 0.128 µg ml^{-1} for erythromycin and 0.08 µg ml^{-1} to 40 µg ml^{-1} for chloramphenicol.

Cultures for each strain that had been growing at 34°C were diluted into BSK II at a concentration of 10^5 cells ml^{-1} and inoculated into the appropriate rows of the 96-well plate. A small volume of antibiotics that had been diluted to the proper concentration (and to eliminate any ethanol effect) was then added to each column of the plate. Plates

were incubated at 34°C in 1.5% CO_2 for one week, then colorimetrically assayed for growth (yellowing due to acidification of the medium, which contains phenol red). As the *rrlB* null mutant strain grows at a reduced rate compared to the wild type and *rrlA* null mutant, the culture was incubated for four additional days before data collection. Images were captured on a light box using a 7.1 megapixel Canon PowerShot SD750 Digital Elph camera on 11 d and 14 d after inoculation.

Chapter 3

Role of *B. burgdorferi* RNase III in rRNA processing

Most Lyme disease bacterial agents, *B. burgdorferi* and related species, possess only a single complete set of the three rRNA genes, with the 16S and 23S-5S rRNA genes separated by over 3 kb, and the 23S-5S rRNA operon tandemly duplicated on the chromosome (1, 83). This organization likely requires alternative transcription regulatory mechanisms not observed for bacteria with canonical and stoichiometric rRNA gene arrangements. *This work seeks to demonstrate how* B. burgdorferi, *with its unusual rRNA gene organization, produces functional ribosomes. To that end, our data provide an initial characterization of* B. burgdorferi *RNase III, including RNase III processing of the rRNA transcripts from the unlinked 16S gene and tandemly duplicated 23S-5S genes, and an investigation of rRNA transcription and ribosome production from the unusual rRNA genomic locus of* B. burgdorferi.

Complementation of a *Bacillus subtilis rncS* null mutant with *B. burgdorferi rnc*

We trans-complemented a well-characterized RNase III mutant to test if the *B. burgdorferi rnc* encoded a functional RNase III. *B. subtilis* was chosen as the heterologous bacterium for these experiments because the *B. burgdorferi* RNase III is more similar to the enzyme from *B. subtilis* than to RNase III from *E. coli* (44% identity vs. 36% identity, respectively). In addition, the collection of ribonucleases carried by *B. burgdorferi* is more similar to that of *B. subtilis* than *E. coli* (Tables 1 and 2).

Furthermore, RNase III is essential in *B. subtilis* and not in other well-studied bacteria (e.g., *E. coli* and *S. aureus*), which allows us to utilize a defined phenotype (7, 260, 261, 262). Herskovitz *et al.* (7) engineered a *B. subtilis rncS* merodiploid with a null allele on the chromosome and a wild-type *rncS* on a temperature-sensitive plasmid (pBSR40). The *B. burgdorferi rnc* gene was fused to the inducible *B. subtilis spac* promoter and cloned into a stable *B. subtilis* plasmid (pBK36-*Bbrnc*). The *rncS* plasmid (pBSR40) was cured by shifting to the non-permissive temperature (45°C) (7).

Growth of the strains *trans*-complemented with either *B. burgdorferi rnc* or *B. subtilis rncS* in either a wild-type (BE589) or null *rncS* (BE600) background was assayed (Fig. 2). The two *B. subtilis* strains with a chromosomally encoded *rncS* gene (BE589) and the *rncS* mutant strain (BE600) carrying *B. subtilis rncS* in *trans* grew at similar rates, as did the BE589 strain with the *B. burgdorferi rnc* gene. The *B. subtilis rncS* null strain carrying both plasmids (pBSR40 and pBK36-*Bbrnc*) grew slower than the other three strains. These four strains started reaching stationary phase around an OD_{600} density of 2.0 at 450 min after growth initiation. The *B. subtilis rncS* mutant (BE600) carrying the *B. burgdorferi rnc* gene (pBK36-*Bbrnc*) grew considerably slower than the other strains tested, but was able to reach an OD_{600} of 2.0 after approximately 800 min. These data demonstrate that *B. burgdorferi* RNase III is capable of complementing the lethal *rncS* defect in *B. subtilis* and that *B. burgdorferi rnc* encodes a functional RNase III.

Fig. 2. *B. burgdorferi rnc* complements a lethal *B. subtilis rncS* null mutant.

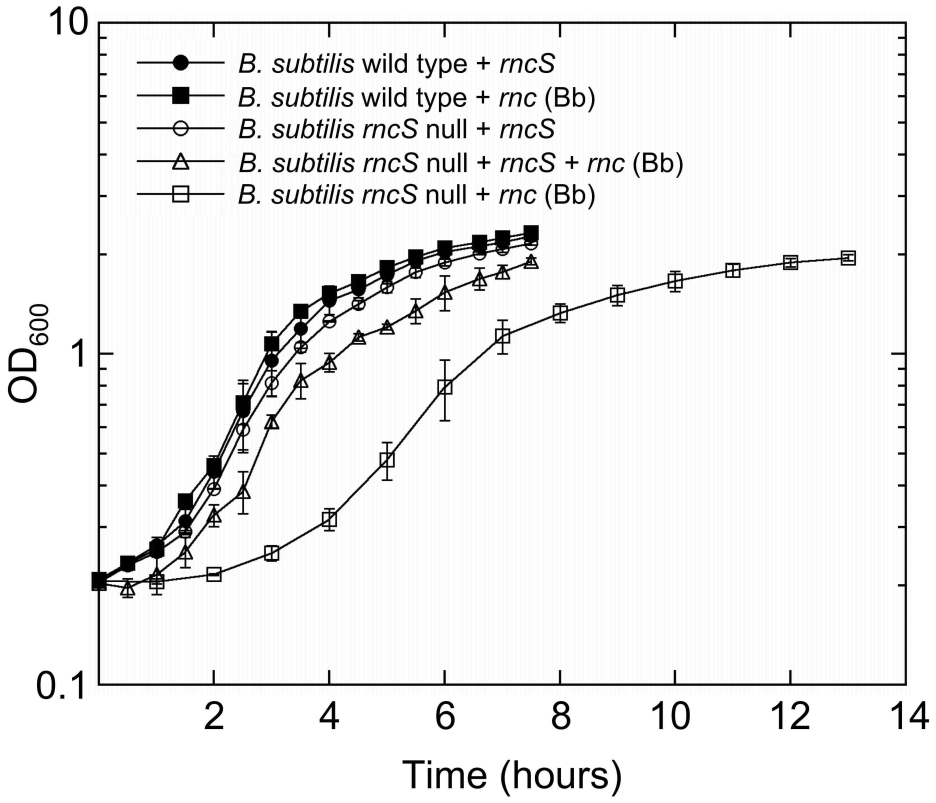

Growth over time was plotted on a logarithmic scale for the following *B. subtilis* strains that were derived from strains described in Herskovitz *et al.* (7): an *rncS* merodiploid (wild type carrying the *rncS* gene in *trans*: wild type + *rncS*), wild type carrying the *B. burgdorferi rnc* gene in *trans*: wild type + *rnc* (Bb); the *rncS* null mutant carrying the *rncS* gene in *trans*: *rncS* null + *rncS*; the *rncS* null mutant carrying both the *rncS* gene in *trans* and the *B. burgdorferi rnc* gene in *trans*: *rncS* null + *rncS* + *rnc* (Bb); and the *rncS* null mutant carrying the *B. burgdorferi rnc* gene in *trans*: *rncS* null + *rnc* (Bb). Cultures were inoculated at an OD_{600} of approximately 0.2; OD_{600} was measured from 1-ml samples that were collected every 30 min (or 1 h for the *rncS* null + *rnc* (Bb) strain) until stationary phase was reached (OD_{600} of approximately 2.0).

Generation of an RNase III (*rnc*) null mutant

We hypothesized that the rRNA transcripts in *B. burgdorferi*, which have a unique organization, are processed as in other bacteria, including cleavage of the 16S and 23S rRNA transcripts by the endoribonuclease RNase III (7, 157, 158). The chromosomal *rnc* gene for this enzyme was replaced though homologous recombination with the gentamicin resistance cassette *flgBp-aacC1*. Three transformants were isolated in two *B. burgdorferi* strains (297 and B31-A3), and appeared after approximately 90 d incubation at 34°C, much longer than the 10 d to 14 d that are usually sufficient for transformed clones to appear. This initial observation suggests that, while not essential, RNase III is nevertheless an important enzyme in *B. burgdorferi*. Additionally, it is possible that the *rnc* null mutants accumulated suppressor mutations that allowed them to grow in the absence of the RNase III enzyme.

The clones were screened for the presence of the *flgBp-aacC1* insertion (Fig. 3B) by PCR using primers specific for the flanking regions of the *rnc* gene (Table 3; Fig. 3A). A second primer set specific for the *flgBp-aacC1* cassette (Table 3) and flanking downstream *rnc* region was also used to verify insertion of the resistance marker into the chromosome (data not shown). Mutants were additionally confirmed by RT-PCR of cDNA demonstrating the absence of the *rnc* transcript (data not shown). Exhaustive attempts to complement the *rnc* null mutants were unsuccessful.

Fig. 3. A *B. burgdorferi rnc* null mutant exhibits growth and morphological phenotypes.

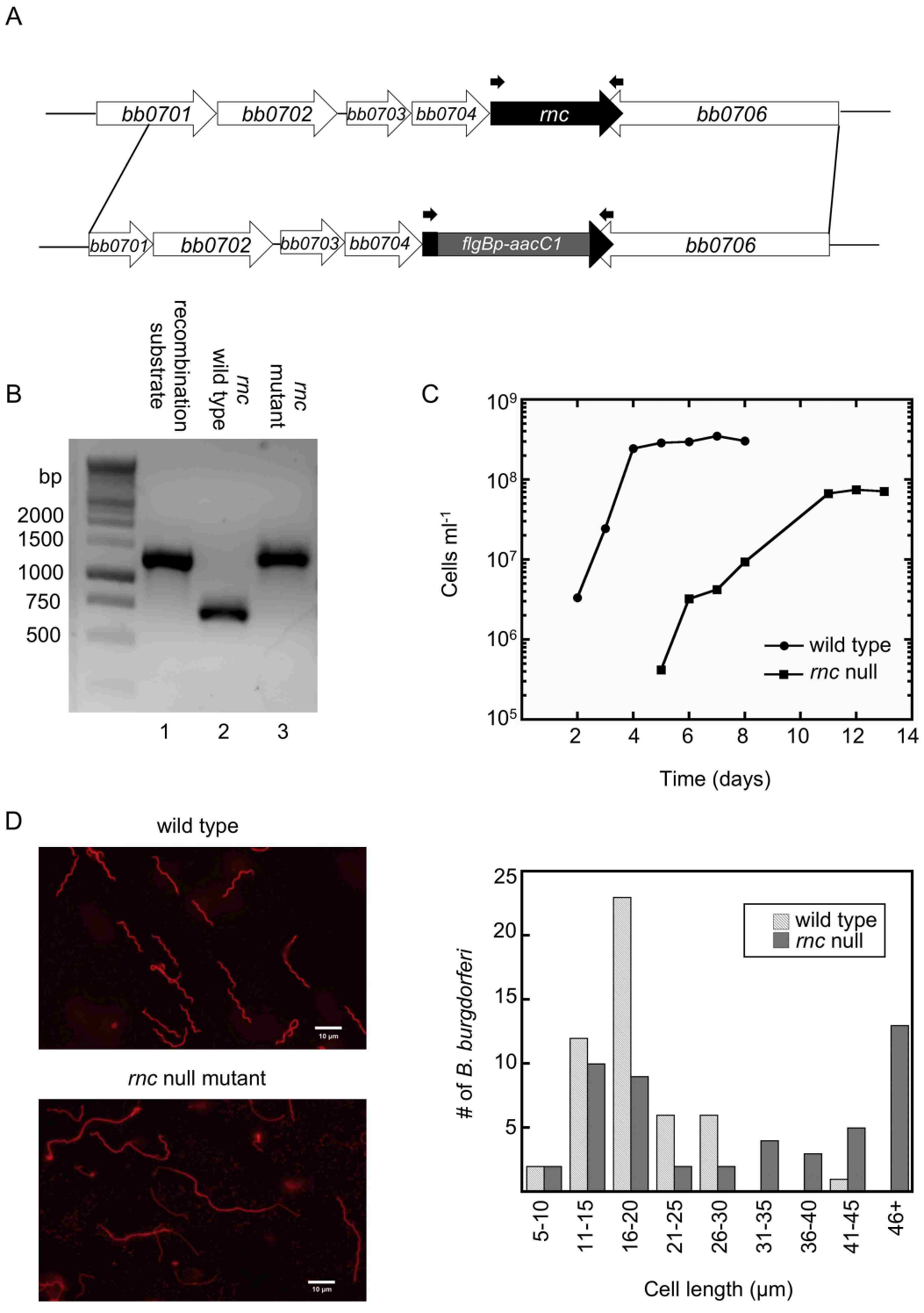

A. Schematic of the genetic approach taken to create the *rnc* null mutant in *B. burgdorferi*. An electroporated plasmid-borne gentamicin resistance cassette (*flgBp-aacC1*) replaced most of the chromosomal *rnc* gene through homologous recombination and subsequent antibiotic selection. Primers (Table 3) used to obtain PCR products shown in Fig. 3B are indicated by the small black arrows above the *rnc* gene and *flgBp-aacC1* cassette. B. Confirmation of an *rnc* null mutant. PCR-amplified chromosomal DNA from a successful *B. burgdorferi* transformant clone and controls were electrophoresed on an ethidium bromide-stained 1% agarose gel using primers (black arrows in 3A; Table 3) flanking the insertion region for the gentamicin resistance cassette. Lane 1: Gentamicin resistance cassette (*flgBp-aacC1*) control from the transformable vector (recombination substrate); Lane 2: Genomic *rnc* control of chromosomal DNA from wild type *B. burgdorferi* (*rnc* wild type); Lane 3: Successful *rnc* null mutant in strain 297 using chromosomal DNA as a template (*rnc* mutant). C. A *B. burgdorferi rnc* null mutant exhibits a severe growth defect *in vitro*. *B. burgdorferi* wild type and the *rnc* null mutant were inoculated in BSK II liquid medium at a cell density of 10^4 cells ml^{-1} and grown at 34°C until stationary phase. Cells were enumerated every 24 h using a Petroff-Hausser counting chamber (2, 3). Growth curves were plotted on a logarithmic scale over time for both strains. D. Microscopy images showing the mixed cell length morphology of the *rnc* null mutant (lower panel) as compared with wild-type *B. burgdorferi* (upper panel). Cells were stained with a wheat-germ agglutinin (WGA)-Alexa Fluor® 594 conjugate (Invitrogen) and assayed by fluorescence microscopy. The length of fifty cells for each strain was measured and the number of *B. burgdorferi* cells were plotted on a bar graph for each bracketed set of cell lengths (μm) to show cell length distribution of wild-type *B. burgdorferi* vs. the *rnc* null mutant.

Examination of the *rnc* null mutant phenotype

The *rnc* null mutants from both strains exhibited growth (Fig. 3C and data not shown) and morphological (Fig. 3D and data not shown) phenotypes. Wild-type *B. burgdorferi* cells reached mid-log cell density within 1 d and stationary phase by 4 d of growth. The *rnc* null mutant did not reach mid-log cell density until about 5 d of growth and the log phase was extended until about 11 d of growth. Cell density at stationary phase reached by the *rnc* null mutant was approximately half a log lower than the cell

density reached by wild type. In addition to the growth phenotype, the *rnc* null mutant cells are significantly longer than wild type (Fig. 3D), which is a phenotype previously found in *B. burgdorferi* mutants lacking the RNA chaperone Hfq (256). A subpopulation of mutant cells has a wild-type length, resulting in a bimodal distribution. These phenotypes may be the result of inefficient or defective ribosome biogenesis or failure to correctly process mRNAs with translation products involved in cell division.

Characterization of rRNA in the *rnc* null mutant

The ends of the three rRNAs in the *rnc* null mutant were determined by 5′ and 3′ RACE to assay the role of RNase III in rRNA processing in *B. burgdorferi*. Total RNA was isolated from both *B. burgdorferi rnc* null mutants as well as wild type. Representative data of the 5′ and 3′ RACE PCR products for each rRNA resolved by gel electrophoresis are shown (Fig. 4A). PCR products were cloned and at least four clones from each reaction were sequenced. The primary nucleotide sequence of each rRNA is shown with black dots above (wild-type sequences) and below (*rnc* null sequences) indicating the experimentally determined location of each rRNA end (Fig. 4B).

Fig. 4. *B. burgdorferi* RNase III processes the 5′ end of the 16S rRNA and the 23S rRNA but not the 5S rRNA nor, unexpectedly, the 3′ end of the 16S rRNA.

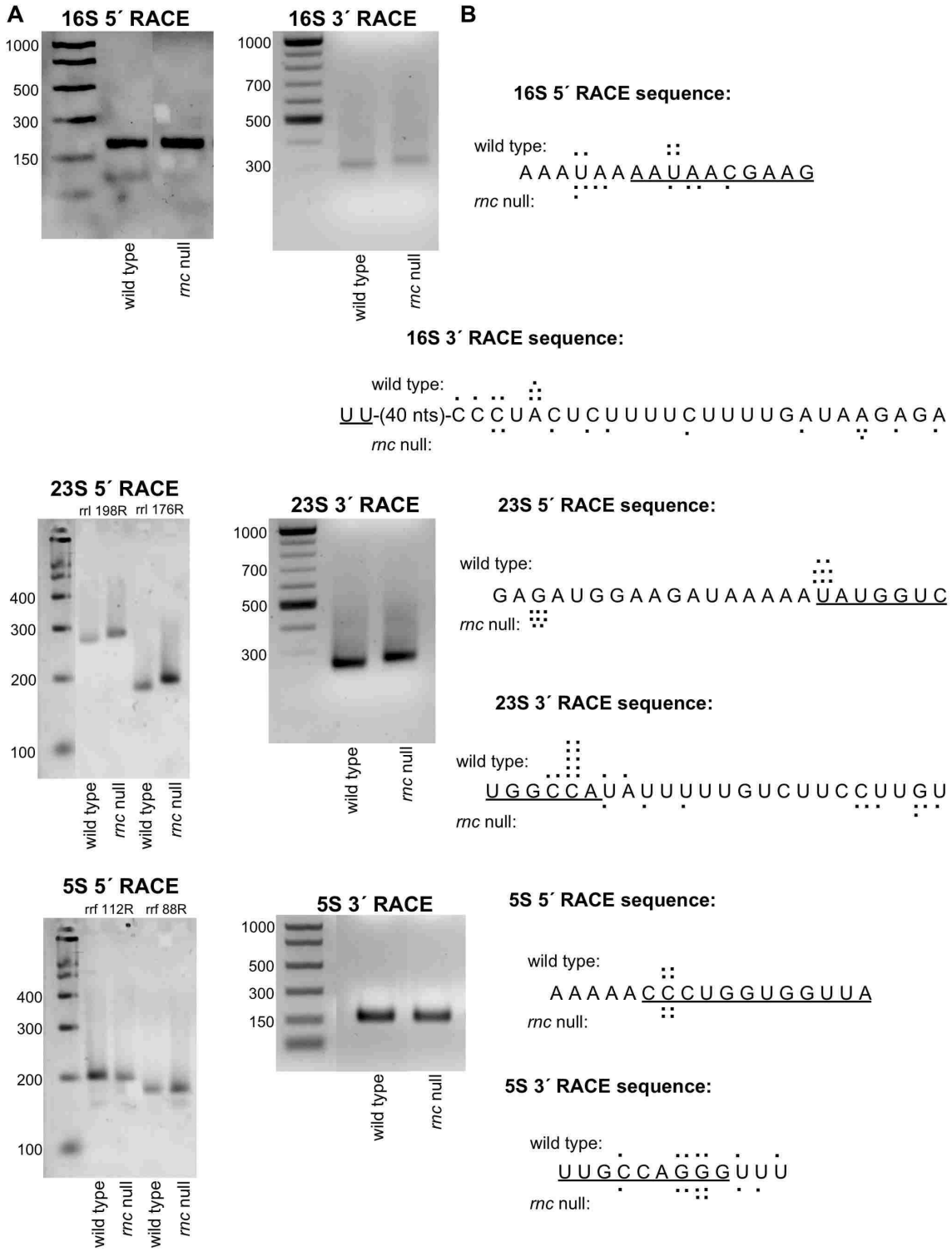

The 5′ and 3′ ends of each of the rRNAs (16S, 23S, and 5S) were examined by 5′ and 3′ Rapid Amplification of cDNA Ends (RACE). A. PCR products for each of the rRNAs generated from *B. burgdorferi* RACE-ready cDNA and one or two gene-specific primers (Table 3) were electrophoresed on an ethidium bromide-stained 2% agarose gel for both wild type and the *rnc* null mutant. Two primers (Table 3) were used for the 23S rRNA (rrl 198R and rrl 176R) and 5S rRNA (rrf 112R and rrf 88R) 5′ RACE reactions (Fig. 4A). B. Primary sequences for each rRNA 5′ and 3′ end are shown with the annotated rRNA sequence underlined. Individual sequencing events from multiple cloned RACE PCR products for each rRNA are represented by black dots above (wild type) and below (*rnc* null mutant) each sequence.

The data demonstrate that the 5′ end of the 16S rRNA is the same in both the wild type and *rnc* null mutant, mapping near the annotated 5′ end. The 3′ end is more variable (Fig. 4). Therefore, RNase III does not appear to be essential for 16S rRNA processing of the 5′ end, a feature that is unique to *B. burgdorferi*. As expected, the RACE data show that RNase III processes the 23S rRNA (Fig. 4). The mature 23S rRNA transcript is longer at both ends in an *rnc* null mutant. The 5′ end of the 23S rRNA in the *rnc* null mutant is 20 nucleotides downstream from the predicted promoter. Additionally, junctional RT-PCR between the two tandem 23S-5S rRNA gene sets reveals the presence of a single transcript containing both 23S-5S rRNA molecules. This large transcript is present in both the wild type and *rnc* null mutant backgrounds, but is in greater abundance in the mutant, highlighting the importance of RNase III in initial separation of these transcripts (Fig. 5). There is no difference in the 5S rRNA 5′ and 3′ transcript ends generated in the *rnc* null mutant compared to wild type, indicating that RNase III has no effect on processing this rRNA, as expected (Fig. 4).

Fig. 5. A single long rRNA transcript is produced from the tandem 23S-5S rRNA genes in both the wild type and *rnc* null mutant.

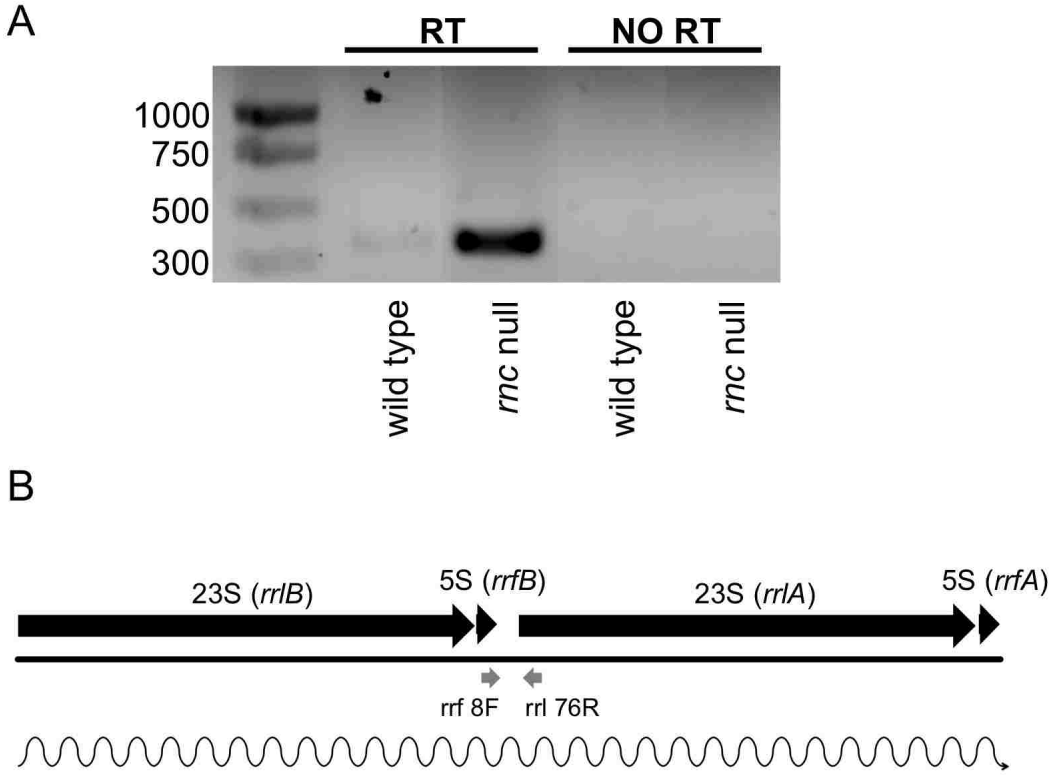

A. RT-PCR analysis was used to assay the junction between the first 5S rRNA gene and the second 23S rRNA gene in *B. burgdorferi*. The junctional primer set (Table 3) used is represented by gray arrows in 5B. RT-PCR products and no RT controls were run on an ethidium bromide-stained 1% agarose gel. B. Gene map depicting the tandem 23S-5S rRNA gene region (black arrows). Junctional primers (Table 3) are represented by gray arrows below the gene map. The squiggly line beneath the gene map depicts the primary rRNA transcript suggested by the junctional RT-PCR data.

Cleavage of an artificial 23S rRNA substrate

We confirmed the biochemical activity of RNase III from *B. burgdorferi* using an *in vitro* cleavage assay. An artificial 23S rRNA stem-loop that serves as an RNase III substrate was generated as previously described (8). The sequence is composed of the double-stranded stem portion of the 23S rRNA transcript with a loop of four unmatched nucleotides (Fig. 6A). RNase III recognizes the double-stranded stems of this RNA and creates a staggered break with a 3′ two-nucleotide overhang. Exonucleases would then trim the 5′ and 3′ transcript ends to their proper length *in vivo*. The artificial 23S rRNA substrate was generated by *in vitro* transcription (MEGAscript; Ambion) and radiolabeled with ^{32}P-UTP. A molar excess of the substrate was incubated with recombinant *B. burgdorferi* RNase III protein as previously described by Amarasinghe *et al.* (8). Cleavage products were produced with inceasing concentrations of RNase III (Fig. 6B), showing enzyme-substrate specificity.

Fig. 6. Recombinant RNase III selectively cleaves an artificial 23S rRNA substrate *in vitro*.

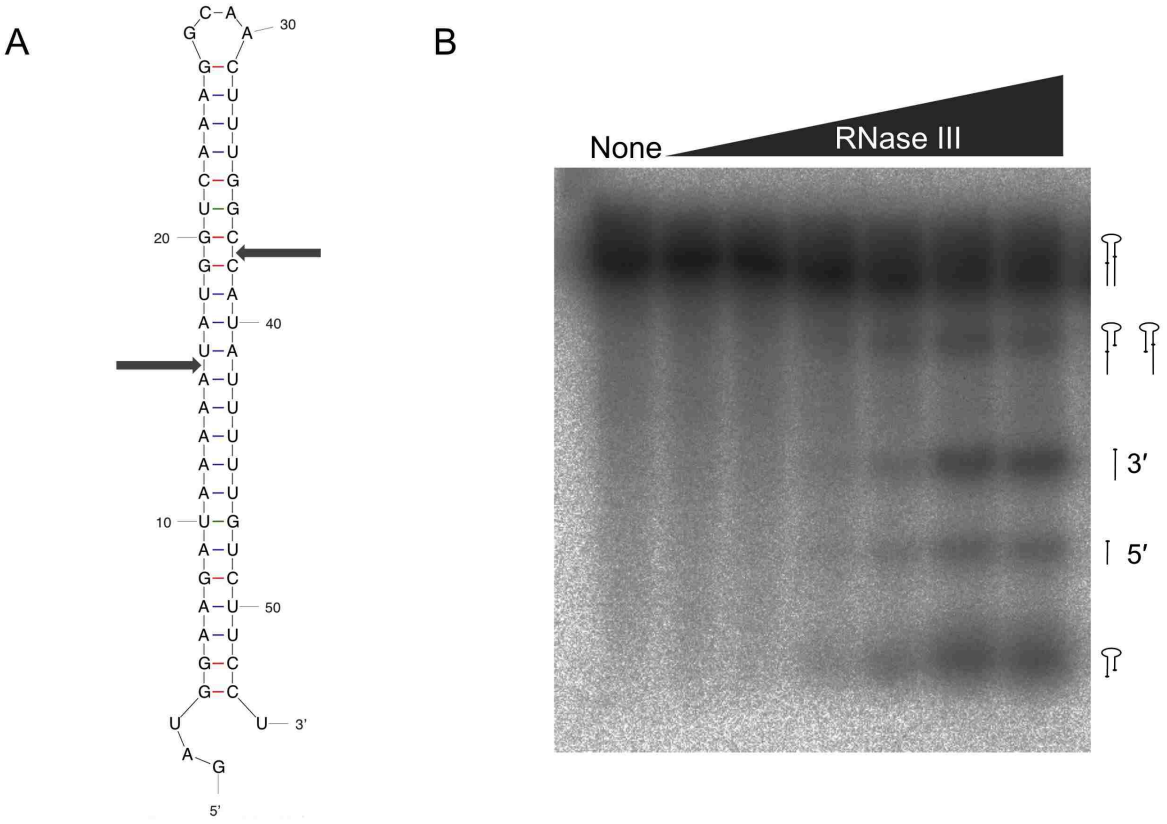

A. Mfold structure depicting the double-stranded secondary structure of the artificial 23S rRNA substrate. Black arrows represent wild type substrate ends as determined by RACE (Fig. 4). Substrate design was based on the method described in Amarasinghe *et al.* (8). B. Phosphorimage showing the specific increase in ^{32}P-UTP-labeled artificial 23S rRNA substrate cleavage products produced at 37°C after 5 min in the presence of increasing concentrations of recombinant *B. burgdorferi* RNase III protein (0 nM to 25 nM; black triangle indicates increasing enzyme concentration). Cartoon structures to the right of the phosphorimage depict predicted cleavage products. Band density likely reflects the number of labeled ^{32}P-UTP molecules present in each cleavage product.

Profile of *rnc* operon structure.

rnc is encoded on the *B. burgdorferi* chromosome in a region dense with genes related to translation. Junctional RT-PCR was performed on cDNA synthesized from *B. burgdorferi* total RNA (Fig. 7A). The data suggest that the *rnc* gene is transcribed as part of a five-gene operon, which includes *bb0701* (encoding a conserved hypothetical protein), *coaD* (encoding pantetheine-phosphate adenylyltransferase), *rpmF* (encoding ribosomal protein L32), and *acpP* (encoding acyl carrier protein) (Fig. 7B).

Fig. 7. The *rnc* gene is transcribed as part of a larger operon.

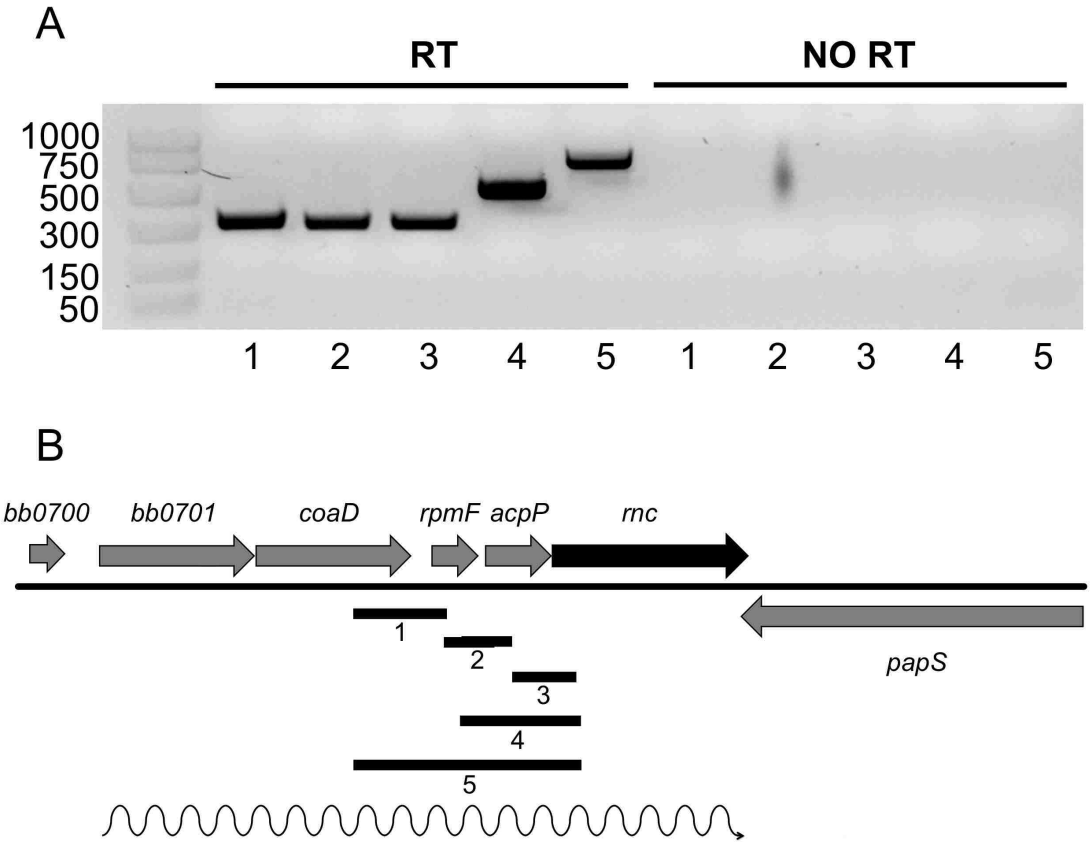

A. Junctional RT-PCR analysis of the coding region 5′ to *rnc* in *B. burgdorferi*. RT-PCR products and no RT controls were run on an ethidium bromide-stained 1% agarose gel. Numbers beneath the gel image and under the small black bars in 7B refer to the following primer sets (Table 3): 1: bb702 351F and bb703 145R; 2: bb703 48F and bb704 177R; 3: bb704 46F and rnc 143R; 4: bb703 48F and rnc 143R; 5: bb702 351F and rnc 143R. B. Gene map depicting the *rnc* chromosomal region. Junctional primer set (Table 3) coverage is represented by numbered black bars below the gene map. A squiggly line beneath the gene map depicts the primary *rnc* operon transcript suggested by the junctional RT-PCR data. Junctional RT-PCR reactions covering the junctions between *bb0700-bb0701* and *bb0701-coaD* were also performed to confirm the 5′ end of the predicted *rnc* operon transcript; the data indicate no junction between *bb0700-bb0701* and a junction present between *bb0701-coaD* (data not shown), which is illustrated by the squiggled line above.

Role of RNase III in *B. burgdorferi* ribosomal RNA processing

As expected, *B. burgdorferi* RNase III, encoded by the *rnc* gene, appears to function in a canonical fashion. This is evidenced by our *in vitro* cleavage data of a artificial RNase III substrate (Fig. 6) and heterologous complementation of a *B. subtilis rncS* mutant (Fig. 2). An *rnc* null mutant exhibits growth and morphological phenotypes likely linked to a defect in ribosome synthesis or lack of proper processing of mRNAs involved in cell division (Fig. 3). Characterization of the 5′ and 3′ ends of the rRNA transcripts in wild-type *B. burgdorferi* and the *rnc* null mutant reveal that RNase III processes the 23S rRNA transcript but not the 5S transcript, as expected (Fig. 4). There is also less separation of the tandem 23S-5S rRNA transcripts in an *rnc* null background (Fig. 5). Unexpectedly, however, the enzyme is only essential for processing the 3′ end of the 16S rRNA transcript (Fig. 4). The 5′ end of this transcript appears to be processed by a yet-undefined mechanism independent of RNase III cleavage. This latter finding prompted us to investigate the structure of the 16S rRNA operon.

Structure of the 16S rRNA operon

In most bacteria, all three rRNA genes (16S-23S-5S) are encoded in a single operon that generates a large polycistronic precursor rRNA transcript for processing. In *B. burgdorferi*, however, the 16S and first 23S gene are separated by over 3 kb. Bugrysheva *et al.* (5) previously demonstrated that the $tRNA_{Ala}$ gene downstream of the 16S rRNA gene forms the 3′ end of the 16S rRNA operon. Junctional RT-PCR was performed on *B. burgdorferi* cDNA to characterize the operon structure upstream of the 16S rRNA gene (Fig. 8A). Surprisingly, the data show that the 16S rRNA transcript is co-transcribed with two upstream genes, *bb0426*, an unnamed member of the nucleoside 2-deoxyribosyltransferase superfamily, and *bb0427*, a predicted methyltransferase (Fig. 8B). This operon structure is unique to Lyme disease *Borrelia* and may be the product of tRNA recombination during evolutionary genome reduction.

Fig. 8. The 16S rRNA gene is encoded as part of a larger operon.

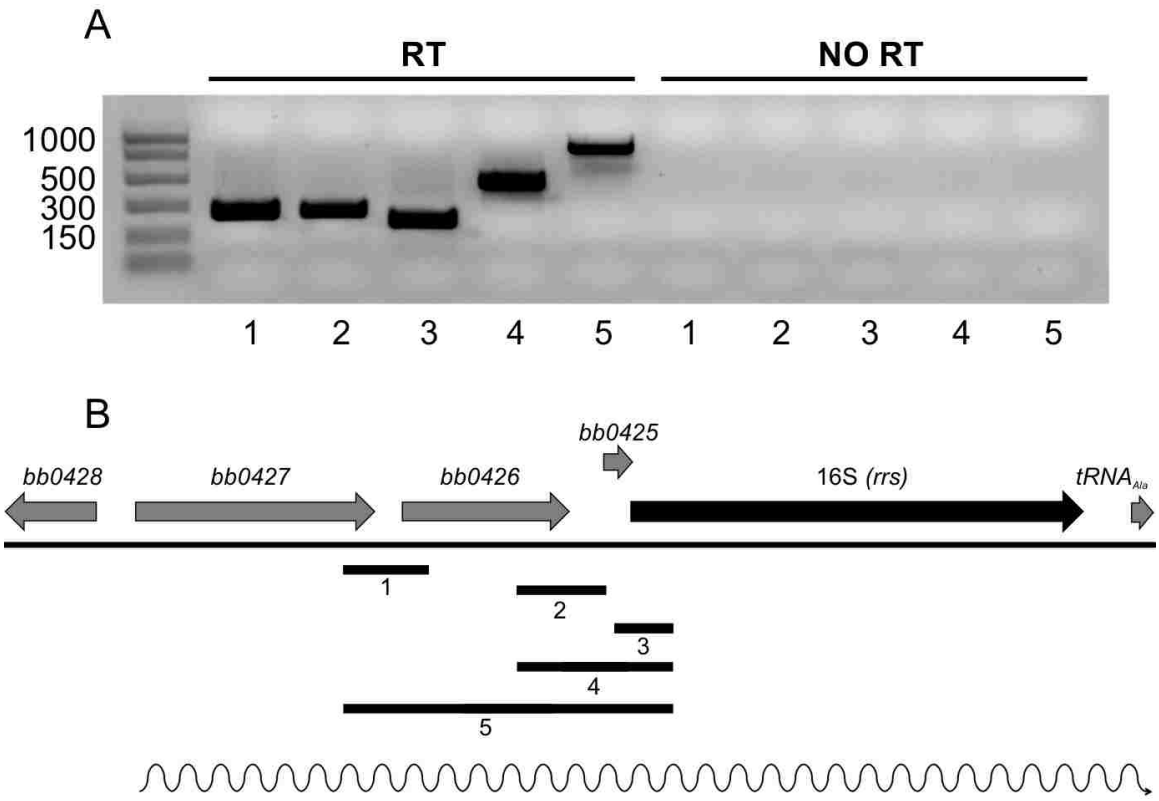

A. Junctional RT-PCR analysis of the coding region 5′ to the 16S rRNA (*rrs*) gene in *B. burgdorferi*. RT-PCR products and no RT controls were run on an ethidium bromide-stained 1% agarose gel. Numbers beneath the gel image and under the small black bars in 8B refer to the following primer sets (Table 3): 1: bb0427 687F and bb0426 90R; 2: bb0426 437F and bb0425 29R; 3: bb0425 10F and rrs 146R; 4: bb0426 437F and rrs 146R; 5: bb0427 687F and rrs 146R. B. Gene map depicting the 16S rRNA *(rrs)* chromosomal region. Junctional primer sets (Table 3) are represented by numbered black bars below the gene map. A squiggly line beneath the gene map depicts the primary 16S (*rrs*) operon structure suggested by the junctional RT-PCR data and includes the 3′ junctional RT-PCR data from Bugrysheva *et al.* (5).

Chapter 4

Characterization of the tandem 23S-5S rRNA genes of *B. burgdorferi*

Tandem duplication of the 23S-5S rRNA operons is a highly conserved feature that is unique to Lyme disease *Borrelia* species. We hypothesized that the duplicated 23S-5S rRNA genes were differentially regulated from the 16S rRNA operon to produce the correct 1:1:1 ratio of the rRNAs. To explore this possibility, we examined possible regulatory mechanisms through single nucleotide polymorphism (SNP) analysis of the the 23S rRNA genes and generation of null mutants in each 23S rRNA gene to create a single full complement of the rRNA genes in these *B. burgdorferi* strains. The data presented here demonstrate that tandem duplication of the 23S rRNA genes in *B. burgdorferi* has led to unique adaptations in rRNA gene regulation not observed in any other bacterial species described to date.

Characteristics of the tandem 23S rRNA genes

Tandem duplication of the *B. burgdorferi* 23S-5S rRNA operons creates an unequal complement of rRNA genes. When a gene is duplicated in this manner, one copy can accumulate mutations without harming the cell. To understand why *B. burgdorferi* encodes conserved tandem copies of the 23S-5S rRNA operons, we investigated the presence of SNPs in all sequenced *B. burgdorferi* strains. No *B. burgdorferi* 297 strain sequence is presently available, so we sequenced the tandem 23S-5S rRNA operon region and submitted the completed sequence to GenBank. Details about this sequence and its

accession number can be found in Chapter 2. Additionally, null mutants for each of the *rrl* genes (*rrlB* and *rrlA*) from strain 297 were created using the same homologous recombination technique used for the *rnc* null mutant (Fig. 3A).

SNP analyses were conducted on the 23S rRNA genes from five *B. burgdorferi* strains: N40, 297, JD1, B31, and ZS7. Sequences were downloaded from GenBank and aligned using ClustalW; the results are shown in Table 4. The location column specifies the position of each SNP compared to the first nucleotide of the 23S rRNA gene. Each strain exhibits a unique set of SNPs spread throughout the 23S rRNA genes. There appears to be no conserved region that is modified between all five strains. Interestingly, each SNP seems to have arisen from a purine-purine or pyrimidine-pyrimidine transition. There is only a single 5S SNP; it is located at the ninth nucleotide in the 297 strain *rrfA* gene and consists of a G→C transversion (data not shown).

Table 4. *B. burgdorferi* 23S rRNA gene SNPs.

***B. burgdorferi* strains**	**SNP characterization**	**Location**
N40 and 297	N40: both C 297: *rrlB* – C *rrlA* - T	162
JD1	JD1: *rrlA* – A *rrlB* - G	422
297	297: *rrlA* – A All other strains: G	794
N40	N40: A and Y All other strains: G	841
N40	N40: G and Y All other strains: A	1029
297	297: *rrlA* – T All other strains: C	1050
297 and B31	297/B31: *rrlA* – G All other strains: A	1298
N40 and 297	N40: both – T 297: *rrlB* – T All other strains: C	1426
297 and ZS7	297 *rrlB* and ZS7: T All other strains: C	1559
297 and ZS7	297 *rrlB* and ZS7: G All other strains: A	1569
JD1 and N40	JD1: both A N40: rrlA – A All other strains: G	1928
N40	N40: both T All other strains: C	2201
B31 and N40	B31/N40: *rrlA* - G All other strains: A	2737
N40	N40: *rrlA* – T All other strains: C	2746
B31 and JD1	JD1: both – C B31: *rrlB* – C All other strains: T	2864
JD1	JD1: both T All other strains: C	2889

Stoichiometry of the 16S and 23S rRNA transcripts

We performed quantitative reverse transcriptase PCR (qRT-PCR) to examine the ratio of 16S rRNA to 23S rRNA present in *B. burgdorferi*. Total RNA was collected from three wild-type *B. burgdorferi* strains (B31-A3, B31-5A4, and 297-BbAH130), two *rnc* null mutant strains (B31-A3 and 297-BbAH130), and the *rrlA* and *rrlB* mutants (297-BbAH130) at several cell growth phases (Table 5). A purified preparation of isolated *B. burgdorferi* ribosomes (B31-A; a generous gift from Paula Schlax of Bates College) were also analyzed. Primers and probes specific for conserved regions of the 16S and 23S rRNA genes (Table 3) were used for the qRT-PCR. Data from this assay are shown in Table 5. Surprisingly, the ratio of the two rRNAs is not equimolar; there is approximately 2.5 to 3 times more 23S rRNA than 16S rRNA in three strains of wild-type *B. burgdorferi* during mid-logarithmic growth. This ratio is lower (1 to 2) for an *rnc* null mutant during this growth phase. As the wild-type cells approach late-logarithmic growth, the 16S to 23S ratio is even greater: 1 to 4. An examination of the *rrlA* and *rrlB* null mutants also at late-logarithmic growth reveals that there are fewer 23S rRNAs produced in both stains than in wild-type *B. burgdorferi*, though an *rrlA* null mutant still produces a ratio similar to that observed for wild-type *B. burgdorferi* in late-logarithmic growth (16S to 23S of 1 to 2.8 for *rrlA*). This result is not surprising; Fig. 9 shows the predicted structure of the tandem 23S rRNA gene promoter region: one promoter was removed for each of the *rrl* null mutants during homologous recombination. Unless transcription from the single remaining *rrl* gene is increased, 23S rRNA transcript levels should decrease compared to wild-type *B. burgdorferi*.

As shown in Fig. 9B, the upstream untranslated regions (UTRs) of the *rrl* genes share identical, conserved σ^{70} promoters, so we hypothesize that transcription could initiate from either promoter, synthesizing both RNAs shown in Fig. 9A. Processing of the proposed RNAs would then generate three 23S rRNA transcripts for every 16S rRNA transcript, if the mechanism of regulation for the rRNA genes is the same. Finally, as *B. burgdorferi* reaches stationary phase, the amount of total rRNA decreases, and the ratio of 16S to 23S rRNA decreases (1 to 1.4). Notably, in the *rnc* null mutant, this ratio remains very similar for both mid-logarithmic (1 to 2.1) and stationary phase (1 to 2.2). Finally, the ratio of 16S to 23S rRNA in isolated *B. burgdorferi* ribosomes is 1:1.4, supporting our data for an excess of 23S rRNA in *B. burgdorferi* cells during normal growth.

Table 5. 16S rRNA to 23S rRNA ratios in *B. burgdorferi*

***B. burgdorferi* strain**	**Growth phase**	**Ratio of 16S:23S rRNA**
B31 (5A4) wild type	mid-logarithmic	1:3
B31 (A3) wild type	mid-logarithmic	1: 2.4
297 (BbAH130) wild type	mid-logarithmic	1:2.5
B31 (A3) *rnc* null	mid-logarithmic	1: 2.1
297 (BbAH130) wild type	late-logarithmic	1:4
297 (BbAH130) *rrlA* null mutant	late-logarithmic	1:2.8
297 (BbAH130) *rrlB* null mutant	late-logarithmic	1:2.2
297 (BbAH130) wild type	stationary phase	1:1.4
297 (BbAH130) *rnc* null	stationary phase	1:2.2
B31 (A) wild type isolated ribosomes	N/A	1:1.4

Fig. 9. 23S rRNA gene promoter regions

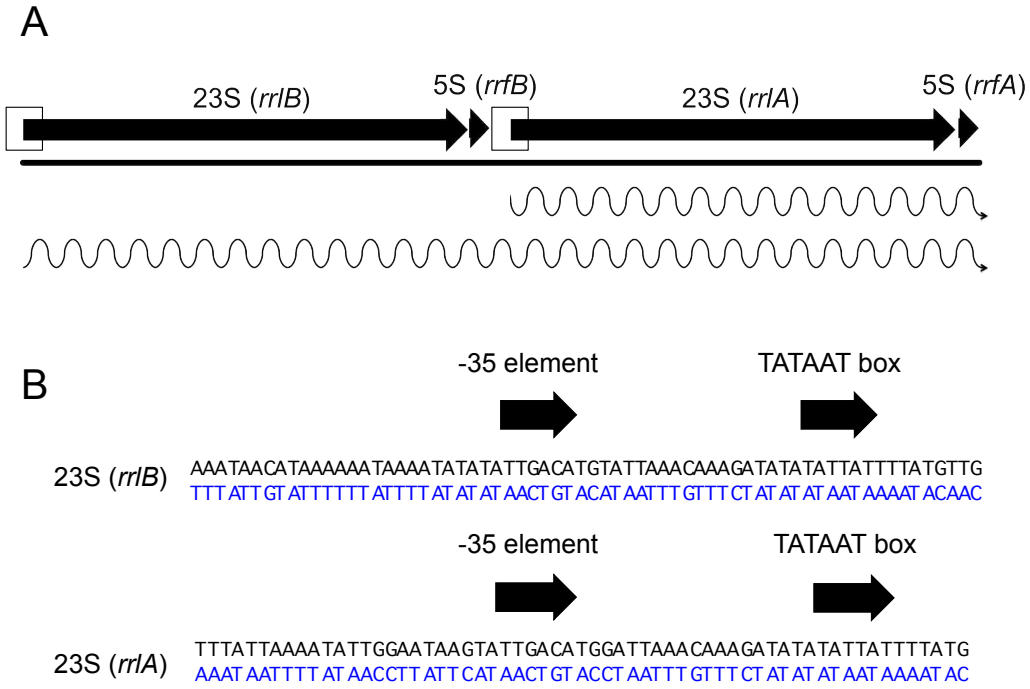

Model of *B. burgdorferi* 23S-5S rRNA operon transcription. A. Tandem 23S-5S rRNA operon region and proposed 23S-5S rRNA transcription products (squiggly lines). The locations of identical promoter regions detailed in 9B are indicated by black boxes. B. 23S rRNA promoter regions are identical for *rrlA* and *rrlB*. Core promoter elements (-35 elements and TATAAT boxes) are shown by black arrows above the *rrlA* and *rrlB* double-stranded DNA sequences.

Primer extension analysis of SNPs from RNA

The ratio of 16S to 23S rRNA transcripts observed by qRT-PCR suggested that both copies of the tandem 23S-5S rRNA operons were used to synthesize rRNA. However, the quantity of complete ribosomes in the cell is limited to the amount of 16S rRNA available to bind 23S and 5S rRNA in the mature ribosome. To examine whether the observed SNPs caused a bias in which 23S rRNA gene transcript was preferentially

selected for ribosome assembly, we performed a primer extension assay on *B. burgdorferi* ribosomes and total RNA (from strain B31-A) using a primer specific for a single SNP difference (Table 3) between the two strains. Transcripts from both 23S rRNA gene copies (*rrlA* and *rrlB*) are present in total RNA (indicating transcription of both genes) and in isolated mature 70S ribosomes (suggesting that there is no SNP-specific bias for transcript selection) for both strains (Fig. 10). Additionally, the ratio shown by the differences in band densities appears to be the same in both total RNA and isolated ribosomes; these data indicate that the 23S rRNA transcripts are incorporated into ribosomes randomly, at the ratio produced. This result is not surprising, as the promoter regions are identical (Fig. 9) and the SNP locations do not offer a rationale for selection (Table 4). Finally, the differences in band densities observed by eye between the two transcripts likely reflect promoter usage.

Fig. 10. 23S rRNA transcripts from *rrlA* and *rrlB*

A

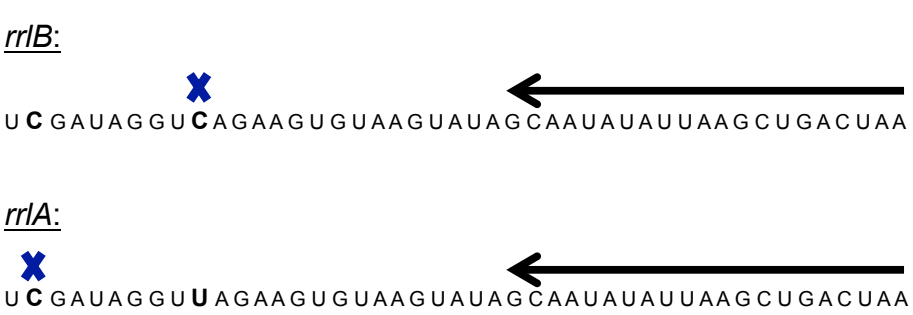

B

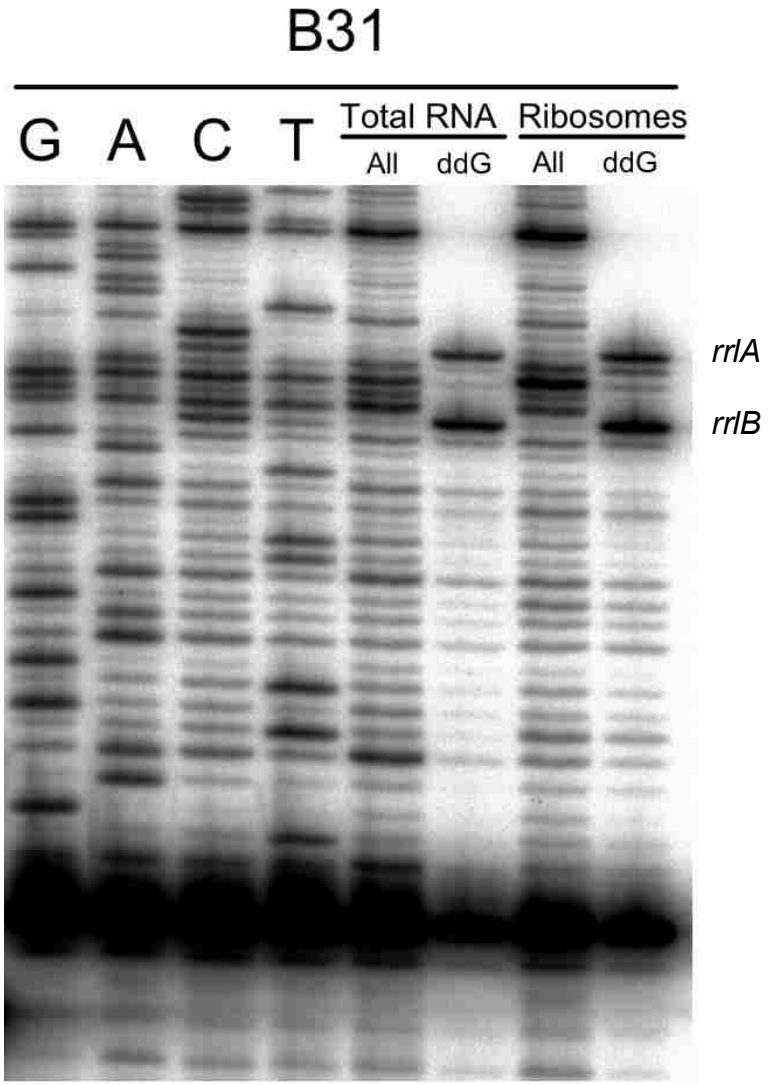

Primer extension analysis of total RNA and isolated ribosomes from *B. burgdorferi* showing that transcripts from both 23S rRNA genes are present in total RNA and mature ribosomes. A. Schematic depicting the SNP location differences and expected primer extension product sizes (terminating at the "X" above the sequence) between the *rrlB* and *rrlA* genes of strain B31. ^{32}P-ATP was used to radiolabel an oligonucleotide probe (Table 3) downstream of the sequenced SNP (black arrow above the nucleotide sequence). Primer extension analysis was performed using a single dideoxynucleotide complementary to the SNP (ddG) to terminate the chain at the first cytosine (represented by the "X" above the nucleotide sequence for each *rrl* gene). B. Phosphorimage showing radiolabeled primer extension products. G, A, C, T lanes: Sequencing lanes for Sanger sequencing of the rRNA template. B31 Total RNA lane: (contains total RNA as a template); "All" contains all four ddNTPs and dNTPs; "ddG" contains only ddGTP and all four dNTPs. The same reactions were performed using purified ribosomes as a template (Ribosome lanes: "All" and "ddG"). Ribosome preparations from *B. burgdorferi* stain B31-A were a generous gift from Paula Schlax (Bates College). The primer extension experiment and gel electrophoresis were performed by Emily Hedrick of the Hill laboratory (The University of Montana, Missoula).

An *rrlB* null mutant exhibits a growth phenotype *in vitro* and is non-infectious *in vivo*

We examined the *rrlA* and *rrlB* null mutants for *in vitro* growth characteristics (Fig. 11), ability to compete *in vitro* with wild-type *B. burgdorferi* (Table 6), and capability of infecting mice after needle inoculation. During *in vitro* growth (Fig. 11), the *rrlA* null mutant grew indistinguishably from wild type, with both cultures reaching a cell density of 10^5 cells ml^{-1} after two days of growth, and stationary phase at 4 d of growth. The *rrlB* mutant, on the other hand, had not progressed past its starting density of 10^4 cells ml^{-1} after 2 d of growth and remained several logs lower than the *rrlA* null mutant

and wild type until reaching a maximal stationary phase at 7 d post-inoculation. Initial entry into stationary phase was delayed by 2 d as compared to the *rrlA* null mutant and wild-type *B. burgdorferi* (4 d versus 6 d).

Fig. 11. An *rrlB*, but not an *rrlA*, null mutant exhibits a growth phenotype

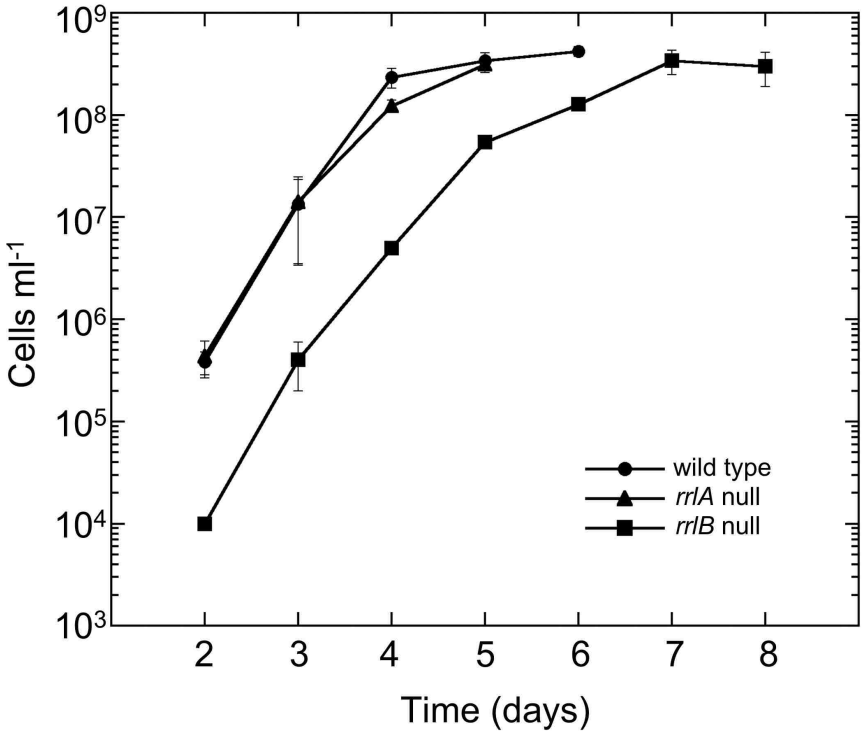

A *B. burgdorferi rrlB,* but not an *rrlA*, null mutant exhibits a growth defect *in vitro*. *B. burgdorferi* wild type and the *rrlB* and *rrlA* null mutants were inoculated in BSK II liquid medium at a cell density of 5 x 10^3 or 1 x 10^4 cells/ml and grown in a 34°C incubator until stationary phase. Cells were enumerated every 24 hours using a Petroff-Hausser counting chamber (2, 3). Growth curves were plotted on a logarithmic scale over time for all three strains.

When placed into direct *in vitro* competition with wild-type *B. burgdorferi* (Table 6), the *rrlA* null mutant was able to successfully compete and accounted for

approximately 60% to 62% of the cells in competition cultures after both 60 generations and 120 generations at 34°C. The *rrlB* null mutant failed to compete with wild-type *B. burgdorferi* as no cells were isolated from competition cultures after 60 or 120 generations at 34°C. The slower growth of the *rrlB* null mutant likely contributed to this finding, though other factors may contribute, as the *rrlB* null mutant is capable of attaining wild-type levels of growth in a longer span of time (Fig. 11).

Table 6. An *rrlB* null mutant cannot outcompete wild type during *in vitro* growth

	Percent of antibiotic-resistant colonies present at:	
***B. burgdorferi* strains (mixed 50:50 in a single culture tube)**	**60 generations**	**120 generations**
297 (BbAH120) wild type + *rrlA* null mutant	60 ± 16 (*rrlA* null)	62 ± 13 (*rrlA* null)
297 (BbAH120) wild type + *rrlB* null mutant	0 ± 0 (*rrlB* null)	0 ± 0 (*rrlB* null)

Duplicate independent experiments were performed with each set of competition strains; experimental data collected for both experiments for each set are presented here.

The *rrlA* and *rrlB* null mutants were needle-inoculated into mice using a technique that mimics tick transmission into the mammalian host. Wild-type *B. burgdorferi* was also needle-inoculated as a control. Ear punches were taken three weeks post-infection and allowed to grow at 34°C for one week before examination by dark-field microscopy. After one week, the wild type and *rrlA* null mutant had grown in all three independent ear punch cultures; no spirochetes were observed for the *rrlB* null mutant cultures. At five weeks post-inoculation, ear punches, bladders, and tibiolateral joints were collected and placed into culture tubes at 34°C; these cultures were also

examined for spirochete growth after one week. As observed for the initial ear punches, all cultures for the wild type and *rrlA* null mutant were positive after one week of growth at 34°C; none of the *rrlB* null mutant cultures exhibited any spirochete growth. The week three *rrlB* null mutant ear punch cultures and five-week ear, bladder, and tibiolateral joint cultures were incubated for an extended period of time to ensure that the growth phenotype was not causing a delay in spirochete culture. After three additional weeks of growth for the week three ear punch cultures and two additional weeks of growth for the week five cultures, no spirochetes were observed during examination by dark-field microscopy. The absence of the *rrlB* null mutant in these cultures was confirmed by PCR using flagellin gene-specific primers (Table 3). Therefore, an *rrlA* mutant is capable of infecting mice by needle inoculation while an *rrlB* null mutant is non-infectious.

Table 7. An *rrlB* null mutant is non-infectious in mice.

5 week post-infection organ cultures	Number of positive mice by culture		
***B. burgdorferi* strain**	**Ear**	**Joint**	**Bladder**
297 (BbAH130) wild type	3/3	3/3	3/3
297 *rrlA* null mutant	3/3	3/3	3/3
297 *rrlB* null mutant	0/3	0/3	0/3

Antibiotic resistance capacity of *B. burgdorferi* single 23S rRNA gene mutants

We selected two antibiotics that target the large ribosomal subunit (chloramphenicol and erythromycin) to test the hypothesis that maintenance of the tandem 23S rRNA genes confer reduced antibiotic susceptibility to *B. burgdorferi*. The *rrlA* and *rrlB* null mutants were inoculated alongside wild-type *B. burgdorferi* into 96-well plates containing a range of each antibiotic. After a 7-d incubation, positive control wells had completely changed color, indicating a culture at stationary phase. However, due to the reduced growth rate of the *rrlB* mutant (Fig. 11), plates were incubated for an additional 4 d before data were recorded to eliminate slow growth as a variable for the observed results. The same results as at 11 d were also observed at 14 d post-inoculation (data not shown). Fig. 12 shows that all three *B. burgdorferi* strains tested exhibited similar patterns of resistance to chloramphenicol. However, the growth end-point for the *rrlB* null mutant when challenged with erythromycin was at an antibiotic concentration twofold lower than that observed for the wild type or *rrlA* null mutant (0.00025 μg ml^{-1} versus 0.0005 μg ml^{-1}), indicating that loss of some aspect of *rrlB* gene regulation or the promoter region confers increased susceptibility of *B. burgdorferi* to erythromycin.

Fig. 12. The *rrlB* null mutant shows increased sensitivity to erythromycin *in vitro*.

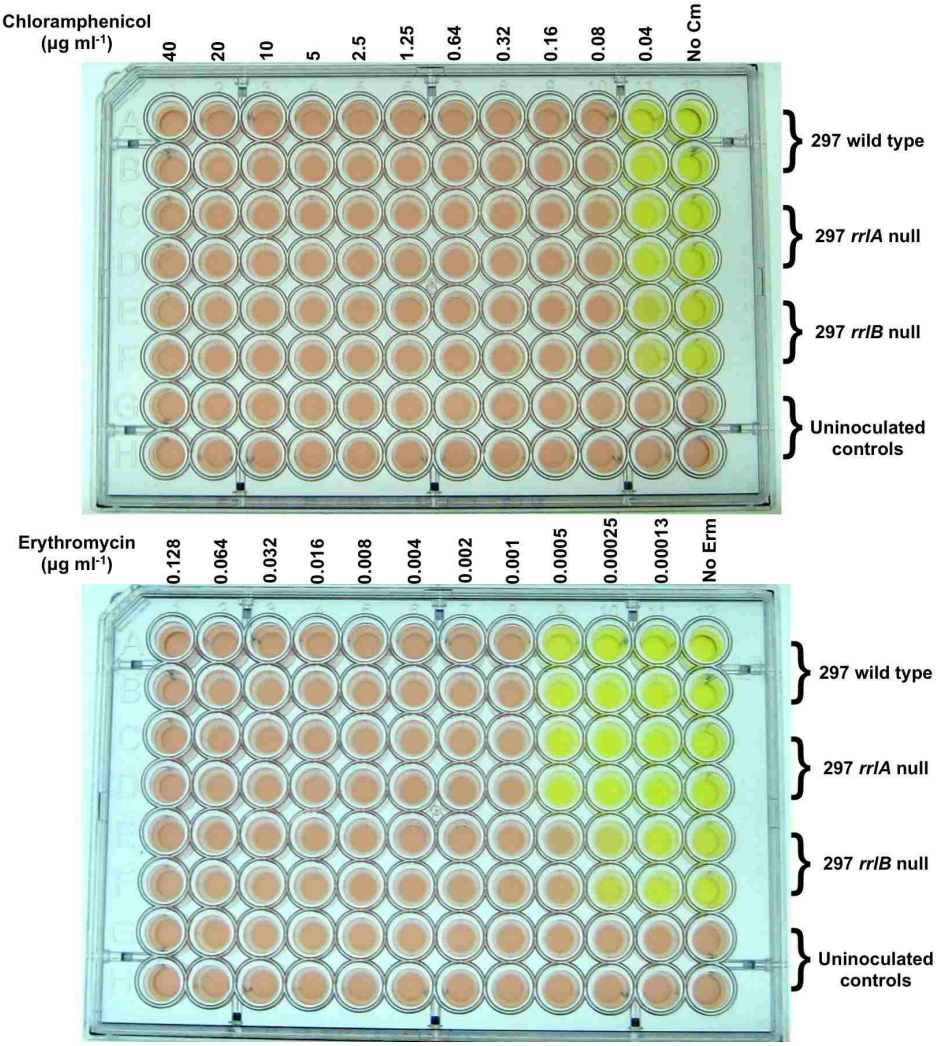

The *rrlB* null mutant is more susceptible to erythromycin than the wild type. Three *B. burgdorferi* strains (297 wild type, *rrlA* null mutant, and *rrlB* null mutant) were inoculated (in duplicate rows) into 96-well plates at a concentration of 10^5 cells ml^{-1} per well. Two rows containing no B. burgdorferi were used as controls. Antibiotics (chloramphenicol or erythromycin) were added to each well at the appropriate concentration (µg ml^{-1}) to create a two-fold dilution scheme (indicated above the plate image). The experimentally determined minimum inhibitory concentration (MIC) for each antibiotic was used as a mid-point for the experiment with twofold dilutions of the antibiotic on either side. Erythromycin: MIC of 0.004 µg ml^{-1} (4) and chloramphenicol: MIC of 1.25 µg ml^{-1} (6). Plates were incubated in 1.5% CO_2 at 34°C for one week before inspection of media color change (pink wells indicate a lack of growth; yellow well signify a media pH change and are indicative of growth). As the *rrlB* null mutant grows slower than the other two strains used for the assay (Fig. 11), data were collected at 11 d post-inoculation. Plates were checked a final time at 14 d post-inoculation and an identical pattern of media coloration observed to 11 d (data not shown).

Insights into the unusual rRNA gene operon of *B. burgdorferi*

Due to the physical separation of the 16S rRNA gene from the 23S-5S rRNA operon and the tandem duplication of the 23S-5S rRNA operon, regulation of the *B. burgdorferi* rRNA genes is expected to be different than that of most bacteria. The 16S rRNA gene appears to be co-transcribed as part of a larger operon independent of the 23S-5S rRNA operons (Fig. 8). As is common with duplicated genes, the 23S rRNA genes of *B. burgdorferi* have accumulated SNPs, though, intriguingly, the location of these SNPs varies between sequenced strains (Table 4). In accordance with the tandem 23S rRNA genes containing identical σ^{70} promoters, the ratio of 16S rRNA to 23S rRNA is not equimolar, suggesting a possible role for the extra 23S rRNA in the cell (Table 5). These ratios are lower in the *rnc*, *rrlA*, and *rrlB* null mutants (Table 5). In accordance with the hypothesis that both *rrl* genes are transcribed, primer extension analysis reveals that rRNA from both *rrl* genes is present in total RNA and incorporated into mature ribosomes (Fig. 10).

Intriguingly, the *rrlB* null mutant displays growth and morphological phenotypes (Fig. 11 and data not shown), is unable to compete with wild type in an *in vitro* competition (Table 6), and is non-infectious in mice (Table 7). The *rrlA* null mutant, on the other hand, lacks a discernible phenotype (Fig. 11, Table 6, and Table 7). Finally, the *rrlB* null mutant exhibits a twofold increase in erythromycin susceptibility, which may be due to decreased 23S rRNA or 50S ribosomal subunits in the cell, loss of the *rrlB* promoter region, or polar effects from the gentamicin cassette (Fig. 12). Altogether, these

results suggest that the rearrangement of the rRNA genes in this organism has contributed to the evolution of unique mechanisms of rRNA regulation.

Chapter 5

Discussion

Ribosomes are essential to all living cells, as they bridge the information stored in DNA to the production of proteins that carry out innumerable functions within the cell. Evolution has driven many bacterial genomes to streamline the process of rRNA transcription: most bacteria encode all three rRNA genes in single operon units on their chromosomes (of which there can be many copies). This allows for rRNA transcription to be tightly regulated for the production of equimolar ratios of the three rRNA transcripts, which leads to efficient ribosome assembly. However, not all organisms possess this tidy rRNA genome arrangement. *B. burgdorferi*, the Lyme disease bacterium, possesses an rRNA gene region with an unusual and unique organization: the 16S rRNA gene is encoded more than 3 kb upstream from the 23S and 5S rRNA genes; the 23S-5S rRNA operons are tandemly duplicated on the chromosome. This novel organization has likely resulted from rearrangement during genome reduction as the spirochete has adapted to a parasitic lifestyle that requires a tick vector and mammalian host. In this work, we have gained additional insight into the novel mechanism of rRNA gene transcription and ribosome assembly in *B. burgdorferi*, including the role of initial *B. burgdorferi* rRNA processing by the highly conserved RNase III.

Our results reveal that *B. burgdorferi* RNase III functions in a canonical manner and that RNase III is likely an important enzyme to members of the Spirochaetae, as in other bacterial phyla. RNase III processes the 23S rRNA transcribed from the unusual tandem 23S-5S rRNA operons as expected. However, while the enzyme processes the 3′

end of the 16S rRNA, it is not required to process the 5′ end of 16S rRNA, a novel finding from this work. This is likely due to the unique genomic location of the 16S rRNA as part of a larger operon that does not contain other rRNA genes. Further probing of the 23S rRNA genes reveals that they are accumulating SNPs, that *B. burgdorferi* utilizes both *rrl* gene copies to produce an excess of 23S rRNA as compared to 16S RNA, and that mutation of the first (*rrlB*), but not the second (*rrlA*), 23S rRNA gene causes a phenotype.

All of these findings suggest that after the rearrangement of its rRNA genes, *B. burgdorferi* has adapted a unique mechanism of rRNA production. This dissertation details the exploration of rRNA transcription and ribosome biogenesis from an unusual rRNA operon that includes tandem 23S rRNA genes, a feature unique to Lyme disease *Borrelia*. Altogether, our results suggest that novel ribosome biogenesis regulatory mechanisms are at work in *B. burgdorferi* that have not been observed in other bacteria to date and are the product of the unusual rRNA operons of this organism.

Characterization of *B. burgdorferi* RNase III

This study is the first characterization of an RNase III homolog from a spirochete. As RNase III homologs can often, but not always, functionally substitute for each other (217, 218, 219, 220), we first attempted heterologous complementation of a *B. subtilis* lethal *rncS* mutant (BE600) (7). The *B. burgdorferi rnc* gene was able to complement a *B. subtilis rncS* mutant (Fig. 2), suggesting that its function is conserved. Although there are several examples of *B. burgdorferi* genes complementing *E. coli* mutants (57, 91, 256,

263, 264, 265, 266, 267, 268, 269, 270), this study is, to our knowledge, the first example of a *B. burgdorferi* gene complementing a *Bacillus* mutant.

RNase III is essential in *B. subtilis* (7), but not in *E. coli* and *S. aureus* (260, 261, 271). A study was recently published detailing the reason for RNase III essentiality in *B. subtilis* (173). Several prophages within the genome produce toxin/antitoxin mRNAs that yield protein products toxic to the *B. subtilis* host cell if present in high enough density. RNase III selectively cleaves the double-stranded toxin-antitoxin mRNA interface, preventing these molecules from being translated (173). Our experimental data (Fig. 2) clearly demonstrate that *B. burgdorferi* encodes an RNase III that is capable of at least partially protecting *B. subtilis* from these molecules, as well as likely fulfilling other characteristic roles of this enzyme in the cell such as rRNA processing.

Notably, the cp32 plasmid of *B. burgdorferi* appears to encode a prophage (81, 82, 91, 92). However, unlike the *B. subtilis* prophage, the known gene products of cp32 enhance *B. burgdorferi* immune evasion and other host interactions (40, 46, 74, 77, 272, 273, 274, 275, 276). RNase III may play a role in regulating mRNAs or non-coding RNAs (ncRNAs) from cp32 or any of the other *B. burgdorferi* plasmids. Given the conservation of some plasmids among all sequenced *B. burgdorferi* strains (including lp54, cp26, and the cp32s) and the lack of endo- and exoribonuclease homologs in *B. burgdorferi* (Tables 1 and 2), plasmid gene products requiring processing probably serve as RNase III substrates (74, 75, 77).

Our *B. burgdorferi rnc* mutant grows slower and reaches a lower cell density at stationary phase than wild type (Fig. 3C). The growth phenotype is likely due to defective ribosomes and an excess of partially processed pre-rRNA, as shown in *E. coli* and *B.*

subtilis (7, 157, 213, 214, 215, 261, 262). RNase III also processes mRNA in order to globally regulate transcript levels (173, 221, 222, 223, 260, 277, 278, 279, 280, 281, 282, 283, 284, 285, 286, 287). An additional role for RNase III in *S. aureus* was found in ncRNA regulation as well as mRNA regulation (283). Loss of mRNA and ncRNA regulation may also contribute to the growth and morphological phenotype of our *B. burgdorferi rnc* mutant (Fig. 3C, 3D).

Dark-field microscopy of individual *B. burgdorferi rnc* mutant cells revealed a long-cell phenotype (Fig. 3C) that might be associated with delayed or improper cell division due to inefficient translation or production of defective cell division machinery. Curiously, the *rnc* mutant population also contained cells of a normal length (Fig. 3C), yielding a bimodal distribution of lengths (Fig. 3D), a phenotype also observed for a *B. burgdorferi hfq* mutant (256). Backup pathways involving alternative RNases may be at work in these cells, as in *E. coli*, but the process is slow, resulting in a subpopulation of normal-length cells (271). Cells could also be accumulating suppressor mutations that promote growth in the absence of RNase III. Indeed, given the length of time to culture a successful *B. burgdorferi* rnc null mutant (90 d), it is likely that suppressor mutations were gained following initial transformation of the *rnc* null recombinant construct that allowed *B. burgdorferi* to grow in the absence of RNase III. Suppressor mutations in an RNase III null mutant background are not without precedence (7, 216) and might explain why isolation of an *rnc* null mutant in *B. burgdorferi* is a rare event.

The *rnc* gene is located on the linear chromosome molecule of *B. burgdorferi* as the final gene in a five-gene operon (Fig. 7). Upstream genes include *bb0701* (encoding a conserved hypothetical protein), *coaD* (encoding pantetheine-phosphate

adenylyltransferase), *rpmF* (encoding ribosomal protein L32), and *acpP* (encoding acyl carrier protein). Two genes in this operon are involved in transcription and translation (*coaD* and *rpmF*, respectively). As RNase III contributes to proper maturation of the ribosome and global mRNA regulation, this operon structure is not surprising. Additionally, as RNase III autoregulates *rnc* transcription through a feedback loop in other bacteria (221, 222, 223), it is possible that the slow growth in the *B. burgdorferi* rnc null mutant can be partially attributed to dysregulation of the *rnc* operon following the loss of this control mechanism. A suppressor mutation that relieves the inhibition caused by improper *rnc* autoregulation might be present in our *rnc* null mutants. Taken together, these results suggest that while RNase III is not essential in *B. burgdorferi*, it is a vital contributor to RNA metabolism in this organism.

Role of RNase III in *B. burgdorferi* ribosomal RNA processing

The primary role for RNase III is rRNA processing of the 16S and 23S rRNAs prior to ribosome assembly(78), so we hypothesized that this would be conserved in *B. burgdorferi* in spite of the unusual rRNA operon architecture. We assayed processing by determining the 5′ and 3′ ends of the mature rRNAs in the *B. burgdorferi rnc* null mutant. Comparison of wild-type *B. burgdorferi* and the *rnc* null mutant by 5′ and 3′ RACE revealed that the 23S and 5S rRNA transcripts are processed in a canonical fashion, in spite of the tandem gene duplication (Figs. 4 and 13B). The 23S rRNA is 15 nucleotides longer at the 5′ end and about 18 nucleotides longer at the 3′ end in the *rnc* null mutant. These data suggest a model for 23S rRNA processing in the *rnc* null mutant. The 23S

rRNA 5′ end in the *rnc* null mutant almost certainly maps to the transcriptional start site as it is approximately 20 nucleotides downstream from the predicted promoter(s), suggesting that no nucleolytic processing is taking place to generate this end (Fig. 13B). On the other hand, the 23S rRNA 3′ end in the *rnc* null mutant maps to the 5′ end of the 5S rRNA unprocessed stem (Fig. 13B), suggesting that exoribonucleases might be responsible for processing this end. In addition, PCR across the junction between the two 5S-23S rRNA operons demonstrated an increase in the amount of a large precursor transcript in the *rnc* null mutant, suggesting a decrease in endonucleolytic processing (Fig. 5). This result is not without precedence, as a 30S unprocessed rRNA species is observed in both *B. subtilis rncS* and *E. coli rnc* null mutants (7, 157, 213, 214, 215). An addition of greater than two nucleotides to the 3′ end of the 23S rRNA can cause a delayed assembly of the mature ribosome subunits (193), which might contribute to the growth phenotype observed in our *rnc* null mutant (Fig. 3C). The 5S rRNA transcript, on the other hand, shows no difference in the 5′ and 3′ rRNA processed ends in the wild type and *rnc* null mutant. These data are also expected, as processing of the 5S rRNA is carried out by RNase E in *E. coli* and RNase M5 in *B. subtilis* (162, 163). *B. burgdorferi* possesses a homolog (BB0626) of RNase M5 (Table 1).

We generated a radiolabeled artificial *B. burgdorferi* 23S substrate containing the double-stranded stem recognized by RNase III (Fig. 6A). When incubated with recombinant RNase III, cleavage products were observed in increasing abundance with the addition of increasing concentrations of enzyme (Fig. 6B). These data show that *B. burgdorferi* RNase III specifically binds and processes the double-stranded 23S rRNA stem structure. This result is not surprising, as the 23S rRNA stem contains identifiable

proximal and distal box elements with no anti-determinant nucleotide sequences (205, 206, 207, 208, 209). The RACE results (Fig. 4) also support these data. We conclude from these data that RNase III processes the 23S rRNA along a canonical pathway in *B. burgdorferi* in spite of the unusual rRNA gene arrangement.

Fig. 13. Model for initial 16S and 23S rRNA processing in *B. burgdorferi*

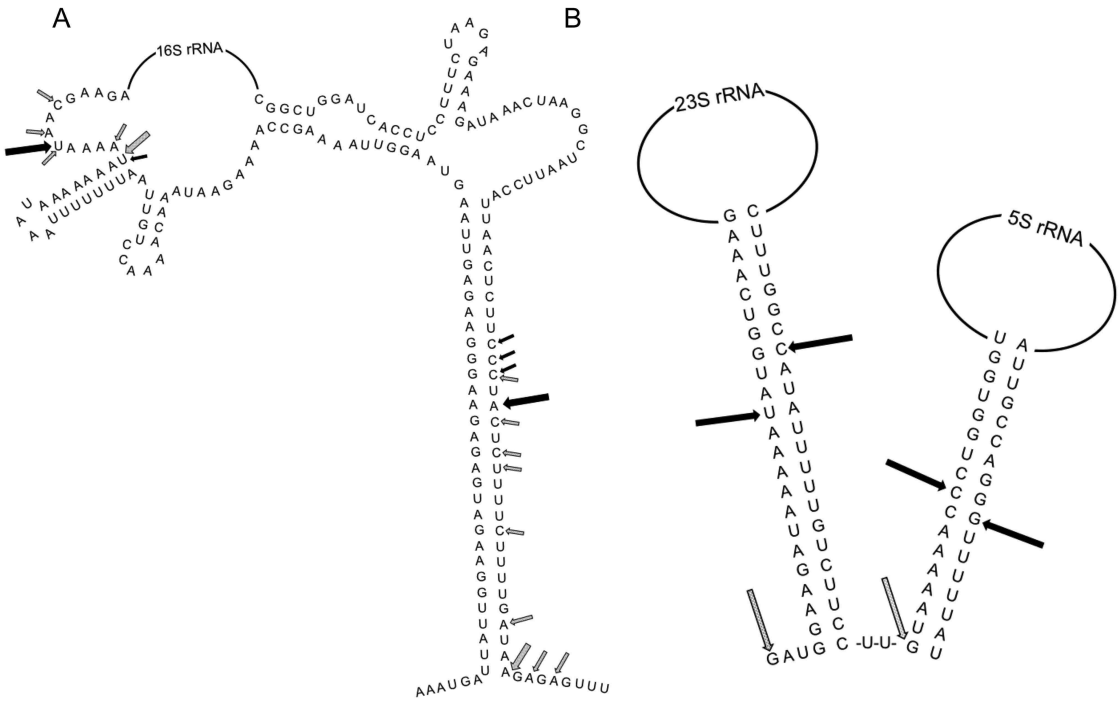

A. Structural model showing the 16S rRNA 5′ and 3′ UTR predicted stem structure. B. Structure of the 23S and 5S double-stranded stem regions (based on Schwartz *et. al* (1) model). Experimentally determined 5′ and 3′ transcript ends for the three rRNAs (16S, 23S, and 5S) based on 5′ and 3′ RACE data (Fig. 4) are represented by black arrows (wild type) and gray arrows (*rnc* null mutant) on the structure. Clear double-stranded stem structures capable of being processed by RNase III are present for the 16S rRNA 3′ end (Fig. 13A) and the 23S rRNA 5′ and 3′ ends (Fig. 13B). In the *rnc* null mutant, the 5′ end of the 23S rRNA likely maps to the transcription start site and the 3′ end is positioned between the 23S and 5S rRNA double-stranded stems and might be processed by exonucleases following RNase M5 cleavage of the adjacent 5S rRNA double-stranded stem. The 5′ end of the 16S rRNA is in a region of stem-loop secondary structure, and does not represent an ideal RNase III substrate (Fig. 13A). The current mechanism required for generation of the 16S rRNA 5′ end is currently unknown, but RNase III does not appear to be involved. The 5′ and 3′ ends of the *B. burgdorferi* 5S rRNA are the same in both the wild type and *rnc* null mutant, as expected (data not shown).

The 16S rRNA gene is spatially separated from the 23S-5S rRNA operons on the chromosome in *B. burgdorferi*. A truncated ORF (*bb0425*) is present upstream and $tRNA_{Ala}$ is downstream of the "marooned" 16S rRNA gene. Junctional RT-PCR data indicate that the 16S rRNA is co-transcribed with the two upstream genes (Fig. 8) and Bugrysheva *et al.* (5) showed that the $tRNA_{Ala}$ was co-transcribed with the 16S rRNA gene, yielding a large polycistronic transcript. An mfold structure (288) of the 16S rRNA 5′ and 3′ flanking regions suggests that the 5′ end of the 16S rRNA transcript lies within a region containing several loops that might interfere with RNase III binding (Fig. 13A). Data from 5′ RACE analysis (Fig. 4) indicate that the 16S rRNA 5′ end is the same in both the *rnc* null mutant and the wild type, implying that RNase III is not required for generating the 5′ end. This phenomenon has not previously been observed in bacteria. The 3′ end, on the other hand, does appear to be processed by RNase III in *B. burgdorferi*.

The predicted structure of the 16S rRNA precursor (Fig. 13A) includes a long double-stranded stem region around the mature 3′ end of the 16S rRNA, which could be a reasonable RNase III substrate. Notably, the mature 16S rRNA 3′ end in both the wild-type and *rnc* null mutant backgrounds maps to over 40 nucleotides downstream from the annotated end (Fig. 4). We propose the following model for generation of the observed 16S rRNA 3′ end in the *rnc* null mutant. RNase P processing of the $tRNA_{Ala}$ 5′ end downstream of the 16S rRNA would release a region of single-stranded RNA that could undergo subsequent processing by a single-stranded exonuclease (PNPase) and single-stranded endonuclease (YbeY) up to the region of the 16S rRNA double-stranded stem, as observed in *E. coli* (176, 177, 215).

The mechanism of 16S rRNA 5′ end maturation is currently unknown in *B. burgdorferi*. An mfold structure containing the mature 16S rRNA 5′ end as determined by RACE (Fig. 13A) shows that the mature end of this rRNA likely maps to a large single-stranded loop region. A self-processing mechanism involving a ribozyme activity of the nascent 16S rRNA may generate the 5′ end of the transcript in *B. burgdorferi* (289, 290). However, a more likely scenario is that an endoribonuclease such as RNase Y processes the AU-rich region of the loop (its preferred nucleotide substrate) (240), with or without prior RNase III cleavage of the stem structure formed near the 3′ end of the rRNA transcript, to generate the mature 16S rRNA 5′ end (Fig. 13A). This enzyme, of which *B. burgdorferi* has a clear homolog identified in this work, was originally characterized for its role in riboswitch degradation in *B. subtilis* (240), and later for its role in global mRNA degradation (239, 240, 241, 242, 243, 244, 245, 246). This phenomenon probably occurs in other *Borrelia* species given the conserved separation of the 16S rRNA gene from the 23S-5S rRNA operons throughout the genus (94).

The 16S rRNA operon structure

In addition to the novel processing mechanism that generates the 5′ end of the 16S rRNA (Fig. 4, 13A), the operon structure of the 16S rRNA gene of *B. burgdorferi* appears have been modified during genome reduction. No clear promoter is discernible near the 5′ end of the 16S rRNA gene (data not shown). This observation prompted us to examine this genome region through junctional RT-PCR analysis (Fig. 8A). Surprisingly, the 16S rRNA gene appears to be transcribed as part of a larger operon, and contains the

overlapping truncated gene *bb0425* and the upstream genes *bb0426*, a member of the nucleoside 2-deoxyribosyltransferase protein superfamily, and *bb0427*, a predicted methyltransferase (Fig. 8B, 14). Co-transcription of the 16S rRNA gene with genes other than the 23S and 5S rRNA genes or intervening tRNA genes is novel to *B. burgdorferi* and suggests a unique adaptation to the conserved mechanism of rRNA gene regulation. An intriguing hypothesis is that the co-transcribed genes of the 16S rRNA operon are constitutively transcribed with the 16S rRNA gene but only translated under certain conditions. This would allow for *B. burgdorferi* to exert temporal control over the translation of the DNA modification enzymes produced by *bb0426* and *bb0427*. Overall, this gene rearrangement likely contributed to the divergence of RNase III processing of the 16S rRNA 5′ end in *Borrelia*.

tRNA can serve as sites of recombination for mobile genetic elements (93, 107, 108). There are two tRNA genes ($tRNA_{Ala}$ and $tRNA_{Ile}$) directly downstream from the 16S rRNA gene (Fig. 14), which could have served as sites for recombination during the genome reduction of *B. burgdorferi* as it adapted to a parasitic lifestyle between vector and host. Additionally, the 16S rRNA gene overlaps a truncated ORF (*bb0425*) that could produce a very short protein of 30 amino acids (Fig. 14). A second truncated ORF that could produce a 97-amino acid protein (*bb0423*) is located directly upstream of the $tRNA_{Ile}$ gene (Fig. 14). We hypothesize that tRNA recombination during genome reduction led to the insertion of the 16S rRNA gene into the center of a larger gene composed of *bb0425* and *bb0423*, which directly led to this unusual operon structure where transcription of the 16S rRNA gene requires transcription of several upstream

genes. The $tRNA_{Ile}$ gene and *bb0424* truncated ORF may have been part of additional recombination events in this region (Fig. 14).

Fig. 14. The tRNA genes of the 16S rRNA operon suggest a mechanism for recombination

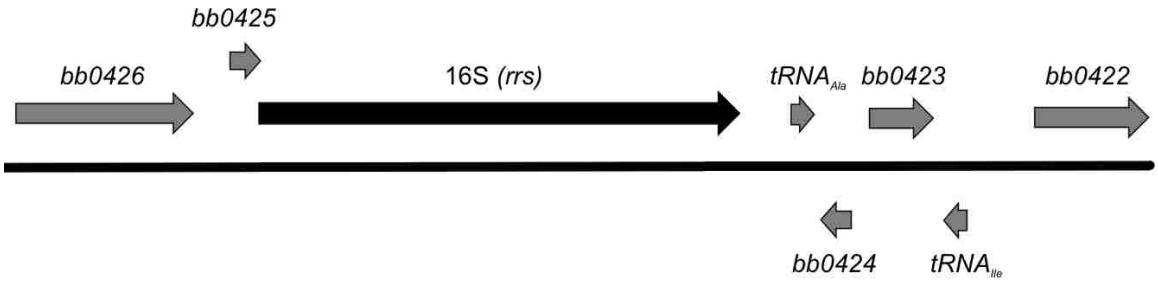

The tRNA genes of the 16S rRNA operon suggest a mechanism for recombination. Two tRNA genes are located downstream of the 16S rRNA gene ($tRNA_{Ala}$ and $tRNA_{Ile}$). We hypothesize that the 16S rRNA gene and $tRNA_{Ala}$ were originally recombined by insertion into a larger gene composed of *bb0425* and *bb0423*. Additional recombination events involving insertion of the second tRNA, $tRNA_{Ile}$, and *bb0424* further divided the *bb0425* and *bb0423* genes. *bb0424* is also likely a truncated ORF.

Insights into conservation of the tandem 23S-5S rRNA genes

The conserved tandem duplication of the 23S-5S rRNA genes is a feature that is unique to Lyme disease *Borrelia* species. While there are mechanisms that promote duplication of the rRNA genes in bacteria (110), the fact that this arrangement is conserved across a diverse array of Lyme disease *Borrelia* species (1, 94, 95, 98, 99) suggests a possible function in *Borrelia* biology. Intriguingly, this duplication leads to an imbalance in the number of complete rRNA gene sets (16S, 23S, and 5S) in *B. burgdorferi*. We originally hypothesized that the 23S-5S rRNA operons were

differentially regulated from the 16S rRNA gene to produce a 1:1:1 stoichiometric ratio of rRNA. However, qRT-PCR analysis (Table 5) suggests a different outcome of this tandem duplication. In wild-type *B. burgdorferi*, there is 2.5 to 3 times more 23S rRNA present during mid-logarithmic growth than 16S rRNA. In spite of this finding, the number of ribosomes present in *B. burgdorferi* is limited by the amount of 16S rRNA present in the cell. This led us to analyze the accumulation of single nucleotide polymorphisms (SNPs) in all sequenced *B. burgdorferi* strains, including sequencing of the 297 strain in this work to determine if there was a sequence-related rationale for producing an excess of 23S rRNA.

The tandem 23S rRNA genes of *B. burgdorferi* have several SNPs in all sequenced strains (Table 5). However, there exists no consensus for a SNP locus common to all strains, suggesting that these are the product of genetic drift. Indeed, the SNPs appear to be distributed throughout the 23S rRNA gene and are present in different densities and locations between strains. The only common feature that is clearly present is that these SNPs are the product of either purine-purine or pyrimidine-pyrimidine transitions. This form of base mutation is much more common than nucleotide transversion due to the similarities of ring structure within each class of nucleotide (291) which mutate to resemble their purine or pyrimidine counterpart after deamination (e.g. 5-methylcytosine deaminates to thymine) and other nucleotide base modifications that commonly arise over time. After mutation, mispairing occurs between pyrimidine and purine nucleotides to create a new set of base paired nucleotides after DNA replication (e.g. a C-G basepair becomes a T-A basepair following deamination of the 5-methylcytosine).

There are a few structural features of the 23S rRNA that are required for its role in translation, particularly domain V, which catalyzes the peptidyl transferase reaction between incoming amino acids and the nascent peptide chain, and may be influenced by these SNPs. An examination of the primary sequence structure of the *B. burgdorferi* 23S rRNA shows that there is only a single SNP in strain N40 at position 2201 that is within this domain. As it is a C-T transition in the N40 *rrlA* gene (or C-U transition in the rRNA molecule), the structure of these two alleles is very similar, and the transition is present in the end of a stem structure, this change does not likely have any influence on the translational capacity of the ribosome. Notably, the most abundant SNPs lie in domains II (five SNPs), III (three SNPs), and VI (four SNPs) (data not shown). These do not appear to interfere with ribosomal subunit association, which relies on 23S rRNA nucleotides A715, A1912, or A1918 (292). Although there is a functional interaction between domain II and domain V in mature ribosomes (293), the SNPs are outside the range of these interactions as well. Overall, the 23S rRNA SNPs appear to be tolerated in locations that do not affect ribosome function, which suggests that rRNA transcripts from both genes could be used in mature ribosomes.

There is a single transversion in the 297 *rrfA* sequence (data not shown). This nucleotide substitution might cause a mismatch in the double-stranded stem formed by the 5′ and 3′ ends of the mature 5S rRNA, but it is located near the internal terminus of the stem and is unlikely to have a major effect on the structure of the 5S rRNA. The accumulation of SNPs in *B. burgdorferi* could be the result of selective pressures in the vertebrate host. An example of this possibility is that the highly infectious 297 strain, which is a human isolate, possesses seven SNPs, while the lower infectivity B31 strain,

which is a tick isolate, shows only three SNPs. However, further analysis is required to determine if there is a selective mechanism for the diversity of SNPs observed in *B. burgdorferi* strains.

Our data definitively demonstrate that both tandem 23S rRNA genes in *B. burgdorferi* are transcribed and incorporated into ribosomes (Table 5, Fig. 10). qRT-PCR of *B. burgdorferi* at a variety of growth phases (Table 5) suggests that, during logarithmic growth, wild-type *B. burgdorferi* transcribes 2.5 to 3 times more 23S rRNA than 16S rRNA, and that this amount increases during late-logarithmic growth. However, upon entry into stationary phase, the amount of rRNA decreases so that there is only 1.4 times more 23S rRNA than 16S rRNA. This latter phenomenon is not unexpected, as total rRNA is reduced during stationary phase in other bacteria (134) and the nearly 1:1 ratio likely reflects the amount of rRNA required for cells to maintain themselves during stationary phase. This ratio (1:1.4 16S rRNA: 23S rRNA) is also observed for qRT-PCR of an isolated ribosome fraction and supports this hypothesis.

We also analyzed the 16S to 23S rRNA ratio in several mutants (*rnc* null, *rrlA* null, *rrlB* null). Surprisingly, the *rnc* null mutant showed similar levels of 23S rRNA during both mid-logarithmic and stationary phase growth (Table 5). We postulate that this could be the result of failure to separate a population of the long tandemly transcribed (from the *rrlB* promoter; Fig. 9) pre-23S-5S rRNA transcript. Indeed, we observe an overabundance of this transcript in the *rnc* null mutant versus wild type (Fig. 5). In this scenario, degradation of these aberrant transcripts upon entry into stationary phase may not be as efficient, so there is a greater amount of 23S rRNA in these mutants. The lower amount of 23S rRNA observed in the *rnc* mutant during logarithmic growth

could also reflect decreased transcription due to some undefined sensing mechanism that detects an abundance of unprocessed tandem 23S-5S rRNA transcript, thus reducing transcription until the cell can correctly process the transcripts.

As expected, less 23S rRNA transcript is produced during logarithmic growth in the single 23S deletion mutants *rrlA* and *rrlB* (Table 5). This likely reflects the loss of one of the 23S rRNA promoters and genes in these mutants (Fig. 9). The *rrlA* null mutant produces about a third less 23S rRNA than wild type, whereas the *rrlB* null mutant generates half as many transcripts as wild type during this growth phase (Table 5). An *rrlB* null mutant also grows slower than the *rrlA* null mutant (Fig. 11), which suggests that there is a difference in the promoter regions or promoter regulation.

We propose the following model for 23S-5S rRNA transcription in *B. burgdorferi*: the *rrlB* promoter is the dominant promoter for rRNA synthesis and, in the *rrlA* null mutant, produces the amount of rRNA required for normal growth, so our *rrlA* null mutant exhibits the same growth pattern as wild type (Fig. 11). Creating a null mutation in some, but not all, of the *rrn* operons of *E. coli* results in similar levels of rRNA as produced in wild-type cells, demonstrating that it possesses more genes than it needs for maximal rRNA production, at least during *in vitro* growth (125, 126). The *rrlB* null mutant, on the other hand, eliminates the putative major 23S rRNA promoter and relies solely on the *rrlA* promoter (Fig. 9). In agreement with this hypothesis, band densities for each *rrl* transcript visualized after primer extension analysis (Fig. 10) suggest that there are more *rrlB* transcripts present in total RNA and isolated ribosomes. We inserted a gentamicin resistance cassette into the location of the *rrlB* gene in this strain. The slow growth of our *rrlB* null mutant (Fig. 11) may instead, or in addition, be

due to some other, as yet undefined, regulatory mechanism or polar effect of the gentamicin resistance cassette.

As previously discussed, we originally hypothesized that transcription was regulated to ensure a stoichiometric production or assembly of the 16S, 23S, and 5S rRNAs. As the qRT-PCR results showed that transcription initiated from both 23S rRNA genes to produce an overabundance of 23S (and presumably 5S) rRNA (Table 5, Fig. 9), we decided to use primer extension of independent SNPs from two strains of *B. burgdorferi* in order to determine if only one of the 23S rRNA alleles was incorporated into ribosomes. Fig. 10 shows that both 23S rRNAs are produced in *B. burgdorferi*, and, furthermore, that transcripts from both genes appear to be incorporated into mature ribosomes at a ratio similar to that seen in total RNA. While these results do not suggest a role of the 23S rRNA SNPs in regulation of transcription, they do imply that both gene copies are functional and used in mature ribosomes. However, the SNPs in the *rrlA* gene (as it is dispensable for growth) could be evolving to enable *B. burgdorferi* ribosomes to differentially function under selective environmental pressures.

An *rrlB* null mutant exhibits *in vitro* and *in vivo* phenotypes

To examine other factors that might contribute to the maintenance of two tandem 23S rRNA gene copies in *B. burgdorferi*, we generated null mutants for each gene and examined the resulting phenotypes under several different conditions: *in vitro* growth at 34°C (Fig. 11), *in vitro* competition with an equivalent number of wild-type cells (Table 6), ability to infect mice (Table 7), and susceptibility to antibiotics that target the large

subunit (Fig. 12). In all conditions tested, the *rrlA* null mutant had no phenotype and was able to compete with the wild type. A previously described *rrlA* null mutant generated by transposon mutagenesis also did not have a growth phenotype (103). These results are consistent with our data, and indicate that while the *rrlA* gene is transcribed and the resulting 23S rRNA is used in ribosomes, this gene is dispensable for normal growth, even during infection of the vertebrate host (Table 7).

The *rrlB* null mutant, however, displayed a definitive phenotype. While the *rrlB* mutant could reach stationary phase at the same density as the *rrlA* null mutant and wild type, growth was slower and log phase was extended by 2 d (Fig. 11). Some reasons for this phenotype are discussed above. The *rrlB* mutant also failed to compete with the wild type during an *in vitro* growth competition and was completely lost from the population by 60 generations (Table 6). The *rrlB* null mutant was also unable to infect mice after needle inoculation (Table 7) and had a twofold increase in susceptibility to erythromycin as compared to wild type (Fig. 12). While there is still twice as much 23S rRNA as 16S rRNA in an *rrlB* null mutant at late-logarithmic growth, suggesting that the maximum number of ribosomes required for growth should be produced (Table 5), some aspect of 23S rRNA regulation in *B. burgdorferi* is affected by removal of the *rrlB* promoter and *rrlB-rrfB* operon. Further research is required to elucidate whether this phenotype is the result of differential regulation of the *rrl* promoters in *B. burgdorferi* or if we are merely observing polar effects from the insertion of a gentamicin cassette at this genomic location.

Concluding remarks

This work begins to dissect the complicated rRNA gene regulation of *B. burgdorferi* and many questions remain unanswered. What is clear is that the evolution of the unusual rRNA gene arrangement in *B. burgdorferi* has led to adaptation of this organism to novel mechanisms of rRNA transcriptional regulation, including incorporation of its single 16S rRNA gene into a larger operon containing unrelated genes, and dysregulated transcription that produces an overabundance of 23S and 5S rRNA as compared to 16S rRNA. Generating null mutants in each 23S rRNA gene shows that while the second copy is dispensable for growth (*rrlA*), a profound phenotype is observed when the first copy (*rrlB*) and its promoter are deleted. While the *rrlB* null mutant can grow at a slower rate, it is incapable of infecting mice (Table 7). This suggests that the tandem duplication of the 23S rRNA genes has functional significance in *B. burgdorferi* and that there is an important regulatory mechanism to maintain the genomic arrangement. Further study will undoubtedly reveal additional novel features of this gene region and transcription products that will further our understanding of alternative mechanisms of rRNA regulation. Additionally, the overproduction of 23S rRNA in *B. burgdorferi* may be adaptive for spirochete persistence during the dual host lifestyle. There may also be an alternative use of excess 50S ribosomal subunits under different environmental conditions (such as in the tick vector or vertebrate host). However, it is also possible that the genome of *B. burgdorferi* is still in the process of limited genome reduction and that the tandem duplication of the 23S rRNA genes and

production of excess 23S rRNA will be eliminated during further evolutionary adaptation of *B. burgdorferi*.

Future work should seek to further explore the phenotype of the *rrl* null mutants, including understanding the role of transcription from each 23S rRNA gene in the context of the complete enzootic cycle. Additionally, site-directed mutagenesis or promoter swapping should be undertaken to examine the regulation of the unusual 16S rRNA operon and each of the tandem 23S-5S rRNA promoters so that a more lucid picture of *B. burgdorferi* rRNA transcription can be developed. Finally, a variety of experimental approaches should be undertaken to elucidate the role of the extra 23S rRNA present in *B. burgdorferi* cells, as the spirochete scavenges nutrients from its environment and wasting so many nutrients producing an overabundance of rRNA that will not be incorporated into mature ribosomes seems illogical. This suggests a functional role that may define a novel survival strategy unique to these bacteria. We hope that this work will provide the foundation that will allow the development of a deeper understanding of alternative mechanisms of rRNA regulation and how these contribute to the unique lifestyle exhibited by host-restricted parasitic organisms such as *B. burgdorferi*.

Chapter 6

References

1. **Schwartz JJ, Gazumyan A, Schwartz I.** 1992. rRNA gene organization in the Lyme disease spirochete, *Borrelia burgdorferi. J Bacteriol* **174**:3757-3765.
2. **Caimano MJ, Eggers CH, Hazlett KR, Radolf JD.** 2004. RpoS is not central to the general stress response in *Borrelia burgdorferi* but does control expression of one or more essential virulence determinants. *Infect Immun* **72**:6433-6445.
3. **Galbraith KM, Ng AC, Eggers BJ, Kuchel CR, Eggers CH, Samuels DS.** 2005. *parC* mutations in fluoroquinolone-resistant *Borrelia burgdorferi. Antimicrob Agents Chemother* **49**:4354-4357.
4. **Hunfeld KP, Wichelhaus TA, Rodel R, Acker G, Brade V, Kraiczy P.** 2004. Comparison of in vitro activities of ketolides, macrolides, and an azalide against the spirochete *Borrelia burgdorferi. Antimicrob Agents Chemother* **48**:344-347.
5. **Bugrysheva JV, Godfrey HP, Schwartz I, Cabello FC.** 2011. Patterns and regulation of ribosomal RNA transcription in *Borrelia burgdorferi. BMC Microbiol* **11**:17.
6. **Hunfeld KP, Kraiczy P, Kekoukh E, Schafer V, Brade V.** 2002. Standardised *in vitro* susceptibility testing of *Borrelia burgdorferi* against well-known and newly developed antimicrobial agents--possible implications for new therapeutic approaches to Lyme disease. *Int J Med Microbiol* **291 Suppl 33**:125-137.
7. **Herskovitz MA, Bechhofer DH.** 2000. Endoribonuclease RNase III is essential in *Bacillus subtilis. Mol Microbiol* **38**:1027-1033.
8. **Amarasinghe AK, Calin-Jageman I, Harmouch A, Sun W, Nicholson AW.** 2001. *Escherichia coli* ribonuclease III: affinity purification of hexahistidine-tagged enzyme and assays for substrate binding and cleavage. *Methods Enzymol* **342**:143-158.
9. **Burgdorfer W, Barbour AG, Hayes SF, Benach JL, Grunwaldt E, Davis JP.** 1982. Lyme disease-a tick-borne spirochetosis? *Science* **216**:1317-1319.
10. **Benach JL, Bosler EM, Hanrahan JP, Coleman JL, Habicht GS, Bast TF, Cameron DJ, Ziegler JL, Barbour AG, Burgdorfer W, Edelman R, Kaslow RA.** 1983. Spirochetes isolated from the blood of two patients with Lyme disease. *N Engl J Med* **308**:740-742.
11. **Steere AC, Grodzicki RL, Kornblatt AN, Craft JE, Barbour AG, Burgdorfer W, Schmid GP, Johnson E, Malawista SE.** 1983. The spirochetal etiology of Lyme disease. *N Engl J Med* **308**:733-740.

12. **Radolf JD, Salazar, J.C., and Dattwyler, R.J.** 2010. Lyme disease in humans, p. 487-533. *In* Samuels DS, Radolf JD (ed), Borrelia: *Molecular Biology, Host Interaction and Pathogenesis*. Caister Academic Press, Norfolk, UK.
13. **Radolf JD, Caimano MJ, Stevenson B, Hu LT.** 2012. Of ticks, mice and men: understanding the dual-host lifestyle of Lyme disease spirochaetes. *Nat Rev Microbiol* **10**:87-99.
14. **Antal GM, Lukehart SA, Meheus AZ.** 2002. The endemic treponematoses. *Microbes Infect* **4**:83-94.
15. **Norris SJ, Cox DL, Weinstock GM.** 2001. Biology of *Treponema pallidum*: correlation of functional activities with genome sequence data. *J Mol Microbiol Biotechnol* **3**:37-62.
16. **Vinetz JM.** 2001. Leptospirosis. *Curr Opin Infect Dis* **14**:527-538.
17. **Adler B, de la Pena Moctezuma A.** 2010. *Leptospira* and leptospirosis. *Vet Microbiol* **140**:287-296.
18. **Tsinganou E, Gebbers JO.** 2010. Human intestinal spirochetosis--a review. *Ger Med Sci* **8**:Doc01.
19. **Mikosza AS, Hampson DJ.** 2001. Human intestinal spirochetosis: *Brachyspira aalborgi* and/or *Brachyspira pilosicoli*? *Anim Health Res Rev* **2**:101-110.
20. **Smajs D, Norris SJ, Weinstock GM.** 2012. Genetic diversity in *Treponema pallidum*: implications for pathogenesis, evolution and molecular diagnostics of syphilis and yaws. *Infect Genet Evol* **12**:191-202.
21. **Mitja O, Asiedu K, Mabey D.** 2013. Yaws. *Lancet* **381**:763-773.
22. **Goldstein SF, Li, C., Liu, J., Miller, M., Motaleb, M. A., Norris, S. J., Silversmith, R. E., Wolgemuth, C. W., and Charon, N. W. .** 2010. The chic motility and chemotaxis of *Borrelia burgdorferi*, p. 167-187. *In* Samuels DS, Radolf JD (ed), Borrelia: *Molecular Biology, Host Interaction and Pathogenesis*. Caister Academic Press, Norfolk, UK.
23. **Charon NW, Cockburn A, Li C, Liu J, Miller KA, Miller MR, Motaleb MA, Wolgemuth CW.** 2012. The unique paradigm of spirochete motility and chemotaxis. *Annu Rev Microbiol* **66**:349-370.
24. **Charon NW, Goldstein SF.** 2002. Genetics of motility and chemotaxis of a fascinating group of bacteria: the spirochetes. *Annu Rev Genet* **36**:47-73.
25. **Piesman J, and Schwan, T.G.** 2010. Ecology of *borreliae* and their arthropod vectors, p. 251-278. *In* Samuels DS, Radolf JD (ed), Borrelia: *Molecular Biology, Host Interaction and Pathogenesis*. Caister Academic Press, Norfolk, UK.
26. **Kurtenbach K, Hanincova K, Tsao JI, Margos G, Fish D, Ogden NH.** 2006. Fundamental processes in the evolutionary ecology of Lyme borreliosis. *Nat Rev Microbiol* **4**:660-669.
27. **Mannelli A, Bertolotti L, Gern L, Gray J.** 2012. Ecology of *Borrelia burgdorferi sensu lato* in Europe: transmission dynamics in multi-host systems, influence of molecular processes and effects of climate change. *FEMS Microbiol Rev* **36**:837-861.
28. **Wormser GP, Dattwyler RJ, Shapiro ED, Halperin JJ, Steere AC, Klempner MS, Krause PJ, Bakken JS, Strle F, Stanek G, Bockenstedt L, Fish D, Dumler JS, Nadelman RB.** 2006. The clinical assessment, treatment, and prevention of lyme disease, human granulocytic anaplasmosis, and babesiosis:

clinical practice guidelines by the Infectious Diseases Society of America. *Clin Infect Dis* **43**:1089-1134.

29. **Fraser CM, Casjens S, Huang WM, Sutton GG, Clayton R, Lathigra R, White O, Ketchum KA, Dodson RJ, Hickey EK, Gwinn M, Dougherty B, Tomb JF, Fleischmann RD, Richardson D, Peterson J, Kerlavage AR, Quackenbush J, Salzberg S, Hanson M, van Vugt R, Palmer N, Adams MD, Gocayne J, Weidman J, Utterback T, Watthey L, McDonald L, Artiach P, Bowman C, Garland S, Fujii C, Cotton MD, Horst K, Roberts K, Hatch B, Smith HO, Venter JC.** 1997. Genomic sequence of a Lyme disease spirochaete, *Borrelia burgdorferi. Nature* **390**:580-586.
30. **Weis JJaB, L.K.** 2010. Host Response, p. 413-441. *In* Samuels DS, Radolf JD (ed), Borrelia: *Molecular Biology, Host Interaction and Pathogenesis.* Caister Academic Press, Norfolk, UK.
31. **Salazar JC, Pope CD, Sellati TJ, Feder HM, Jr., Kiely TG, Dardick KR, Buckman RL, Moore MW, Caimano MJ, Pope JG, Krause PJ, Radolf JD.** 2003. Coevolution of markers of innate and adaptive immunity in skin and peripheral blood of patients with erythema migrans. *J Immunol* **171**:2660-2670.
32. **Guo X, Booth CJ, Paley MA, Wang X, DePonte K, Fikrig E, Narasimhan S, Montgomery RR.** 2009. Inhibition of neutrophil function by two tick salivary proteins. *Infect Immun* **77**:2320-2329.
33. **Kotsyfakis M, Sa-Nunes A, Francischetti IM, Mather TN, Andersen JF, Ribeiro JM.** 2006. Antiinflammatory and immunosuppressive activity of sialostatin L, a salivary cystatin from the tick *Ixodes scapularis. J Biol Chem* **281**:26298-26307.
34. **Ramamoorthi N, Narasimhan S, Pal U, Bao F, Yang XF, Fish D, Anguita J, Norgard MV, Kantor FS, Anderson JF, Koski RA, Fikrig E.** 2005. The Lyme disease agent exploits a tick protein to infect the mammalian host. *Nature* **436**:573-577.
35. **Pal UaF, E.** 2010. Tick Interactions, p. 279-297. *In* Samuels DS, Radolf JD (ed), Borrelia: *Molecular Biology, Host Interaction and Pathogenesis.* Caister Academic Press, Norfolk, UK.
36. **Kenedy MR, Lenhart TR, Akins DR.** 2012. The role of *Borrelia burgdorferi* outer surface proteins. *FEMS Immunol Med Microbiol* **66**:1-19.
37. **Norris SJ, Coburn, J., Leong, J. M., Hu, L. T., and Höök, M.** 2010. Pathobiology of Lyme Disease Borrelia, p. 299-331. *In* Samuels DS, Radolf JD (ed), Borrelia: *Molecular Biology, Host Interaction and Pathogenesis.* Caister Academic Press, Norfolk, UK.
38. **Moriarty TJ, Norman MU, Colarusso P, Bankhead T, Kubes P, Chaconas G.** 2008. Real-time high resolution 3D imaging of the lyme disease spirochete adhering to and escaping from the vasculature of a living host. *PLoS Pathog* **4**:e1000090.
39. **Coleman JL, Gebbia JA, Piesman J, Degen JL, Bugge TH, Benach JL.** 1997. Plasminogen is required for efficient dissemination of *B. burgdorferi* in ticks and for enhancement of spirochetemia in mice. *Cell* **89**:1111-1119.
40. **Brissette CA, Haupt K, Barthel D, Cooley AE, Bowman A, Skerka C, Wallich R, Zipfel PF, Kraiczy P, Stevenson B.** 2009. *Borrelia burgdorferi*

infection-associated surface proteins ErpP, ErpA, and ErpC bind human plasminogen. *Infect Immun* **77**:300-306.

41. **Onder O, Humphrey PT, McOmber B, Korobova F, Francella N, Greenbaum DC, Brisson D.** 2012. OspC is potent plasminogen receptor on surface of *Borrelia burgdorferi. J Biol Chem* **287**:16860-16868.
42. **Cabello FC, Godfrey HP, Newman SA.** 2007. Hidden in plain sight: *Borrelia burgdorferi* and the extracellular matrix. *Trends Microbiol* **15**:350-354.
43. **Liang FT, Brown EL, Wang T, Iozzo RV, Fikrig E.** 2004. Protective niche for *Borrelia burgdorferi* to evade humoral immunity. *Am J Pathol* **165**:977-985.
44. **Liang FT, Yan J, Mbow ML, Sviat SL, Gilmore RD, Mamula M, Fikrig E.** 2004. *Borrelia burgdorferi* changes its surface antigenic expression in response to host immune responses. *Infect Immun* **72**:5759-5767.
45. **Zhang JR, Hardham JM, Barbour AG, Norris SJ.** 1997. Antigenic variation in Lyme disease borreliae by promiscuous recombination of VMP-like sequence cassettes. *Cell* **89**:275-285.
46. **Brisson D, Drecktrah D, Eggers CH, Samuels DS.** 2012. Genetics of *Borrelia burgdorferi. Annu Rev Genet* **46**:515-536.
47. **Skare JT, Carroll, J. A., Yang, X. F., Samuels, D. S., and Akins, D. R.** 2010. Gene Regulation, Transcriptomics and Proteomics, p. 67-101. *In* Samuels DS, Radolf JD (ed), Borrelia: *Molecular Biology, Host Interaction and Pathogenesis.* Caister Academic Press, Norfolk, UK.
48. **Samuels DS.** 2011. Gene regulation in *Borrelia burgdorferi. Annu Rev Microbiol* **65**:479-499.
49. **He M, Ouyang Z, Troxell B, Xu H, Moh A, Piesman J, Norgard MV, Gomelsky M, Yang XF.** 2011. Cyclic di-GMP is essential for the survival of the lyme disease spirochete in ticks. *PLoS Pathog* **7**:e1002133.
50. **Pappas CJ, Iyer R, Petzke MM, Caimano MJ, Radolf JD, Schwartz I.** 2011. *Borrelia burgdorferi* requires glycerol for maximum fitness during the tick phase of the enzootic cycle. *PLoS Pathog* **7**:e1002102.
51. **Yang XF, Pal U, Alani SM, Fikrig E, Norgard MV.** 2004. Essential role for OspA/B in the life cycle of the Lyme disease spirochete. *J Exp Med* **199**:641-648.
52. **Scheckelhoff MR, Telford SR, Wesley M, Hu LT.** 2007. *Borrelia burgdorferi* intercepts host hormonal signals to regulate expression of outer surface protein A. *Proc Natl Acad Sci U S A* **104**:7247-7252.
53. **Pal U, Li X, Wang T, Montgomery RR, Ramamoorthi N, Desilva AM, Bao F, Yang X, Pypaert M, Pradhan D, Kantor FS, Telford S, Anderson JF, Fikrig E.** 2004. TROSPA, an *Ixodes scapularis* receptor for *Borrelia burgdorferi. Cell* **119**:457-468.
54. **Battisti JM, Bono JL, Rosa PA, Schrumpf ME, Schwan TG, Policastro PF.** 2008. Outer surface protein A protects Lyme disease spirochetes from acquired host immunity in the tick vector. *Infect Immun* **76**:5228-5237.
55. **Bugrysheva J, Dobrikova EY, Godfrey HP, Sartakova ML, Cabello FC.** 2002. Modulation of *Borrelia burgdorferi* stringent response and gene expression during extracellular growth with tick cells. *Infect Immun* **70**:3061-3067.

56. **Bugrysheva J, Dobrikova EY, Sartakova ML, Caimano MJ, Daniels TJ, Radolf JD, Godfrey HP, Cabello FC.** 2003. Characterization of the stringent response and *rel*$_{(Bbu)}$ expression in *Borrelia burgdorferi*. *J Bacteriol* **185**:957-965.
57. **Bugrysheva JV, Bryksin AV, Godfrey HP, Cabello FC.** 2005. *Borrelia burgdorferi rel* is responsible for generation of guanosine-3'-diphosphate-5'-triphosphate and growth control. *Infect Immun* **73**:4972-4981.
58. **Revel AT, Talaat AM, Norgard MV.** 2002. DNA microarray analysis of differential gene expression in *Borrelia burgdorferi*, the Lyme disease spirochete. *Proc Natl Acad Sci U S A* **99**:1562-1567.
59. **Fingerle V, Rauser S, Hammer B, Kahl O, Heimerl C, Schulte-Spechtel U, Gern L, Wilske B.** 2002. Dynamics of dissemination and outer surface protein expression of different European *Borrelia burgdorferi sensu lato* strains in artificially infected *Ixodes ricinus* nymphs. *J Clin Microbiol* **40**:1456-1463.
60. **Gilmore RD, Jr., Piesman J.** 2000. Inhibition of *Borrelia burgdorferi* migration from the midgut to the salivary glands following feeding by ticks on OspC-immunized mice. *Infect Immun* **68**:411-414.
61. **Leuba-Garcia S, Martinez R, Gern L.** 1998. Expression of outer surface proteins A and C of *Borrelia afzelii* in *Ixodes ricinus* ticks and in the skin of mice. *Zentralbl Bakteriol* **287**:475-484.
62. **Montgomery RR, Malawista SE, Feen KJ, Bockenstedt LK.** 1996. Direct demonstration of antigenic substitution of *Borrelia burgdorferi ex vivo*: exploration of the paradox of the early immune response to outer surface proteins A and C in Lyme disease. *J Exp Med* **183**:261-269.
63. **Ohnishi J, Piesman J, de Silva AM.** 2001. Antigenic and genetic heterogeneity of *Borrelia burgdorferi* populations transmitted by ticks. P*roc Natl Acad Sci U S A* **98**:670-675.
64. **Rathinavelu S, de Silva AM.** 2001. Purification and characterization of *Borrelia burgdorferi* from feeding nymphal ticks (*Ixodes scapularis*). *Infect Immun* **69**:3536-3541.
65. **Schwan TG, Piesman J.** 2000. Temporal changes in outer surface proteins A and C of the lyme disease-associated spirochete, *Borrelia burgdorferi*, during the chain of infection in ticks and mice. *J Clin Microbiol* **38**:382-388.
66. **Schwan TG, Piesman J, Golde WT, Dolan MC, Rosa PA.** 1995. Induction of an outer surface protein on *Borrelia burgdorferi* during tick feeding. *Proc Natl Acad Sci U S A* **92**:2909-2913.
67. **Hubner A, Yang X, Nolen DM, Popova TG, Cabello FC, Norgard MV.** 2001. Expression of *Borrelia burgdorferi* OspC and DbpA is controlled by a RpoN-RpoS regulatory pathway. *Proc Natl Acad Sci U S A* **98**:12724-12729.
68. **Piesman J, Mather TN, Sinsky RJ, Spielman A.** 1987. Duration of tick attachment and *Borrelia burgdorferi* transmission. *J Clin Microbiol* **25**:557-558.
69. **Rollend L, Fish D, Childs JE.** 2013. Transovarial transmission of *Borrelia* spirochetes by *Ixodes scapularis*: a summary of the literature and recent observations. *Ticks Tick Borne Dis* **4**:46-51.
70. **Donahue JG, Piesman J, Spielman A.** 1987. Reservoir competence of white-footed mice for Lyme disease spirochetes. *Am J Trop Med Hyg* **36**:92-96.

71. **Magnarelli LA, Anderson JF, Hyland KE, Fish D, McAninch JB.** 1988. Serologic analyses of *Peromyscus leucopus*, a rodent reservoir for *Borrelia burgdorferi*, in northeastern United States. *J Clin Microbiol* **26**:1138-1141.
72. **Barthold SW, Cadavid, D., and Philipp, M. T. .** 2010. Animal models of Borreliosis, p. 359-411. *In* Samuels DS, Radolf JD (ed), Borrelia: *Molecular Biology, Host Interaction and Pathogenesis.* Caister Academic Press, Norfolk, UK.
73. **Spielman A, Wilson ML, Levine JF, Piesman J.** 1985. Ecology of *Ixodes dammini*-borne human babesiosis and Lyme disease. *Annu Rev Entomol* **30**:439-460.
74. **Casjens S, Palmer N, van Vugt R, Huang WM, Stevenson B, Rosa P, Lathigra R, Sutton G, Peterson J, Dodson RJ, Haft D, Hickey E, Gwinn M, White O, Fraser CM.** 2000. A bacterial genome in flux: the twelve linear and nine circular extrachromosomal DNAs in an infectious isolate of the Lyme disease spirochete *Borrelia burgdorferi. Mol Microbiol* **35**:490-516.
75. **Casjens SR, Mongodin EF, Qiu WG, Luft BJ, Schutzer SE, Gilcrease EB, Huang WM, Vujadinovic M, Aron JK, Vargas LC, Freeman S, Radune D, Weidman JF, Dimitrov GI, Khouri HM, Sosa JE, Halpin RA, Dunn JJ, Fraser CM.** 2012. Genome stability of Lyme disease spirochetes: comparative genomics of *Borrelia burgdorferi* plasmids. *PLoS One* **7**:e33280.
76. **Chaconas G, Kobryn K.** 2010. Structure, function, and evolution of linear replicons in *Borrelia. Annu Rev Microbiol* **64**:185-202.
77. **Casjens SR, Eggers, C.H., and Schwartz, I.** 2010. *Borrelia* genomics: Chromosome, Plasmids, Bacteriophages and Genetic Variation, p. 27-53. *In* Samuels DS, Radolf JD (ed), Borrelia: *Molecular Biology, Host Interaction and Pathogenesis*. Caister Academic Press, Norfolk, UK.
78. **Srivastava AK, Schlessinger D.** 1990. Mechanism and regulation of bacterial ribosomal RNA processing. *Annu Rev Microbiol* **44**:105-129.
79. **Barbour AG.** 1984. Isolation and cultivation of Lyme disease spirochetes. *Yale J Biol Med* **57**:521-525.
80. **Gherardini F, Boylan, J., Lawrence, K., and Skare, J.** 2010. Metabolism and Physiology of *Borrelia*, p. 103-138. *In* Samuels DS, Radolf JD (ed), Borrelia: *Molecular Biology, Host Interaction and Pathogenesis*. Caister Academic Press, Norfolk, UK.
81. **Eggers CH, Samuels DS.** 1999. Molecular evidence for a new bacteriophage of *Borrelia burgdorferi. J Bacteriol* **181**:7308-7313.
82. **Eggers CH, Kimmel BJ, Bono JL, Elias AF, Rosa P, Samuels DS.** 2001. Transduction by *phi*BB-1, a bacteriophage of *Borrelia burgdorferi. J Bacteriol* **183**:4771-4778.
83. **Fukunaga M, Yanagihara Y, Sohnaka M.** 1992. The 23S/5S ribosomal RNA genes (*rrl/rrf*) are separate from the 16S ribosomal RNA gene (*rrs*) in B*orrelia burgdorferi*, the aetiological agent of Lyme disease. *J Gen Microbiol* **138**:871-877.
84. **Lynch M.** 2006. Streamlining and simplification of microbial genome architecture. *Annu Rev Microbiol* **60**:327-349.

85. **McCutcheon JP, Moran NA.** 2012. Extreme genome reduction in symbiotic bacteria. *Nat Rev Microbiol* **10**:13-26.
86. **Posey JE, Gherardini FC.** 2000. Lack of a role for iron in the Lyme disease pathogen. *Science* **288**:1651-1653.
87. **Kobryn K, Chaconas G.** 2002. ResT, a telomere resolvase encoded by the Lyme disease spirochete. *Mol Cell* **9**:195-201.
88. **Labandeira-Rey M, Skare JT.** 2001. Decreased infectivity in *Borrelia burgdorferi* strain B31 is associated with loss of linear plasmid 25 or 28-1. *Infect Immun* **69**:446-455.
89. **Purser JE, Norris SJ.** 2000. Correlation between plasmid content and infectivity in *Borrelia burgdorferi. Proc Natl Acad Sci U S A* **97**:13865-13870.
90. **Strother KO, Broadwater A, De Silva A.** 2005. Plasmid requirements for infection of ticks by *Borrelia burgdorferi. Vector Borne Zoonotic Dis* **5**:237-245.
91. **Damman CJ, Eggers CH, Samuels DS, Oliver DB.** 2000. Characterization of *Borrelia burgdorferi* BlyA and BlyB proteins: a prophage-encoded holin-like system. *J Bacteriol* **182**:6791-6797.
92. **Zhang H, Marconi RT.** 2005. Demonstration of cotranscription and 1-methyl-3-nitroso-nitroguanidine induction of a 30-gene operon of *Borrelia burgdorferi*: evidence that the 32-kilobase circular plasmids are prophages. *J Bacteriol* **187**:7985-7995.
93. **Andersson SG, Kurland CG.** 1995. Genomic evolution drives the evolution of the translation system. *Biochem Cell Biol* **73**:775-787.
94. **Ojaimi C, Davidson BE, Saint Girons I, Old IG.** 1994. Conservation of gene arrangement and an unusual organization of rRNA genes in the linear chromosomes of the Lyme disease spirochaetes *Borrelia burgdorferi, B. garinii and B. afzelii. Microbiology* **140 (Pt 11)**:2931-2940.
95. **Gazumyan A, Schwartz JJ, Liveris D, Schwartz I.** 1994. Sequence analysis of the ribosomal RNA operon of the Lyme disease spirochete, *Borrelia burgdorferi. Gene* **146**:57-65.
96. **Kuznetsova E, Proudfoot M, Gonzalez CF, Brown G, Omelchenko MV, Borozan I, Carmel L, Wolf YI, Mori H, Savchenko AV, Arrowsmith CH, Koonin EV, Edwards AM, Yakunin AF.** 2006. Genome-wide analysis of substrate specificities of the *Escherichia coli* haloacid dehalogenase-like phosphatase family. *J Biol Chem* **281**:36149-36161.
97. **Xu H, Caimano MJ, Lin T, He M, Radolf JD, Norris SJ, Gherardini F, Wolfe AJ, Yang XF.** 2010. Role of acetyl-phosphate in activation of the Rrp2-RpoN-RpoS pathway in *Borrelia burgdorferi. PLoS Pathog* **6**.
98. **Dykhuizen DaB, D.** 2010. Evolutionary Genetics of *Borrelia burgdorferi sensu lato*, p. 221-249. *In* Samuels DS, Radolf JD (ed), Borrelia: *Molecular Biology, Host Interaction and Pathogenesis*. Caister Academic Press, Norfolk, UK.
99. **Schutzer SE, Fraser-Liggett CM, Casjens SR, Qiu WG, Dunn JJ, Mongodin EF, Luft BJ.** 2011. Whole-genome sequences of thirteen isolates of *Borrelia burgdorferi. J Bacteriol* **193**:1018-1020.
100. **Schutzer SE, Fraser-Liggett CM, Qiu WG, Kraiczy P, Mongodin EF, Dunn JJ, Luft BJ, Casjens SR.** 2012. Whole-Genome Sequences of *Borrelia bissettii*, *Borrelia valaisiana*, and *Borrelia spielmanii*. *J Bacteriol* **194**:545-546.

101. **Casjens SR, Mongodin EF, Qiu WG, Dunn JJ, Luft BJ, Fraser-Liggett CM, Schutzer SE.** 2011. Whole-Genome Sequences of Two *Borrelia afzelii* and Two *Borrelia garinii* Lyme Disease Agent Isolates. *J Bacteriol* **193**:6995-6996.
102. **Marconi RT, Liveris D, Schwartz I.** 1995. Identification of novel insertion elements, restriction fragment length polymorphism patterns, and discontinuous 23S rRNA in Lyme disease spirochetes: phylogenetic analyses of rRNA genes and their intergenic spacers in *Borrelia japonica* sp. nov. and genomic group 21038 (*Borrelia andersonii* sp. nov.) isolates. *J Clin Microbiol* **33**:2427-2434.
103. **Morozova OV, Dubytska LP, Ivanova LB, Moreno CX, Bryksin AV, Sartakova ML, Dobrikova EY, Godfrey HP, Cabello FC.** 2005. Genetic and physiological characterization of 23S rRNA and *ftsJ* mutants of *Borrelia burgdorferi* isolated by mariner transposition. *Gene* **357**:63-72.
104. **Asai T, Condon C, Voulgaris J, Zaporojets D, Shen B, Al-Omar M, Squires C, Squires CL.** 1999. Construction and initial characterization of *Escherichia coli* strains with few or no intact chromosomal rRNA operons. *J Bacteriol* **181**:3803-3809.
105. **Asai T, Zaporojets D, Squires C, Squires CL.** 1999. An *Escherichia coli* strain with all chromosomal rRNA operons inactivated: complete exchange of rRNA genes between bacteria. *Proc Natl Acad Sci U S A* **96**:1971-1976.
106. **Nanamiya H, Sato M, Masuda K, Wada T, Suzuki S, Natori Y, Katano M, Akanuma G, Kawamura F.** 2010. *Bacillus subtilis* mutants harbouring a single copy of the rRNA operon exhibit severe defects in growth and sporulation. *Microbiology* **156**:2944-2952.
107. **Reiter WD, Palm P, Yeats S.** 1989. Transfer RNA genes frequently serve as integration sites for prokaryotic genetic elements. *Nucleic Acids Res* **17**:1907-1914.
108. **Williams KP.** 2002. Integration sites for genetic elements in prokaryotic tRNA and tmRNA genes: sublocation preference of integrase subfamilies. *Nucleic Acids Res* **30**:866-875.
109. **Moritz C, Brown WM.** 1986. Tandem duplication of D-loop and ribosomal RNA sequences in lizard mitochondrial DNA. *Science* **233**:1425-1427.
110. **Lim K, Furuta Y, Kobayashi I.** 2012. Large variations in bacterial ribosomal RNA genes. *Mol Biol Evol* **29**:2937-2948.
111. **Ree HK, Zimmermann RA.** 1990. Organization and expression of the 16S, 23S and 5S ribosomal RNA genes from the archaebacterium *Thermoplasma acidophilum. Nucleic Acids Res* **18**:4471-4478.
112. **Andersson SG, Zomorodipour A, Winkler HH, Kurland CG.** 1995. Unusual organization of the rRNA genes in *Rickettsia prowazekii. J Bacteriol* **177**:4171-4175.
113. **Chen X, Finch LR.** 1989. Novel arrangement of rRNA genes in *Mycoplasma gallisepticum*: separation of the 16S gene of one set from the 23S and 5S genes. *J Bacteriol* **171**:2876-2878.
114. **Taschke C, Klinkert MQ, Wolters J, Herrmann R.** 1986. Organization of the ribosomal RNA genes in *Mycoplasma hyopneumoniae*: the 5S rRNA gene is separated from the 16S and 23S rRNA genes. *Mol Gen Genet* **205**:428-433.

115. **Huang Y, Robertson JA, Stemke GW.** 1995. An unusual rRNA gene organization in *Mycoplasma fermentans* (incognitus strain). *Can J Microbiol* **41**:424-427.
116. **Rurangirwa FR, Brayton KA, McGuire TC, Knowles DP, Palmer GH.** 2002. Conservation of the unique rickettsial rRNA gene arrangement in *Anaplasma. Int J Syst Evol Microbiol* **52**:1405-1409.
117. **Fukunaga M, Mifuchi I.** 1989. Unique organization of *Leptospira interrogans* rRNA genes. *J Bacteriol* **171**:5763-5767.
118. **Ren SX, Fu G, Jiang XG, Zeng R, Miao YG, Xu H, Zhang YX, Xiong H, Lu G, Lu LF, Jiang HQ, Jia J, Tu YF, Jiang JX, Gu WY, Zhang YQ, Cai Z, Sheng HH, Yin HF, Zhang Y, Zhu GF, Wan M, Huang HL, Qian Z, Wang SY, Ma W, Yao ZJ, Shen Y, Qiang BQ, Xia QC, Guo XK, Danchin A, Saint Girons I, Somerville RL, Wen YM, Shi MH, Chen Z, Xu JG, Zhao GP.** 2003. Unique physiological and pathogenic features of *Leptospira interrogans* revealed by whole-genome sequencing. *Nature* **422**:888-893.
119. **Nascimento AL, Ko AI, Martins EA, Monteiro-Vitorello CB, Ho PL, Haake DA, Verjovski-Almeida S, Hartskeerl RA, Marques MV, Oliveira MC, Menck CF, Leite LC, Carrer H, Coutinho LL, Degrave WM, Dellagostin OA, El-Dorry H, Ferro ES, Ferro MI, Furlan LR, Gamberini M, Giglioti EA, Goes-Neto A, Goldman GH, Goldman MH, Harakava R, Jeronimo SM, Junqueira-de-Azevedo IL, Kimura ET, Kuramae EE, Lemos EG, Lemos MV, Marino CL, Nunes LR, de Oliveira RC, Pereira GG, Reis MS, Schriefer A, Siqueira WJ, Sommer P, Tsai SM, Simpson AJ, Ferro JA, Camargo LE, Kitajima JP, Setubal JC, Van Sluys MA.** 2004. Comparative genomics of two *Leptospira interrogans* serovars reveals novel insights into physiology and pathogenesis. *J Bacteriol* **186**:2164-2172.
120. **Andersson SG, Stothard DR, Fuerst P, Kurland CG.** 1999. Molecular phylogeny and rearrangement of rRNA genes in Rickettsia species. *Mol Biol Evol* **16**:987-995.
121. **Nomura M, Morgan EA.** 1977. Genetics of bacterial ribosomes. *Annu Rev Genet* **11**:297-347.
122. **Doi RH, Igarashi RT.** 1966. Heterogeneity of the conserved ribosomal ribonucleic acid sequences of *Bacillus subtilis. J Bacteriol* **92**:88-96.
123. **Ellwood M, Nomura M.** 1980. Deletion of a ribosomal ribonucleic acid operon in *Escherichia coli. J Bacteriol* **143**:1077-1080.
124. **Widom RL, Jarvis ED, LaFauci G, Rudner R.** 1988. Instability of rRNA operons in *Bacillus subtilis. J Bacteriol* **170**:605-610.
125. **Jinks-Robertson S, Gourse RL, Nomura M.** 1983. Expression of rRNA and tRNA genes in *Escherichia coli*: evidence for feedback regulation by products of rRNA operons. *Cell* **33**:865-876.
126. **Condon C, French S, Squires C, Squires CL.** 1993. Depletion of functional ribosomal RNA operons in *Escherichia coli* causes increased expression of the remaining intact copies. *Embo J* **12**:4305-4315.
127. **Condon C, Philips J, Fu ZY, Squires C, Squires CL.** 1992. Comparison of the expression of the seven ribosomal RNA operons in *Escherichia coli. Embo J* **11**:4175-4185.

128. **Condon C, Liveris D, Squires C, Schwartz I, Squires CL.** 1995. rRNA operon multiplicity in *Escherichia coli* and the physiological implications of *rrn* inactivation. *J Bacteriol* **177**:4152-4156.
129. **Hillebrand A, Wurm R, Menzel A, Wagner R.** 2005. The seven *E. coli* ribosomal RNA operon upstream regulatory regions differ in structure and transcription factor binding efficiencies. *Biol Chem* **386**:523-534.
130. **Kolmsee T, Delic D, Agyenim T, Calles C, Wagner R.** 2011. Differential stringent control of *Escherichia coli* rRNA promoters: effects of ppGpp, DksA and the initiating nucleotides. *Microbiology* **157**:2871-2879.
131. **Samarrai W, Liu DX, White AM, Studamire B, Edelstein J, Srivastava A, Widom RL, Rudner R.** 2011. Differential responses of *Bacillus subtilis* rRNA promoters to nutritional stress. *J Bacteriol* **193**:723-733.
132. **Bremer HaD, P. P.** 1996. Modulation of chemical composition and other parameters of the cell by growth rate, p. 1553-1569. *In* Neidhardt FC, Ingraham, J. L., Brooks Low, K., Magasanik, B., Schaechter, M., and Umbarger, H. E. (ed), Escherichia coli *and* Salmonella typhimurium: *Cellular and Molecular Biology.* ASM Press, Washington, DC.
133. **Jin DJ, Cagliero C, Zhou YN.** 2012. Growth rate regulation in *Escherichia coli. FEMS Microbiol Rev* **36**:269-287.
134. **Piir K, Paier A, Liiv A, Tenson T, Maivali U.** 2011. Ribosome degradation in growing bacteria. *EMBO Rep* **12**:458-462.
135. **Scott M, Gunderson CW, Mateescu EM, Zhang Z, Hwa T.** 2010. Interdependence of cell growth and gene expression: origins and consequences. *Science* **330**:1099-1102.
136. **Grundy FJ, Henkin TM.** 1992. Characterization of the *Bacillus subtilis rpsD* regulatory target site. *J Bacteriol* **174**:6763-6770.
137. **Keener JaN, M.** 1996. Regulation of Ribosome Biosynthesis, p. 1417-1431. *In* Neidhardt FC, Ingraham, J. L., Brooks Low, K., Magasanik, B., Schaechter, M., and Umbarger, H. E. (ed), Escherichia coli *and* Salmonella typhimurium: *Cellular and Molecular Biology.* ASM Press, Washington, DC.
138. **Zengel JM, Lindahl L.** 1994. Diverse mechanisms for regulating ribosomal protein synthesis in *Escherichia coli. Prog Nucleic Acid Res Mol Biol* **47**:331-370.
139. **Gausing K.** 1977. Regulation of ribosome production in *Escherichia coli*: synthesis and stability of ribosomal RNA and of ribosomal protein messenger RNA at different growth rates. *J Mol Biol* **115**:335-354.
140. **Paul BJ, Ross W, Gaal T, Gourse RL.** 2004. rRNA transcription in *Escherichia coli. Annu Rev Genet* **38**:749-770.
141. **Gaal T, Bartlett MS, Ross W, Turnbough CL, Jr., Gourse RL.** 1997. Transcription regulation by initiating NTP concentration: rRNA synthesis in bacteria. *Science* **278**:2092-2097.
142. **Barker MM, Gourse RL.** 2001. Regulation of rRNA transcription correlates with nucleoside triphosphate sensing. *J Bacteriol* **183**:6315-6323.
143. **Krasny L, Gourse RL.** 2004. An alternative strategy for bacterial ribosome synthesis: *Bacillus subtilis* rRNA transcription regulation. *Embo J* **23**:4473-4483.

144. **Cashel M.** 1969. The control of ribonucleic acid synthesis in *Escherichia coli*. IV. Relevance of unusual phosphorylated compounds from amino acid-starved stringent strains. *J Biol Chem* **244**:3133-3141.
145. **Potrykus K, Cashel M.** 2008. (p)ppGpp: still magical? *Annu Rev Microbiol* **62**:35-51.
146. **Srivatsan A, Wang JD.** 2008. Control of bacterial transcription, translation and replication by (p)ppGpp. *Curr Opin Microbiol* **11**:100-105.
147. **Dalebroux ZD, Svensson SL, Gaynor EC, Swanson MS.** 2010. ppGpp conjures bacterial virulence. *Microbiol Mol Biol Rev* **74**:171-199.
148. **Wolz C, Geiger T, Goerke C.** 2010. The synthesis and function of the alarmone (p)ppGpp in firmicutes. *Int J Med Microbiol* **300**:142-147.
149. **Mittenhuber G.** 2001. Comparative genomics and evolution of genes encoding bacterial (p)ppGpp synthetases/hydrolases (the Rel, RelA and SpoT proteins). *J Mol Microbiol Biotechnol* **3**:585-600.
150. **Braeken K, Moris M, Daniels R, Vanderleyden J, Michiels J.** 2006. New horizons for (p)ppGpp in bacterial and plant physiology. *Trends Microbiol* **14**:45-54.
151. **Murray HD, Schneider DA, Gourse RL.** 2003. Control of rRNA expression by small molecules is dynamic and nonredundant. *Mol Cell* **12**:125-134.
152. **Wagner R.** 2002. Regulation of ribosomal RNA synthesis in *E. coli*: effects of the global regulator guanosine tetraphosphate (ppGpp). *J Mol Microbiol Biotechnol* **4**:331-340.
153. **Magnusson LU, Farewell A, Nystrom T.** 2005. ppGpp: a global regulator in *Escherichia coli. Trends Microbiol* **13**:236-242.
154. **Milon P, Tischenko E, Tomsic J, Caserta E, Folkers G, La Teana A, Rodnina MV, Pon CL, Boelens R, Gualerzi CO.** 2006. The nucleotide-binding site of bacterial translation initiation factor 2 (IF2) as a metabolic sensor. *Proc Natl Acad Sci U S A* **103**:13962-13967.
155. **Buglino J, Shen V, Hakimian P, Lima CD.** 2002. Structural and biochemical analysis of the Obg GTP binding protein. *Structure* **10**:1581-1592.
156. **Concepcion MB, Nelson DR.** 2003. Expression of spoT in *Borrelia burgdorferi* during serum starvation. *J Bacteriol* **185**:444-452.
157. **Nikolaev N, Silengo L, Schlessinger D.** 1973. Synthesis of a large precursor to ribosomal RNA in a mutant of *Escherichia coli. Proc Natl Acad Sci U S A* **70**:3361-3365.
158. **Nikolaev N, Silengo L, Schlessinger D.** 1973. A role for ribonuclease 3 in processing of ribosomal ribonucleic acid and messenger ribonucleic acid precursors in *Escherichia coli. J Biol Chem* **248**:7967-7969.
159. **Gegenheimer P, Apirion D.** 1975. *Escherichia coli* ribosomal ribonucleic acids are not cut from an intact precursor molecule. *J Biol Chem* **250**:2407-2409.
160. **Gegenheimer P, Apirion D.** 1980. Precursors to 16S and 23S ribosomal RNA from a ribonuclear III-strain of *Escherichia coli* contain intact RNase III processing sites. *Nucleic Acids Res* **8**:1873-1891.
161. **Deutscher MP.** 2009. Maturation and degradation of ribosomal RNA in bacteria. Prog Mol Biol Transl Sci **85**:369-391.

162. **Sogin ML, Pace B, Pace NR.** 1977. Partial purification and properties of a ribosomal RNA maturation endonuclease from *Bacillus subtilis*. *J Biol Chem* **252**:1350-1357.
163. **Misra TK, Apirion D.** 1979. RNase E, an RNA processing enzyme from *Escherichia coli*. *J Biol Chem* **254**:11154-11159.
164. **Li Z, Deutscher MP.** 1995. The tRNA processing enzyme RNase T is essential for maturation of 5S RNA. *Proc Natl Acad Sci U S A* **92**:6883-6886.
165. **Li Z, Pandit S, Deutscher MP.** 1999. Maturation of 23S ribosomal RNA requires the exoribonuclease RNase T. *RNA* **5**:139-146.
166. **Kaczanowska M, Ryden-Aulin M.** 2007. Ribosome biogenesis and the translation process in *Escherichia coli*. *Microbiol Mol Biol Rev* **71**:477-494.
167. **Li Z, Pandit S, Deutscher MP.** 1999. RNase G (CafA protein) and RNase E are both required for the 5' maturation of 16S ribosomal RNA. *Embo J* **18**:2878-2885.
168. **Wachi M, Umitsuki G, Shimizu M, Takada A, Nagai K.** 1999. *Escherichia coli cafA* gene encodes a novel RNase, designated as RNase G, involved in processing of the 5' end of 16S rRNA. *Biochem Biophys Res Commun* **259**:483-488.
169. **Oussenko IA, Abe T, Ujiie H, Muto A, Bechhofer DH.** 2005. Participation of 3'-to-5' exoribonucleases in the turnover of *Bacillus subtilis* mRNA. *J Bacteriol* **187**:2758-2767.
170. **Condon C.** 2007. Maturation and degradation of RNA in bacteria. *Curr Opin Microbiol* **10**:271-278.
171. **Britton RA, Wen T, Schaefer L, Pellegrini O, Uicker WC, Mathy N, Tobin C, Daou R, Szyk J, Condon C.** 2007. Maturation of the 5' end of *Bacillus subtilis* 16S rRNA by the essential ribonuclease YkqC/RNase J1. *Mol Microbiol* **63**:127-138.
172. **Mathy N, Benard L, Pellegrini O, Daou R, Wen T, Condon C.** 2007. 5'-to-3' exoribonuclease activity in bacteria: role of RNase J1 in rRNA maturation and 5' stability of mRNA. *Cell* **129**:681-692.
173. **Durand S, Gilet L, Condon C.** 2012. The essential function of *B. subtilis* RNase III is to silence foreign toxin genes. *PLoS Genet* **8**:e1003181.
174. **Even S, Pellegrini O, Zig L, Labas V, Vinh J, Brechemmier-Baey D, Putzer H.** 2005. Ribonucleases J1 and J2: two novel endoribonucleases in *B.subtilis* with functional homology to *E.coli* RNase E. *Nucleic Acids Res* **33**:2141-2152.
175. **Taverniti V, Forti F, Ghisotti D, Putzer H.** 2011. *Mycobacterium smegmatis* RNase J is a 5'-3' exo-/endoribonuclease and both RNase J and RNase E are involved in ribosomal RNA maturation. *Mol Microbiol* **82**:1260-1276.
176. **Jacob AI, Kohrer C, Davies BW, RajBhandary UL, Walker GC.** 2013. Conserved bacterial RNase YbeY plays key roles in 70S ribosome quality control and 16S rRNA maturation. *Mol Cell* **49**:427-438.
177. **Davies BW, Kohrer C, Jacob AI, Simmons LA, Zhu J, Aleman LM, Rajbhandary UL, Walker GC.** 2010. Role of *Escherichia coli* YbeY, a highly conserved protein, in rRNA processing. *Mol Microbiol* **78**:506-518.
178. **Rasouly A, Davidovich C, Ron EZ.** 2010. The heat shock protein YbeY is required for optimal activity of the 30S ribosomal subunit. *J Bacteriol* **192**:4592-4596.

179. **Tu C, Zhou X, Tropea JE, Austin BP, Waugh DS, Court DL, Ji X.** 2009. Structure of ERA in complex with the 3' end of 16S rRNA: implications for ribosome biogenesis. *Proc Natl Acad Sci U S A* **106**:14843-14848.
180. **Grinwald M, Ron EZ.** 2013. The *Escherichia coli* translation-associated heat shock protein YbeY is involved in rRNA transcription antitermination. *PLoS One* **8**:e62297.
181. **Purusharth RI, Madhuri B, Ray MK.** 2007. Exoribonuclease R in *Pseudomonas syringae* is essential for growth at low temperature and plays a novel role in the 3' end processing of 16 and 5 S ribosomal RNA. *J Biol Chem* **282**:16267-16277.
182. **King TC, Sirdeskmukh R, Schlessinger D.** 1986. Nucleolytic processing of ribonucleic acid transcripts in procaryotes. *Microbiol Rev* **50**:428-451.
183. **Redko Y, Bechhofer DH, Condon C.** 2008. Mini-III, an unusual member of the RNase III family of enzymes, catalyses 23S ribosomal RNA maturation in *B. subtilis. Mol Microbiol* **68**:1096-1106.
184. **Song WS, Lee M, Lee K.** 2011. RNase G participates in processing of the 5'-end of 23S ribosomal RNA. *J Microbiol* **49**:508-511.
185. **Gutgsell NS, Jain C.** 2012. Role of precursor sequences in the ordered maturation of *E. coli* 23S ribosomal RNA. *RNA* **18**:345-353.
186. **Gutgsell NS, Jain C.** 2010. Coordinated regulation of 23S rRNA maturation in *Escherichia coli. J Bacteriol* **192**:1405-1409.
187. **Redko Y, Condon C.** 2009. Ribosomal protein L3 bound to 23S precursor rRNA stimulates its maturation by Mini-III ribonuclease. *Mol Microbiol* **71**:1145-1154.
188. **Redko Y, Condon C.** 2010. Maturation of 23S rRNA in *Bacillus subtilis* in the absence of Mini-III. *J Bacteriol* **192**:356-359.
189. **Ghora BK, Apirion D.** 1978. Structural analysis and *in vitro* processing to p5 rRNA of a 9S RNA molecule isolated from an *rne* mutant of *E. coli. Cell* **15**:1055-1066.
190. **Sogin ML, Pace NR.** 1974. *In vitro* maturation of precursors of 5S ribosomal RNA from *Bacillus subtilis. Nature* **252**:598-600.
191. **Condon C, Brechemier-Baey D, Beltchev B, Grunberg-Manago M, Putzer H.** 2001. Identification of the gene encoding the 5S ribosomal RNA maturase in *Bacillus subtilis*: mature 5S rRNA is dispensable for ribosome function. *RNA* **7**:242-253.
192. **Roy-Chaudhuri B, Kirthi N, Culver GM.** 2010. Appropriate maturation and folding of 16S rRNA during 30S subunit biogenesis are critical for translational fidelity. *Proc Natl Acad Sci U S A* **107**:4567-4572.
193. **Gutgsell NS, Jain C.** 2012. Gateway role for rRNA precursors in ribosome assembly. *J Bacteriol* **194**:6875-6882.
194. **Robertson HD, Webster RE, Zinder ND.** 1968. Purification and properties of ribonuclease III from *Escherichia coli. J Biol Chem* **243**:82-91.
195. **Mian IS.** 1997. Comparative sequence analysis of ribonucleases HII, III, II PH and D. *Nucleic Acids Res* **25**:3187-3195.
196. **Kaberdin VR, Singh D, Lin-Chao S.** 2011. Composition and conservation of the mRNA-degrading machinery in bacteria. *J Biomed Sci* **18**:23.

197. **Bernstein E, Caudy AA, Hammond SM, Hannon GJ.** 2001. Role for a bidentate ribonuclease in the initiation step of RNA interference. *Nature* **409**:363-366.
198. **Lee Y, Ahn C, Han J, Choi H, Kim J, Yim J, Lee J, Provost P, Radmark O, Kim S, Kim VN.** 2003. The nuclear RNase III Drosha initiates microRNA processing. *Nature* **425**:415-419.
199. **Filippov V, Solovyev V, Filippova M, Gill SS.** 2000. A novel type of RNase III family proteins in eukaryotes. *Gene* **245**:213-221.
200. **Blaszczyk J, Tropea JE, Bubunenko M, Routzahn KM, Waugh DS, Court DL, Ji X.** 2001. Crystallographic and modeling studies of RNase III suggest a mechanism for double-stranded RNA cleavage. *Structure* **9**:1225-1236.
201. **Gan J, Tropea JE, Austin BP, Court DL, Waugh DS, Ji X.** 2006. Structural insight into the mechanism of double-stranded RNA processing by ribonuclease III. *Cell* **124**:355-366.
202. **Lamontagne B, Larose S, Boulanger J, Elela SA.** 2001. The RNase III family: a conserved structure and expanding functions in eukaryotic dsRNA metabolism. *Curr Issues Mol Biol* **3**:71-78.
203. **Sun W, Jun E, Nicholson AW.** 2001. Intrinsic double-stranded-RNA processing activity of *Escherichia coli* ribonuclease III lacking the dsRNA-binding domain. *Biochemistry* **40**:14976-14984.
204. **Inada T, Nakamura Y.** 1995. Lethal double-stranded RNA processing activity of ribonuclease III in the absence of *suhB* protein of *Escherichia coli. Biochimie* **77**:294-302.
205. **Zhang K, Nicholson AW.** 1997. Regulation of ribonuclease III processing by double-helical sequence antideterminants. *Proc Natl Acad Sci U S A* **94**:13437-13441.
206. **Nicholson AW.** 1999. Function, mechanism and regulation of bacterial ribonucleases. *FEMS Microbiol Rev* **23**:371-390.
207. **Kim K, Sim SH, Jeon CO, Lee Y, Lee K.** 2011. Base substitutions at scissile bond sites are sufficient to alter RNA-binding and cleavage activity of RNase III. *FEMS Microbiol Lett* **315**:30-37.
208. **Shi Z, Nicholson RH, Jaggi R, Nicholson AW.** 2011. Characterization of *Aquifex aeolicus* ribonuclease III and the reactivity epitopes of its pre-ribosomal RNA substrates. *Nucleic Acids Res* **39**:2756-2768.
209. **Pertzev AV, Nicholson AW.** 2006. Characterization of RNA sequence determinants and antideterminants of processing reactivity for a minimal substrate of *Escherichia coli* ribonuclease III. *Nucleic Acids Res* **34**:3708-3721.
210. **Gan J, Shaw G, Tropea JE, Waugh DS, Court DL, Ji X.** 2008. A stepwise model for double-stranded RNA processing by ribonuclease III. *Mol Microbiol* **67**:143-154.
211. **Sun W, Pertzev A, Nicholson AW.** 2005. Catalytic mechanism of E*scherichia coli* ribonuclease III: kinetic and inhibitor evidence for the involvement of two magnesium ions in RNA phosphodiester hydrolysis. *Nucleic Acids Res* **33**:807-815.
212. **Robertson HD.** 1982. *Escherichia coli* ribonuclease III cleavage sites. *Cell* **30**:669-672.

213. **Dunn JJ, Studier FW.** 1973. T7 early RNAs and *Escherichia coli* ribosomal RNAs are cut from large precursor RNAs *in vivo* by ribonuclease 3. *Proc Natl Acad Sci U S A* **70**:3296-3300.
214. **Pettijohn DE, Stonington OG, Kossman CR.** 1970. Chain termination of ribosomal RNA synthesis *in vitro*. *Nature* **228**:235-239.
215. **Gegenheimer P, Watson N, Apirion D.** 1977. Multiple pathways for primary processing of ribosomal RNA in *Escherichia coli*. *J Biol Chem* **252**:3064-3073.
216. **King TC, Schlessinger D.** 1983. S1 nuclease mapping analysis of ribosomal RNA processing in wild type and processing deficient *Escherichia coli*. *J Biol Chem* **258**:12034-12042.
217. **Wang W, Bechhofer DH.** 1997. *Bacillus subtilis* RNase III gene: cloning, function of the gene in *Escherichia coli*, and construction of *Bacillus subtilis* strains with altered *rnc* loci. *J Bacteriol* **179**:7379-7385.
218. **Rauhut R, Jager A, Conrad C, Klug G.** 1996. Identification and analysis of the *rnc* gene for RNase III in *Rhodobacter capsulatus*. *Nucleic Acids Res* **24**:1246-1251.
219. **Conrad C, Rauhut R, Klug G.** 1998. Different cleavage specificities of RNases III from *Rhodobacter capsulatus* and *Escherichia coli*. *Nucleic Acids Res* **26**:4446-4453.
220. **Mitra S, Bechhofer DH.** 1994. Substrate specificity of an RNase III-like activity from *Bacillus subtilis*. *J Biol Chem* **269**:31450-31456.
221. **Xu W, Huang J, Cohen SN.** 2008. Autoregulation of AbsB (RNase III) expression in *Streptomyces coelicolor* by endoribonucleolytic cleavage of *absB* operon transcripts. J Bacteriol **190**:5526-5530.
222. **Matsunaga J, Simons EL, Simons RW.** 1996. RNase III autoregulation: structure and function of *rncO*, the posttranscriptional "operator". *RNA* **2**:1228-1240.
223. **Bardwell JC, Regnier P, Chen SM, Nakamura Y, Grunberg-Manago M, Court DL.** 1989. Autoregulation of RNase III operon by mRNA processing. *Embo J* **8**:3401-3407.
224. **Hartmann RK, Gossringer M, Spath B, Fischer S, Marchfelder A.** 2009. The making of tRNAs and more - RNase P and tRNase Z. *Prog Mol Biol Transl Sci* **85**:319-368.
225. **Lehnik-Habrink M, Lewis RJ, Mader U, Stulke J.** 2012. RNA degradation in *Bacillus subtilis*: an interplay of essential endo- and exoribonucleases. *Mol Microbiol* **84**:1005-1017.
226. **Carpousis AJ.** 2007. The RNA degradosome of *Escherichia coli*: an mRNA-degrading machine assembled on RNase E. *Annu Rev Microbiol* **61**:71-87.
227. **Carpousis AJ, Luisi BF, McDowall KJ.** 2009. Endonucleolytic initiation of mRNA decay in *Escherichia coli*. *Prog Mol Biol Transl Sci* **85**:91-135.
228. **Jester BC, Romby P, Lioliou E.** 2012. When ribonucleases come into play in pathogens: a survey of gram-positive bacteria. *Int J Microbiol* **2012**:592196.
229. **Subbarayan PR, Deutscher MP.** 2001. *Escherichia coli* RNase M is a multiply altered form of RNase I. *RNA* **7**:1702-1707.
230. **Otsuka Y, Ueno H, Yonesaki T.** 2003. *Escherichia coli* endoribonucleases involved in cleavage of bacteriophage T4 mRNAs. *J Bacteriol* **185**:983-990.

231. **Otsuka Y, Yonesaki T.** 2005. A novel endoribonuclease, RNase LS, in *Escherichia coli. Genetics* **169**:13-20.
232. **Tadokoro T, Kanaya S.** 2009. Ribonuclease H: molecular diversities, substrate binding domains, and catalytic mechanism of the prokaryotic enzymes. *Febs J* **276**:1482-1493.
233. **Nakamura A, Koide Y, Miyazaki H, Kitamura A, Masaki H, Beppu T, Uozumi T.** 1992. Gene cloning and characterization of a novel extracellular ribonuclease of *Bacillus subtilis. Eur J Biochem* **209**:121-127.
234. **Oussenko IA, Sanchez R, Bechhofer DH.** 2004. *Bacillus subtilis* YhcR, a high-molecular-weight, nonspecific endonuclease with a unique domain structure. *J Bacteriol* **186**:5376-5383.
235. **Andrade JM, Pobre V, Silva IJ, Domingues S, Arraiano CM.** 2009. The role of 3'-5' exoribonucleases in RNA degradation. *Prog Mol Biol Transl Sci* **85**:187-229.
236. **Ghosh S, Deutscher MP.** 1999. Oligoribonuclease is an essential component of the mRNA decay pathway. *Proc Natl Acad Sci U S A* **96**:4372-4377.
237. **Oussenko IA, Sanchez R, Bechhofer DH.** 2002. *Bacillus subtilis* YhaM, a member of a new family of 3'-to-5' exonucleases in gram-positive bacteria. *J Bacteriol* **184**:6250-6259.
238. **Lehnik-Habrink M, Newman J, Rothe FM, Solovyova AS, Rodrigues C, Herzberg C, Commichau FM, Lewis RJ, Stulke J.** 2011. RNase Y in *Bacillus subtilis*: a Natively disordered protein that is the functional equivalent of RNase E from *Escherichia coli. J Bacteriol* **193**:5431-5441.
239. **Commichau FM, Rothe FM, Herzberg C, Wagner E, Hellwig D, Lehnik-Habrink M, Hammer E, Volker U, Stulke J.** 2009. Novel activities of glycolytic enzymes in *Bacillus subtilis*: interactions with essential proteins involved in mRNA processing. *Mol Cell Proteomics* **8**:1350-1360.
240. **Shahbabian K, Jamalli A, Zig L, Putzer H.** 2009. RNase Y, a novel endoribonuclease, initiates riboswitch turnover in *Bacillus subtilis. Embo J* **28**:3523-3533.
241. **Yao S, Bechhofer DH.** 2010. Initiation of decay of *Bacillus subtilis rpsO* mRNA by endoribonuclease RNase Y. *J Bacteriol* **192**:3279-3286.
242. **Lehnik-Habrink M, Schaffer M, Mader U, Diethmaier C, Herzberg C, Stulke J.** 2011. RNA processing in *Bacillus subtilis*: identification of targets of the essential RNase Y. *Mol Microbiol* **81**:1459-1473.
243. **Yao S, Richards J, Belasco JG, Bechhofer DH.** 2011. Decay of a model mRNA in *Bacillus subtilis* by a combination of RNase J1 5' exonuclease and RNase Y endonuclease activities. *J Bacteriol* **193**:6384-6386.
244. **Durand S, Gilet L, Bessieres P, Nicolas P, Condon C.** 2012. Three essential ribonucleases-RNase Y, J1, and III-control the abundance of a majority of *Bacillus subtilis* mRNAs. *PLoS Genet* **8**:e1002520.
245. **Marincola G, Schafer T, Behler J, Bernhardt J, Ohlsen K, Goerke C, Wolz C.** 2012. RNase Y of *Staphylococcus aureus* and its role in the activation of virulence genes. *Mol Microbiol* **85**:817-832.

246. **Laalami S, Bessieres P, Rocca A, Zig L, Nicolas P, Putzer H.** 2013. B*acillus subtilis* RNase Y activity *in vivo* analysed by tiling microarrays. *PLoS One* **8**:e54062.
247. **Elias AF, Stewart PE, Grimm D, Caimano MJ, Eggers CH, Tilly K, Bono JL, Akins DR, Radolf JD, Schwan TG, Rosa P.** 2002. Clonal polymorphism of *Borrelia burgdorferi* strain B31 MI: implications for mutagenesis in an infectious strain background. *Infect Immun* **70**:2139-2150.
248. **Samuels DS.** 1995. Electrotransformation of the spirochete *Borrelia burgdorferi. Methods Mol Biol* **47**:253-259.
249. **Bono JL, Elias AF, Kupko JJ, 3rd, Stevenson B, Tilly K, Rosa P.** 2000. Efficient targeted mutagenesis in *Borrelia burgdorferi. J Bacteriol* **182**:2445-2452.
250. **Bertani G.** 1951. Studies on lysogenesis. I. The mode of phage liberation by lysogenic *Escherichia coli. J Bacteriol* **62**:293-300.
251. **Spizizen J.** 1958. Transformation of biochemically deficient strains of *Bacillus Subtilis* by deoxyribonucleate. *Proc Natl Acad Sci U S A* **44**:1072-1078.
252. **Cutting SM, Vander Horn, P.B.** 1990. Genetic Analysis, p. 27-74. *In* Harwood CR, Cutting, S.M. (ed), *Molecular Biological Methods for* Bacillus. Wiley, John & Sons, Incorporated, Chichester.
253. **Gilbert MA, Morton EA, Bundle SF, Samuels DS.** 2007. Artificial regulation of *ospC* expression in *Borrelia burgdorferi. Mol Microbiol* **63**:1259-1273.
254. **Lybecker MC, Samuels DS.** 2007. Temperature-induced regulation of RpoS by a small RNA in *Borrelia burgdorferi. Mol Microbiol* **64**:1075-1089.
255. **Hoon-Hanks LL, Morton EA, Lybecker MC, Battisti JM, Samuels DS, Drecktrah D.** 2012. *Borrelia burgdorferi malQ* mutants utilize disaccharides and traverse the enzootic cycle. *FEMS Immunol Med Microbiol* **66**:157-165.
256. **Lybecker MC, Abel CA, Feig AL, Samuels DS.** 2010. Identification and function of the RNA chaperone Hfq in the Lyme disease spirochete *Borrelia burgdorferi. Mol Microbiol* **78**:622-635.
257. **Sigmund CD, Ettayebi M, Borden A, Morgan EA.** 1988. Antibiotic resistance mutations in ribosomal RNA genes of *Escherichia coli. Methods Enzymol* **164**:673-690.
258. **Criswell D, Tobiason VL, Lodmell JS, Samuels DS.** 2006. Mutations conferring aminoglycoside and spectinomycin resistance in *Borrelia burgdorferi. Antimicrob Agents Chemother* **50**:445-452.
259. **Elias AF, Bono JL, Kupko JJ, 3rd, Stewart PE, Krum JG, Rosa PA.** 2003. New antibiotic resistance cassettes suitable for genetic studies in *Borrelia burgdorferi. J Mol Microbiol Biotechnol* **6**:29-40.
260. **Huntzinger E, Boisset S, Saveanu C, Benito Y, Geissmann T, Namane A, Lina G, Etienne J, Ehresmann B, Ehresmann C, Jacquier A, Vandenesch F, Romby P.** 2005. *Staphylococcus aureus* RNAIII and the endoribonuclease III coordinately regulate *spa* gene expression. *Embo J* **24**:824-835.
261. **Talkad V, Achord D, Kennell D.** 1978. Altered mRNA metabolism in ribonuclease III-deficient strains of *Escherichia coli. J Bacteriol* **135**:528-541.

262. **King TC, Sirdeshmukh R, Schlessinger D.** 1984. RNase III cleavage is obligate for maturation but not for function of *Escherichia coli* pre-23S rRNA. *Proc Natl Acad Sci U S A* **81**:185-188.
263. **Margolis N, Hogan D, Tilly K, Rosa PA.** 1994. Plasmid location of *Borrelia* purine biosynthesis gene homologs. *J Bacteriol* **176**:6427-6432.
264. **Tilly K, Fuhrman J, Campbell J, Samuels DS.** 1996. Isolation of *Borrelia burgdorferi* genes encoding homologues of DNA-binding protein HU and ribosomal protein S20. *Microbiology* **142 (Pt 9)**:2471-2479.
265. **Knight SW, Samuels DS.** 1999. Natural synthesis of a DNA-binding protein from the C-terminal domain of DNA gyrase A in *Borrelia burgdorferi. Embo J* **18**:4875-4881.
266. **Lin B, Short SA, Eskildsen M, Klempner MS, Hu LT.** 2001. Functional testing of putative oligopeptide permease (Opp) proteins of *Borrelia burgdorferi*: a complementation model in opp(-) *Escherichia coli. Biochim Biophys Acta* **1499**:222-231.
267. **Purser JE, Lawrenz MB, Caimano MJ, Howell JK, Radolf JD, Norris SJ.** 2003. A plasmid-encoded nicotinamidase (PncA) is essential for infectivity of *Borrelia burgdorferi* in a mammalian host. *Mol Microbiol* **48**:753-764.
268. **Liveris D, Mulay V, Schwartz I.** 2004. Functional properties of *Borrelia burgdorferi recA*. *J Bacteriol* **186**:2275-2280.
269. **Putteet-Driver AD, Zhong J, Barbour AG.** 2004. Transgenic expression of RecA of the spirochetes *Borrelia burgdorferi* and *Borrelia hermsii* in *Escherichia coli* revealed differences in DNA repair and recombination phenotypes. *J Bacteriol* **186**:2266-2274.
270. **Eggers CH, Caimano MJ, Radolf JD.** 2004. Analysis of promoter elements involved in the transcriptional initiation of RpoS-dependent *Borrelia burgdorferi* genes. *J Bacteriol* **186**:7390-7402.
271. **Apirion D, Gegenheimer P.** 1981. Processing of bacterial RNA. *FEBS Lett* **125**:1-9.
272. **Alitalo A, Meri T, Lankinen H, Seppala I, Lahdenne P, Hefty PS, Akins D, Meri S.** 2002. Complement inhibitor factor H binding to Lyme disease spirochetes is mediated by inducible expression of multiple plasmid-encoded outer surface protein E paralogs. *J Immunol* **169**:3847-3853.
273. **Brissette CA, Bykowski T, Cooley AE, Bowman A, Stevenson B.** 2009. *Borrelia burgdorferi* RevA antigen binds host fibronectin. *Infect Immun* **77**:2802-2812.
274. **Brissette CA, Verma A, Bowman A, Cooley AE, Stevenson B.** 2009. The *Borrelia burgdorferi* outer-surface protein ErpX binds mammalian laminin. *Microbiology* **155**:863-872.
275. **Kraiczy P, Hartmann K, Hellwage J, Skerka C, Kirschfink M, Brade V, Zipfel PF, Wallich R, Stevenson B.** 2004. Immunological characterization of the complement regulator factor H-binding CRASP and Erp proteins of *Borrelia burgdorferi. Int J Med Microbiol* **293 Suppl 37**:152-157.
276. **Metts MS, McDowell JV, Theisen M, Hansen PR, Marconi RT.** 2003. Analysis of the OspE determinants involved in binding of factor H and OspE-

targeting antibodies elicited during *Borrelia burgdorferi* infection in mice. *Infect Immun* **71**:3587-3596.
277. **Resch A, Afonyushkin T, Lombo TB, McDowall KJ, Blasi U, Kaberdin VR.** 2008. Translational activation by the noncoding RNA DsrA involves alternative RNase III processing in the rpoS 5'-leader. *RNA* **14**:454-459.
278. **Regnier P, Grunberg-Manago M.** 1990. RNase III cleavages in non-coding leaders of *Escherichia coli* transcripts control mRNA stability and genetic expression. *Biochimie* **72**:825-834.
279. **Robert-Le Meur M, Portier C.** 1992. *E.coli* polynucleotide phosphorylase expression is autoregulated through an RNase III-dependent mechanism. *Embo J* **11**:2633-2641.
280. **Aristarkhov A, Mikulskis A, Belasco JG, Lin EC.** 1996. Translation of the *adhE* transcript to produce ethanol dehydrogenase requires RNase III cleavage in *Escherichia coli. J Bacteriol* **178**:4327-4332.
281. **Freire P, Amaral JD, Santos JM, Arraiano CM.** 2006. Adaptation to carbon starvation: RNase III ensures normal expression levels of *bolA1p* mRNA and sigma(S). *Biochimie* **88**:341-346.
282. **Gravenbeek ML, Jones GH.** 2008. The endonuclease activity of RNase III is required for the regulation of antibiotic production by *Streptomyces coelicolor. Microbiology* **154**:3547-3555.
283. **Lioliou E, Sharma CM, Caldelari I, Helfer AC, Fechter P, Vandenesch F, Vogel J, Romby P.** 2012. Global regulatory functions of the *Staphylococcus aureus* endoribonuclease III in gene expression. *PLoS Genet* **8**:e1002782.
284. **Lim B, Sim SH, Sim M, Kim K, Jeon CO, Lee Y, Ha NC, Lee K.** 2012. RNase III controls the degradation of corA mRNA in *Escherichia coli. J Bacteriol* **194**:2214-2220.
285. **Gatewood ML, Bralley P, Weil MR, Jones GH.** 2012. RNA-Seq and RNA immunoprecipitation analyses of the transcriptome of *Streptomyces coelicolor* identify substrates for RNase III. *J Bacteriol* **194**:2228-2237.
286. **Gatewood ML, Jones GH.** 2012. Expression of a polycistronic messenger RNA involved in antibiotic production in an *rnc* mutant of *Streptomyces coelicolor. Arch Microbiol* **194**:147-155.
287. **Gatewood ML, Bralley P, Jones GH.** 2011. RNase III-dependent expression of the *rpsO-pnp* operon of *Streptomyces coelicolor. J Bacteriol* **193**:4371-4379.
288. **Zuker M.** 2003. Mfold web server for nucleic acid folding and hybridization prediction. *Nucleic Acids Res* **31**:3406-3415.
289. **Serganov A, Patel DJ.** 2007. Ribozymes, riboswitches and beyond: regulation of gene expression without proteins. *Nat Rev Genet* **8**:776-790.
290. **Cochrane JC, Strobel SA.** 2008. Catalytic strategies of self-cleaving ribozymes. *Acc Chem Res* **41**:1027-1035.
291. **Wakeley J.** 1996. The excess of transitions among nucleotide substitutions: new methods of estimating transition bias underscore its significance. *Trends Ecol Evol* **11**:158-162.
292. **Maivali U, Remme J.** 2004. Definition of bases in 23S rRNA essential for ribosomal subunit association. *RNA* **10**:600-604.

293. **Douthwaite S, Prince JB, Noller HF.** 1985. Evidence for functional interaction between domains II and V of 23S ribosomal RNA from an erythromycin-resistant mutant. *Proc Natl Acad Sci U S A* **82**:8330-8334.